N.M.R. STUDIES OF TIN HYDRIDES

A Thesis

presented to the Faculty of Science
of the University of London

in candidature for

the Degree of Doctor of Philosophy

by

Mohammed Jamil Ahamed

The Bourne Laboratory,
Royal Holloway College,
University of London,
Egham,
Surrey TW20 OEX

December, 1976.

ABSTRACT

The proton magnetic resonance spectra of various organo tin hydrides have been studied. Spectra were normally run under conditions of high scale expansion (0.2 Hz or 0.4 Hz cm^{-1}) and numerous heteronuclear double resonance experiments performed. The values of chemical shifts and coupling constants were compared with previously reported data. Proton spectra of di-cyclohexyl tin hydride and di-benzyl tin hydride have been reported for the first time.

Some of the hydrides were deuterated [$(CH_3)_2SnH_2$, $(C_6H_5)_2SnH_2$, $C_6H_5SnH_3$ and $(C_6H_5CH_2)_2SnH_2$] and the effects of deuterium substitution both on shielding and on spin spin coupling constants have been measured. ^{119}Sn spectra at 22.37 MHz were obtained by the pulse FT method and values for ^{119}Sn chemical shift and tin-proton and tin-deuterium coupling constants obtained. Isotopic effects were observed both on shifts and coupling constants as a result of deuterium substitution. A linear dependence for ^{119}Sn shifts on the number of substituents in methyl and phenyl stannanes has been found.

The spin-lattice relaxation times (T_1) of the naturally abundant magnetic tin satellites in the proton spectra of these hydrides have been measured and were found to be shorter than the

relaxation times of the central feature resulting from molecules containing non-magnetic tin. Correlation times (τ_c) were calculated from the dipolar contribution to the total relaxation time. The temperature dependence of ^{13}C spin-lattice relaxation time in di-methyl tin hydride has also been studied. The dipole dipole contribution was determined by measurement of the proton nuclear Overhauser enhancement of the methyl carbon.

A computer program has been used for the iterative curve fitting of the experimental spectra of deuterated di-phenyl tin hydride to determine the quadrupole relaxation time (T_q) of the deuterium nucleus.

This Thesis is dedicated to

my Mother

and

Riaz

****

ACKNOWLEDGEMENTS

I should like to express my deepest gratitude to my supervisor Dr Duncan Gillies for his invaluable guidance in this project. I should also like to thank Professor Randall (Queen Mary College) Dr Shaw (Varian Associates) and Dr Stenhouse of P C M U for the use of valuable equipment, without which much of this work would have been impossible. My thanks also go to the technical staff of this Department, in particular Mr Lane and Mr Ashdown for their help, and Mrs Partin who so kindly typed this thesis. I am also indebted to the Royal Holloway College for the tenure of a post graduate award and to the British Council for an award under the Overseas Students' Fees Award Scheme. Finally, I should like to thank all my friends, librarian and secretarial staff of this Department without whose courtesy and help the work would have been more arduous and less pleasant.

****

CONTENTS

CHAPTER I

GENERAL DESCRIPTION OF THE N.M.R. EXPERIMENT

Section I. 1 Basic Principles of N. M. R.

The fundamental properties of nuclei are mass and positive charge. But nuclei with odd mass number or odd charge number or both possess an additional property of spinning or intrinsic angular momentum. Associated with the spin angular momentum is a magnetic moment which interacts with an applied field B_o.

The angular momentum is measured in units of $\hbar I$. Where I is the spin quantum number and $\hbar = h/2\pi$, h is Planck's constant. I may have integral or half integral values depending on mass and atomic number. A further property is that nuclei with spin 1/2 have a spherical charge distribution whereas nuclei with $I > 1/2$ have non-spherical charge distribution and have an electric quadrupole moment.

When this spinning nucleus is placed in an external magnetic field it starts precessing about the axis of the field.. This occurs due to the opposing effect of the rotational inertia of the nucleus as the applied magnetic field tends to turn the nuclear magnetic moment around into the field direction.

The angular precession frequency, ω_o, which is called the Larmor frequency is given by

$$\omega_o = \gamma B_o$$

where γ is the gyromagnetic ratio and is defined as

$$\gamma = \frac{\text{Magnetic Moment}}{\text{Angular Momentum}} = \frac{\mu}{I}$$

This relation gives the value of the magnetic moment. The energy E of interaction between this dipole moment and the applied field B_o is given by

$$E = \mu B_o \cos\theta$$

where θ is the angle between axis of dipole and the direction of the magnetic field. [T] There are only certain allowed values for θ.

For proton (as an example) having spin $I = 1/2$, there are two possible orientations parallel and anti-parallel to the applied field. Therefore, the above equation can be written as

$$E = -\mu_z B_o$$

When an isolated nucleus is placed in a magnetic field B_o along the z direction, where μ_z is the component of the nuclear magnetic moment in the z direction. If an oscillating magnetic field with an angular frequency ω_1 is applied along the x-axis and its frequency is varied slowly, there will be no observable effect except when ω_1 approximately equals ω_o and energy is absorbed by the precessing nuclei from the radio frequency coil. It is the detection of this resonant absorption of energy which constitutes the Nuclear Magnetic Resonance phenomenon.

According to quantum theory the z component of the angular momentum I can only have $(2I + 1)$ values. Thus the $(2I + 1)$ states of the nucleus have now discrete levels of energy given by

$$E = -\gamma \hbar \, m_I \, B_o$$

where m_I is the magnetic quantum number. The difference in energy between two neighbouring levels (which differ by one in m_I), is thus

$$\Delta E = \gamma \hbar B_o \left[m - (m-1) \right] = \gamma \hbar B_o$$

In a macroscopic system, an oscillating magnetic field induces transitions between the two spin states. The frequency of oscillation to meet the resonance condition is given by the equation

$$h\nu = \Delta E = \gamma \hbar B_o$$

or

$$\nu = \frac{\gamma}{2\pi} \cdot B_o$$

The application of an oscillating magnetic field B_1 can be treated by a time dependent perturbation theory if $B_1 \ll B_o$.

The energy of a system is observable, and the corresponding operator $\hat{\mathcal{H}}$ is known as the Hamiltonian operator. In high resolution N.M.R. experiments apart from the interaction of nuclei with the static magnetic field B_o there is an indirect spin-spin coupling between nuclei themselves which involves the scalar product of the spin vectors. The total Hamiltonian is a combination of the two. Therefore, the total Hamiltonian in the dimensions of frequency for a set of nuclei can be represented as

$$\hat{\mathcal{H}}_{\text{total}} = \sum_j \frac{\gamma_j}{2\pi} B_0 \hat{I}_{jz} + \sum_{j<k} J_{jk} \hat{I}_j \hat{I}_k$$

But the field experienced by the nuclei is not exactly equal to the applied field B_o. To the first part the Hamiltonian a screening constant σ is introduced which has the value equal to

one third of the trace of the screening tensor. Hence the Hamiltonian can be represented as

$$\hat{\mathcal{H}}_{total} = -\sum_j \frac{\gamma_j}{2\pi} B_o (1-\sigma_j) \hat{I}_{jz} + \sum_{j<k} J_{jk} \hat{I}_j \cdot \hat{I}_k$$

This Hamiltonian operates on the various eigenfunctions ψ_n of the system to given the energy of the state En, as described by the Schrodinger equation.

$$\hat{\mathcal{H}} \psi_n = E\psi_n$$

For P nuclei the eigenfunctions ψ_n are expressed in the basis set of the so-called 2^P basic product functions of the type $\phi_n = \alpha(1)$, $\beta(2)\,\alpha(3) \ldots \alpha(p)$ or $\alpha\beta\alpha \ldots$ Eigenfunctions form an orthonormal set of functions. This is conveniently expressed using Dirac notation as

$$\langle \psi_m | \psi_n \rangle = \langle m | n \rangle = \delta_{mn}$$

where δ is known as Kronecker delta and $\delta_{mn} = 1$ if m=n otherwise zero. We write the Schrodinger equation as

$$\langle \psi_m | \hat{\mathcal{H}} | \psi_n \rangle = E \langle \psi_m | \psi_n \rangle = \delta_{mn}$$

or

$$\left| \langle \psi_m | \hat{\mathcal{H}} | \psi_n \rangle - E\delta_{mn} \right| = 0$$

This secular equation is expressed in the form of a matrix and by diagonalisation one obtains the solution which gives the stationary states (eigenfunctions) and stationary state energies (123–125).

The radio frequency field Hamiltonian is given by

$$\hat{\mathcal{H}}_1 = -\hbar B_1 (e^{i\omega t}_1 + e^{-i\omega t}_1) \sum_n \gamma_n \hat{I}_{nx}$$

which induces transition between states with different m values. The resulting probability per unit time of a spin state m changing to state n can be found from time-dependent perturbation theory.

It is

$$P_{mn} = (\frac{2\pi}{h}) \left| \langle n | \hat{\mathcal{H}}_1 | m \rangle \right|^2 \delta (E_n - E_m - \hbar\omega_1)$$

where $\hat{\mathcal{H}}_1 = -\hbar B_1 \sum_n \gamma_n \hat{I}_{nx}$

we can write

$$P_{mn} = \gamma^2 B_1^2 \left| \langle n | \hat{I}_x | m \rangle \right|^2 \delta(\nu_{nm} - \nu)$$

where $\langle n | \hat{I}_x | m \rangle$ represents the quantum mechanical matrix elements of $\hat{I}_x$ between states n and m, and ν_{nm} is the frequency corresponding to the difference between the two states

if $\nu_{nm} = \nu$, then $\delta(\nu_{nm} - \nu) =$ unity

otherwise zero. Absorption occurs when the spectrometer frequency coincides with the natural frequency. In practice absorption occurs across a spread of frequencies which can be represented by a line shape function which is usually Lorentzian in high resolution n.m.r., so that the expression for P_{nm} becomes

$$P_{nm} = \gamma^2 B_1^2 \langle n | \hat{I}_x | m \rangle g(\nu)$$

The selection rules and relative transition probabilities can be most readily obtained by rewriting $\hat{I}_x$ in terms of shift operators

$$\langle n | \hat{I}_x | m \rangle = 1/2 \langle n | \hat{I}_+ + \hat{I}_- | m \rangle$$

where $\hat{I}_+$ raises the m value by one unit

$$\hat{I}_+ | I, m \rangle = \left[I(I+1) - m(m+1) \right]^{1/2} | I, m+1 \rangle$$

$$\text{and } \hat{I}_- \left| I, m \right\rangle = \left[I(I+1) - m(m-1) \right]^{1/2} \left| I, m-1 \right\rangle$$

Section I.2 Description of Spin Systems.

For describing nuclear spins in a molecule a universally accepted but not always consistently adopted nomenclature is used suggested by Pople, Schneider and Bernstein[123] and reviewed by Corio[124] and Roberts[125]. Each different nucleus is assigned a letter and the number of "magnetically equivalent" nuclei in each group is indicated by a subscript number. Nuclei or groups of nuclei which have chemical shift difference comparable to their coupling constants are assigned letters which are close in alphabet, AB, ABC... etc. Nuclei which are far apart in chemical shift are assigned letters which are far apart in the alphabet, e.g. AX, AMX... etc. If two nuclei are chemically equivalent but magnetically non-equivalent, they are denoted by the same letters but one is assigned a prime symbol AA', A'A"A"' etc.

In addition to this type of notation a further notation is introduced. According to this the multiplicity caused by that nucleus should go at the top left of the alphabet letters representing the nucleus. For example, if we are investigating the hydride proton in diphenyl tin deuterated hydride, the $Sn\begin{smallmatrix}H\\D\end{smallmatrix}$ part can be represented as $^{2}A^{3}X$.

Section I.3 Chemical Shifts

In an atom a static magnetic field induces an orbital motion of electrons which gives rise to a secondary field which is proportional to the applied field and opposes it. In the case of atoms because of spherical symmetry it is isotropic and diamagnetic in nature. In the case of molecules this secondary field is not purely diamagnetic because of non spherical distribution of the electronic cloud. Therefore screening of the nucleus is anisotropic and is a tensor property. The field "felt" by the nucleus in a static magnetic field B_o may be written as

$$B_{(\theta)} = B_o (1 - \sigma)$$

where θ is the angle of orientation of the molecule with reference to the laboratory fixed axis. In liquids and gases the random collisions lead to an effectively isotropic shielding of the nucleus and it is possible to write that

$$B = B_o (1 - \sigma)$$

where

$$\sigma = 1/3 (\sigma_{xx} + \sigma_{yy} + \sigma_{zz})$$

and σ is a dimensionless screening constant independent of B_o but dependent on the electronic environment of the nucleus concerned. This shielding of nuclei by electrons from the applied magnetic field gives rise to the phenomenon of the chemical shift. As nuclei in different environments have different electronic shieldings which make them magnetically non equivalent . these nuclei will absorb energy at different frequencies to meet the resonance

condition. The difference between the shift of a nucleus which is being observed and some reference, is proportional to the magnitude of the applied field B_o. It is more convenient to express chemical shift by a dimensionless parameter δ in the units of p.p.m. (parts per million) defined by the following equation

$$\delta = \frac{(\nu_{sample} - \nu_{reference})}{\nu_{spectrometer}} \times 10^6$$

The δ values are positive if the sample absorbs to higher frequency of the reference absorption.

I.3.1 Classification of Shielding Effects.

When a nucleus is chemically bound, the shielding arises in two ways. The term which relates the normal circulation of electrons and depends on the electron density distribution around the atom, is the local diamagnetic shielding. The second term which involves the circulation of electrons in chemical bonds is referred as local paramagnetic shielding. In addition, shielding may arise from the circulation of electrons present around the other atoms in the molecule. Shielding of this kind is known as long range shielding. This is due to the anisotropic effect in which the circulations induced by the applied field are greater for some orientations of the molecule than for others. In a schematic way they are represented as follows and are discussed separately but briefly.

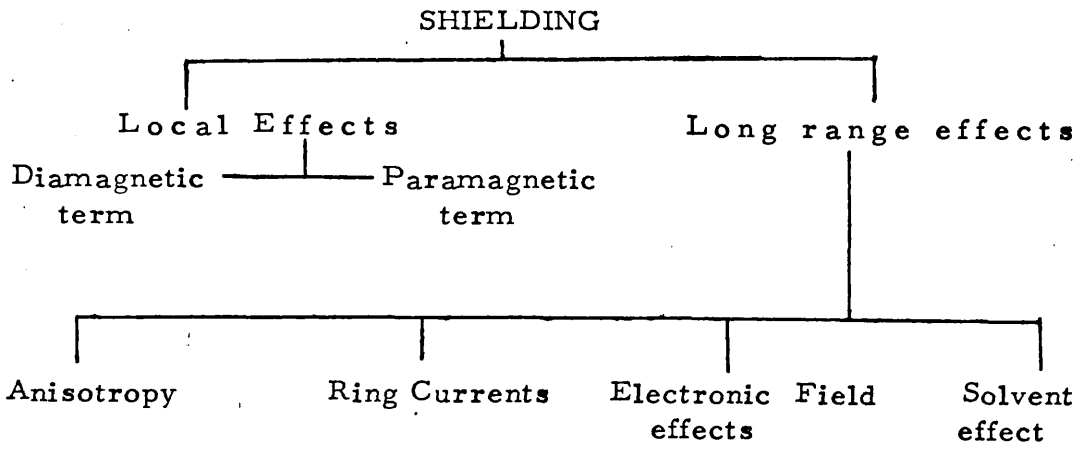

A) Diamagnetic Term σ_d

Electron density is responsible for diamagnetism, which arises from the currents induced by the magnetic field and is represented by Lamb's [126] formula. It also depends on the electronegativity of the substituent on that atom. This term is not very important for tin and other heavy atoms because the major contribution in these cases arise from the inner electrons, which are not very much affected by the variation of chemical environment of tin.

B) Paramagnetic Term σ_p

The local paramagnetic term arises from the induced paramagnetic currents which reinforces the applied field B_o, is generally considered to dominate the shielding (deshielding in fact).

It requires a knowledge of the wave function and energies of all excited states. A simplified representation in S.I. form is given by

$$\sigma^{p}_{local} = -\frac{\mu_o}{4\pi}\frac{e^2h^2}{2m^2\Delta E}\left[\langle r^{-3}\rangle_p Q_{np} + \langle r^{-3}\rangle_d Q_{nd}\right]$$

where μ_o represents the permeability constant. ΔE, is the mean excitation energy, which determines the extent to which the ground

and excited states are mixed by the application of magnetic field. There is very little known about the effect of various substituents on ΔE in tin compounds.

$\langle r^{-3} \rangle_p$ and $\langle r^{-3} \rangle_d$ are mean inverse cubes of distances of the valence shell p and d electrons from the nucleus. These quantities increase with increasing atomic number in a group in periodic table. The terms Q_p and Q_d, represent inbalance in the p and d orbitals respectively, of the atom.

Changes in Q_{5p} dominate the shielding of four coordinated tin compounds. Therefore, sometimes Q_{5d} may be ignored.

C) Long Range Shielding

The appearance of aromatic protons at lower fields than aliphatic ones can be explained due to ring currents. When the applied field B_o is at right angles to the plane of the molecule, the circulating currents of delocalised electrons in benzene ring oppose the applied field in the middle of the molecule but is parallel at the outer region, which makes protons deshielded.

If the secondary magnetic field for two possible orientations of a system in an applied field has different values which opposes the applied field in one orientation and reinforces along the other, the observed shielding in the case of a liquid will

be an average over all the orientations. This type of shielding present in the system due to neighbouring atoms or groups of atoms is known as the neighbour anisotropy effect.

The solvent effects or the medium effects are intermolecular type interactions. The polar solvents usually increase the inductive effect of electronegative substituents in solutes.

The presence of strong polar groups in a molecule gives rise to intra molecular electric fields, which affect the overall charge distribution around the molecule and which results in a change in screening constants.

Section I.4 Spin-spin coupling.

The high resolution N.M.R. spectra of molecules show multiplets rather than single lines. The observed splittings are independent of the applied magnetic field. The magnitude generally increases with the increasing atomic number and this interaction between two non equivalent nuclei is proportional to the scalar product of $\hat{I}_i \cdot \hat{I}_j$. The energy of interaction can be written as

$$E_{ij_o} = h J_{ij} [\hat{I}_i \hat{I}_j]$$

Where J, is a proportionality constant, known as coupling constant and is expressed in Hz, may have positive or negative value. The magnitude depends on the electronic geometry of the molecule. It is calculated from wave functions which describe the electronic states of the molecule.

Fig. I.I. shows a schematic representation of energy

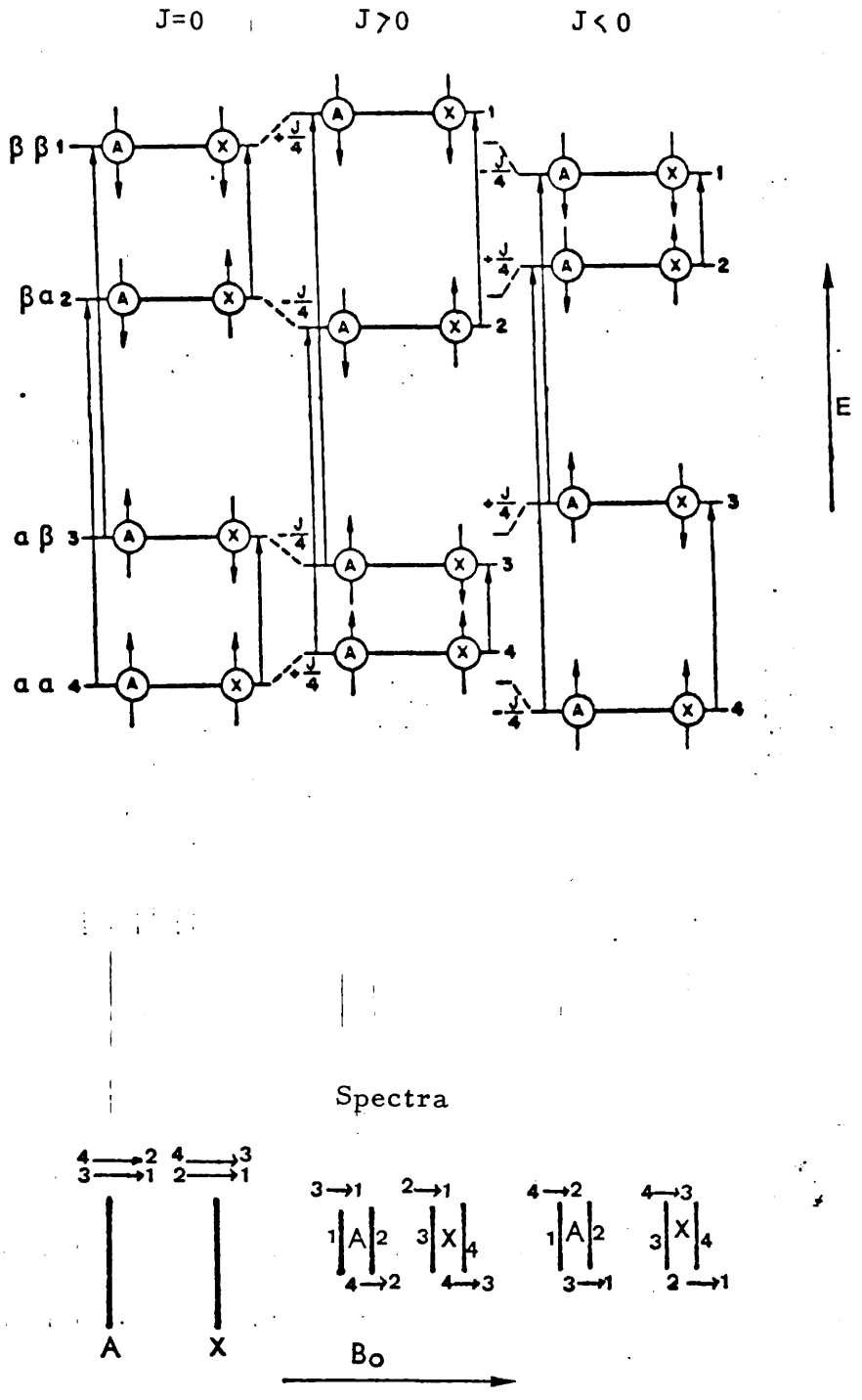

Fig. I. I. Magnetic energy levels of an AX spin system where γ_A and γ_X both are positive.

levels in an AX system, without coupling, and the case when $J > 0$ or $J < 0$. It is also assumed that $\mu_A > \mu_X$. E_1, is the state of highest energy because both moments are aligned against the applied field, and state 4 has the lowest energy where both spins lie parallel to the applied field. When there is no coupling between these two moments, the two transitions of each nucleus have the same energy and the spectrum consists of two lines. In case of positive coupling, the energy levels of unpaired spin will be raised by J/4 and those with the paired spin go down by the same amount. The transitions do not have equal energies any more and the spectrum consists of a total of four lines. In the case when $J < 0$, the energies of parallel spin states goes down, while that of paired spins goes up and the spectrum is shown with the transitions in Fig.I.I.

There are several terms which contribute to coupling constants, some of them are described here briefly.

I.4.1 Direct Dipolar coupling of Nuclear Spins.

The nuclear moments interact directly which can be represented classically by an equation

$$E = \frac{\mu_o}{4\pi} \left[\frac{\underline{\mu}_i \cdot \underline{\mu}_j}{r^3} - \frac{3 (\underline{\mu}_i \cdot \underline{r}) (\underline{\mu}_j \cdot \underline{r})}{r^5} \right]$$

where r, is the radius vector from μ_i to μ_j and μ_o is the permeability constant,

$$\text{and } \underline{\mu}_i = \gamma_i \hbar \underline{I}_i$$

$$\underline{\mu}_j = \gamma_j \hbar \underline{I}_j$$

In terms of quantum mechanics, it is a first order interaction and the Hamiltonian for this interaction can be written as follows

$$\hat{\mathcal{H}}_d = \sum_{ij} \gamma_i \gamma_j \hbar^2 \left\langle 0 \left| r^{-3} \right| 0 \right\rangle \left(3 \hat{I}_{iz} \hat{I}_{jz} - \hat{\underline{I}}_i \hat{\underline{I}}_j \right)$$

The matrix element reduces to an average of r_i^{-3} over the electronic ground state vibrations. The term $(3 \hat{I}_{iz} \hat{I}_{jz} - \hat{\underline{I}}_i \hat{\underline{I}}_j)$ becomes zero in liquids, because all orientations are possible due to molecular motion.

I.4.2 Coupling between Electrons and Nuclear Spins

This coupling involves more than one mechanism. There could be direct dipole interaction between the two magnetic moments. The interaction arises when one nucleus interacts with the surrounding electrons, which then affect the magnetic surroundings of the second nucleus.

The nuclear spin can also interact with the magnetic moment of electron orbital (the electron orbital term). The resulting induced electronic currents produce a magnetic field at the second nucleus. This "electro-nuclear" spin coupling contributes very little to the interaction responsible for the coupling constant.

I. 4. 3 Fermi Contact Interaction via Electrons

For most coupling situations the Fermi contact term is considered to be dominant. This term depends on the s electron density at the nucleus, because it is only the s atomic states which have finite electron density at the nucleus, it is expected that coupling will depend on s character in the bond. The potential energy of two dipoles μ_i and μ_j separated by a distance r_{ij} can be treated classically

In case of an s orbital the electron can penetrate the nucleus and the interaction can be represented by the Fermi contact Hamiltonian[127]

$$\hat{\mathcal{H}}_{eN} = \frac{16\pi\beta\hbar}{3} \sum_{e} \sum_{N} \gamma_N \delta(r_{eN}) \hat{\underline{S}}_e \cdot \hat{\underline{I}}_N$$

where $\delta(r_{eN})$ is a Dirac delta function which shows that this interaction is zero except at the nucleus, $\hat{\underline{S}}$ is the electron spin and $\hat{\underline{I}}_N$ is the nuclear spin vector.

Second order perturbation theory gives a contribution to the ground state energy of the form

$$-\sum_{n \neq o} \frac{\langle 0 | \hat{\mathcal{H}}_{eN} | n \rangle \langle n | \hat{\mathcal{H}}_{eN} | 0 \rangle}{(E_n - E_0)}$$

0, refers to the ground-state and n the excited state, E_o and E_n are their energies respectively, $\hat{\mathcal{H}}_{eN}$ is the electron nuclear pertubbation. According to the expression

$$E_{nn'} = h J_{NN'} \hat{\underline{I}}_N \hat{\underline{I}}_{N'}$$

the energy of interaction between two spin states is proportional to

the coupling constant $J_{NN'}$.

The expression for $J_{NN'}$ is given by

$$J_{NN'} = 2/3\hbar \left(\frac{16\ \pi\ \beta\ \hbar}{3}\right)^2 \quad \gamma_N\ \gamma_{N'}$$

$$\sum_{n\neq o} \frac{\langle 0 \left| \sum_e \delta(r_{eN}) \hat{S}_e \right| n \rangle \langle n \left| \sum_{e'} \delta(r_{e'N'}) \hat{S}_{e'} \right| 0 \rangle}{(E_n - E_0)}$$

I.4.4 The Reduced Coupling Constant

It is apparent that each contribution to the coupling constant is proportional to the product of the magnetogyric ratios. The effect of isotopic substitution on the spin-spin coupling constant is mainly due to the change in the magnetogyric ratio, since it does not affect the electronic wave functions very much. Hence, it was suggested to define another constant which depends solely on the electronic environment, to compare the coupling constants of different elements. Pople and Santry[128] introduced, the reduced coupling constant, denoted by K and defined as

$$K_{NN'} = J_{NN'} \quad \left(\frac{2\ \pi}{\hbar} \quad \frac{1}{\gamma_N \gamma_{N'}}\right)$$

in S.I. units K has units of $N\ A^{-2}\ m^{-3}$.

With this definition the coupling energy can be written in terms of magnetic moments as

$$E_{NN'} = K_{NN'}\ \mu_N\ \mu_{N'}$$

There is a general tendency for the reduced coupling constant to increase with increasing atomic number of coupled nuclei.

Section I. 5 Double Resonance

I. 5. 1 Spin Decoupling

Double resonance methods are frequently used to assist in the interpretation of complex N. M. R. spectra. In the case of spin decoupling, the N. M. R. spectrum is observed with one frequency B_1, while a second r. f. field B_2 is applied in order to perturb the system of nuclei. Under these conditions multiplet splittings arising from spin coupling to the nuclei irradiated by B_2 may collapse. The simplest application is merely to identify signals by simplifying the complex spectra to obtain the values of chemical shifts. Spin decoupling has also been used to determine the signs of coupling constants.

A further effect arising from the high irradiation power level is saturation of signals near the point of irradiation. The intensities observed in double resonance spectra may differ because of the Nuclear Overhauser Effect (NOE) which will be discussed later.

Decoupling is easy to observe only when the chemical shift separation is much greater than the coupling. The simplest case is that of AX system. The multiplet signal of A is reduced to a single peak by irradiation at the resonance frequency of X, provided the intensity irradiation is sufficiently high such that

$$\frac{\gamma B_2}{2\pi} \gg 2\left|J_{AX}\right|$$

I. 5. 2 I N D O R

In the internuclear double resonance technique, a suitable proton line in the proton spectrum is monitored continuously (fixed ω_1),

while a second r.f., ω_2, is used to sweep through the area of interest. In this way spectral information from one nucleus may be observed via the resonance of another nucleus. Usually one uses the sensitivity and convenience of proton spectra to gain information about a nucleus which is less convenient and/or sensitive to observe. One is able to observe INDOR spectra which look very similar to the actual spectra, and from which the resonance frequency may be readily observed.

I.5.3 Nuclear Overhauser Effect

In many double resonance experiments changes in the overall intensities of the observed lines are observed which occur due to the changes in the populations of energy levels due to the second irradiating r.f. field. It is this which is known as the Nuclear Overhauser Effect (N.O.E.), arises when two nuclei are physically close; a necessary condition is that there is a dipole-dipole interaction.

Grant[130], Solomon[129] and Randall[131] have shown for an AX system that the ratio of magnetic polarization of spin A with and without strong decoupling field centered at the resonance frequency of X, is given by

$$\frac{\langle M_z^A \rangle}{\langle M_z^A \rangle_o} = \frac{Id}{Ic} = 1 + \frac{W_2 - W_o}{W_o + 2W_1^A + W_2} \cdot \frac{\gamma_x}{\gamma_A}$$

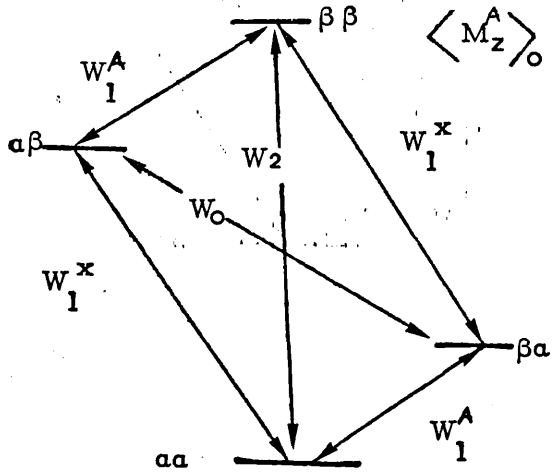

where Id/Ic is the ratio of intensities of resonance signals decoupled/coupled

If the only mechanism responsible for relaxation is through dipole dipole interaction, the transition probabilities have the following ratios

$$W_2 = W_1^{(A)} = W_0 = 12 : 3 : 2$$

on substituting these values we obtain

$$\frac{Id}{Ic} = 1 + \frac{\gamma_x}{2\gamma_A}$$

If we denote $Id/Ic = \eta_{max} = 1 + \frac{\gamma_x}{2\gamma_A}$

and the observed fraction gain in intensity by double resonance condition by η , it is possible to show that

$$N.O.E. = \eta = \eta_{max} \times T_1^A / T_1{}^A{}_{DD}$$

Where $T_1(A)$ = total relaxation time of A and contribution from AX d.d - interaction

N.O.E. determination gives us a method to separate the dipole dipole contribution from the total

This is done by the N.O.E. suppressed procedure. Two pulse sequences are recorded one with the decoupler on all the time and the signal intensity is denoted by I (decoupled) and one with the decoupler on only during the 90^o pulse and acquisition time. The intensity of this N.O.E. suppressed signal can be represented by I (suppressed) The N,O.E. is then calculated by substituting the values in the following expression

$$N.O.E. = \frac{I\ (decoupled)}{I\ (\ suppressed)} - 1$$

The decoupled spectrum without N.O.E is obtained by gated decoupling[132]. The sequence of pulses can be understood by the Fig. I.II The interval between transmitter pulses should be greater than $5T_1$

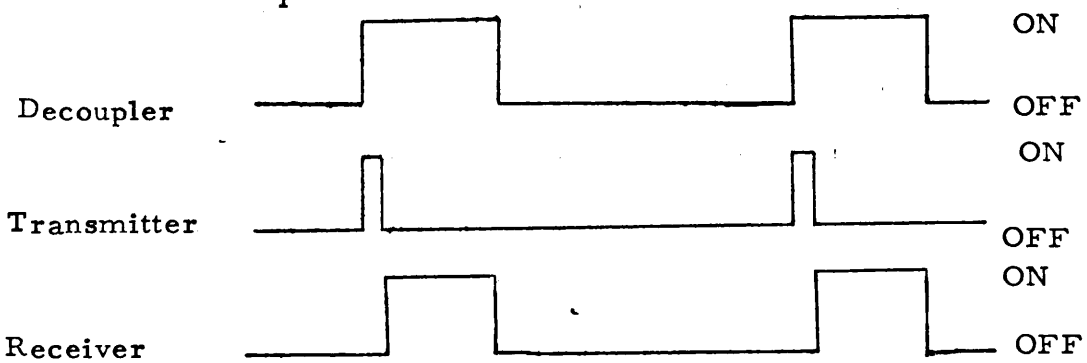

Fig. I.II Gated decoupling

For certain nuclei the magnetic moment in antiparallel to their spin angular momentum. Therefore, they have a negative gyromagnetic ratio, which makes η_{max} negative if one of the two interacting nuclei has negative γ, the negative N.O.E. will either lower the intensity or invert the signal depending on the magnitude of γ.

CHAPTER II

EXPERIMENTAL TECHNIQUES

Section II.1 C.W. Spectrometer

II.1.1 The Magnet

The basic requirement in an N.M.R. spectrometer is a strong, stable and homogeneous magnetic field. In this work a modified Varian Associates HA60IL system N.M.R. spectrometer has been used, Fig.II.I shows the block circuit diagram of this spectrometer. which has an electromagnet capable of giving a resolution of 0.3 Hz at 60 MHz (Proton resonance frequency at 14.1 K G). The magnet is provided with safety devices against overheating. A device, called magnetic flux stabilizer, is used to achieve high magnetic field stability. It compensates for any change in the field. The residual field drift which is still present is eliminated by the incorporation of field/frequency lock. This system uses an n.m.r. signal detected in the dispersion mode as an error signal to compensate for any changes in the field/frequency condition. A homogeneous field is achieved by shimming coils mounted on the pole faces which are capable of producing weak magnetic field gradients. Spinning the sample about the Y-axis at a rate greater than the desired resolution (in Hz) also helps to increase the magnetic field homogeneity at the sample. The lock channel is of fixed frequency. The resonance signal from the reference substance (H_2O, C_6H_6, $CHCl_3$ and T.M.S. etc are used in case of proton lock) is obtained by varying B_o with sweep coils mounted on the face of the magnet. The first upfield side band of the modulation frequency is used as a locking signal

and is displayed on the oscilloscope.

II .1.2 The Audio Oscilator

To observe the spectrum a stable r.f. source of low power (ca.1W) is required. A frequency synthesizer "Schlumberger" of type FSX 3006, capable of sweeping any decade was used to observe the proton resonance.

II .1.3 Detection of Signals

The crossed coil method is used in this spectrometer to detect the signal. Two separate coils are used at right angles to each other. The r.f. energy is transmitted through a transmitter coil at the sample. When the resonance conditions are met, a weak e.m.f. is induced in the receiver coil. It is amplified in a pre-amplifier which is placed very close to the receiver coil.

II .2 INDOR

In this mode a 2nd synthesizer (Schlumberger F.S.2) was used in place of the "FSX" to provide a fixed audio frequency for the observation channel. The "FSX" was then used to sweep the frequency of the irradiating channel.

II .3 Double Resonance

A General Radio frequency synthesizer of type 1061, was used for irradiating the sample at the fixed frequency. The block diagram for heteronuclear double resonance is given in Fig.II.I

II .4 C A T

Normally the frequency of the "FSX" synthesizer is

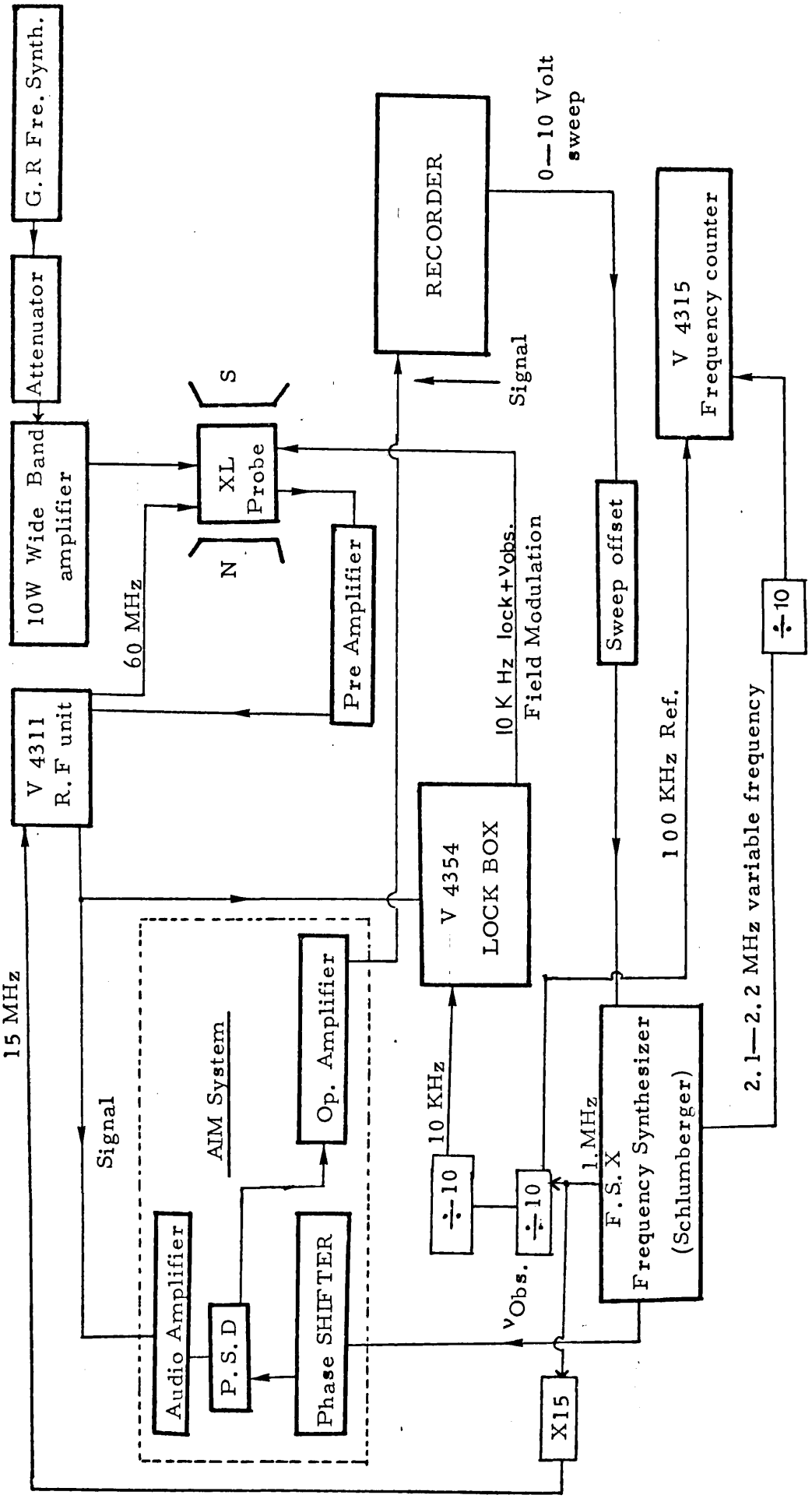

Fig. II. I.N.M.R Spectrometer (CW)

swept by a voltage derived from a potentiometer which is directly attached to the x-axis motion of the recorder. In CAT mode a ramp voltage from the CAT is used instead

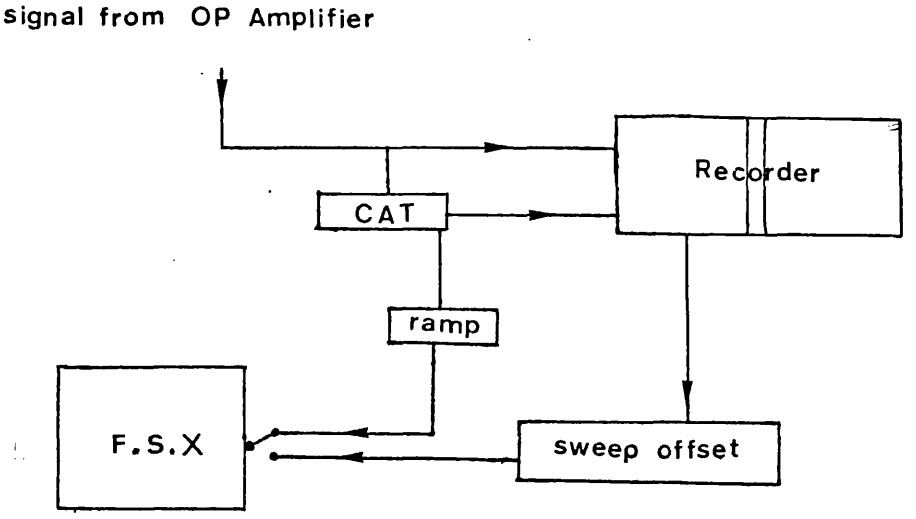

II. 5 Calibration

Spectra were calibrated using the Varian V- 4315 frequency counter, which used as its reference a 100 K Hz signal from the "FSX" frequency synthesizer. The counter measured the interpolation frequency (2.1 x 2.2 MHz) in the FSX synthesizer after division by ten. In this way a calibration accurate to one part in 10,000 of the swept decade can be achieved in one second.

II .6 Pulse F. T. Spectrometer

The mathematical concept of Fourier transformation is used to interconvert the time and frequency domains. The transform is generally represented by an equation of the type

$$f(x) = \int_{-\infty}^{+\infty} f(y)\, e^{-ixy}\, dy$$

where $f(x)$ is said to be the Fourier Transform of $f(y)$, the inverse transformation gives the following

$$f(y) = \frac{1}{2\pi} \int_{-\infty}^{+\infty} f(x)\, \exp(ixy)\, dx$$

In N.M.R. spectroscopy we are dealing with the magnetization M, of the spin system as a function of angular frequency ($\omega = 2\pi\nu$). Therefore, it can be written as

$$M(\omega) = \int_{-\infty}^{+\infty} M(\tau)\, e^{-i\omega\tau}\, d\tau$$

where M (τ) represents the magnetisation as a function of time after an "event". In pulse spectroscopy all the resonances are excited at the same time, therefore the magnetization after the "event" is the property of the whole system. This transformation is done by a computer (P.D.P 11 in our case) using a program based on Cooley-Tuckey Algorithm and modified by Bergland.

The excitation of spins in a static magnetic field is done by subjecting the system to a sequence of rectangular pulses of short duration along the x-axis. The radiofrequency pulses are produced by gating a pair of Hatfield double balanced modulators with subsequent broad band amplification and finally a narrow band amplification by a 150 W "Polaron" amplifier where out put was applied to the coil of a Varian Associates XL probe.

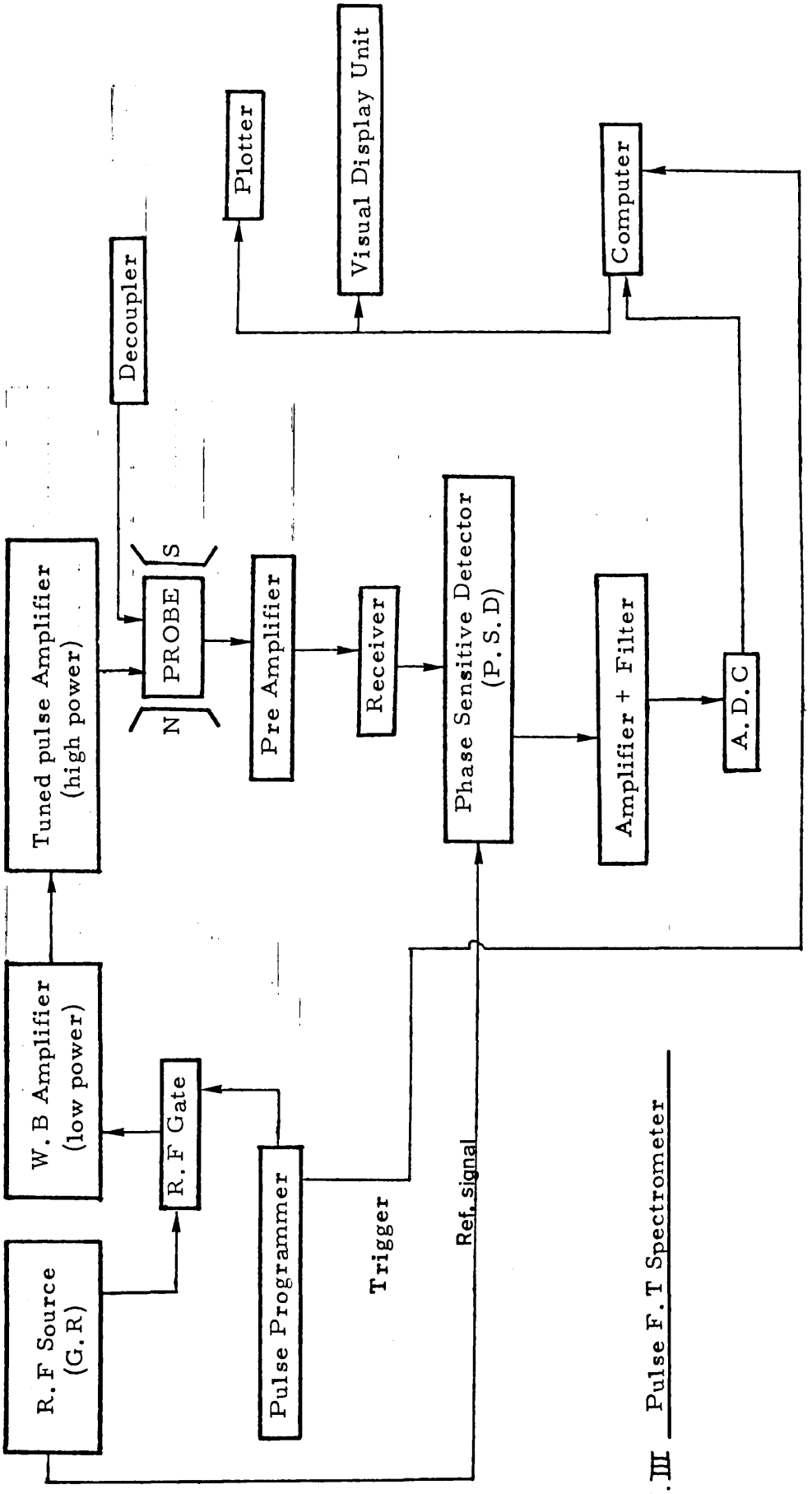

Fig. II. III Pulse F. T Spectrometer

The F.I.D. signal is amplified in a pre-amplifier, which is placed physically in the probe. It then goes via a Decca preamplifier to a Decca receiver. The signal is converted to an intermediate frequency (I.F.) by mixing with a local oscillator frequency, which is then followed by I.F. phase detection. The F.I.D. is then further D.C. amplified.

For either better sensitivity or sensitivity enhancement, the data prior to transformation are weighted, which is a multiplication process in the time domain.

Section II . 1. Organotin Hydrides or Stannanes [71],[102]

The hydrides are highly reactive, decomposing at room temperature into tin and hydrogen. Stannane, SnH_4 is very unstable, but progressive substitution of alkyl or aryl groups for hydrogen results in increased stability. The known organotin hydrides are mostly colourless distillable liquids. The most widely used method to prepare a variety of tin hydrides is the reduction of the corresponding organotin halide by lithium aluminium hydride in ether.

$$R_nSnCl_{(4-n)} + LiAlH_4 \longrightarrow R_nSnH_{(4-n)} + LiACl_4$$

It is the most convenient laboratory method, and it is probable that the reaction proceeds quantitatively in most cases. Their mode of decomposition depends on their storage; in general, contact with air, acids, metals and vacuum grease is avoided. The decomposition generally leads to tetra-alkyl- or tetra-aryl- tin, metallic tin and hydrogen

$$4\ R_n\ SnH_{(4-n)} \longrightarrow n\ R_4Sn + (4-n)Sn + 2\ (4-n)\ H_2$$

Organotin compounds in general are toxic, but none are extremely so, their physiological and toxicological properties have not been fully investigated. Precautions should be taken in handling to avoid inhalation of vapours or contact with the skin.

II. 1.1 Diphenyl Tin Dihydride and partially Deuterated Hydride [96]

$(C_6H_5)_2\ SnH_2$ has a reported b.pt. 89-93°/0.5 mm, and decomposes in air to a bright yellow solid which is probably diphenyl tin polymer

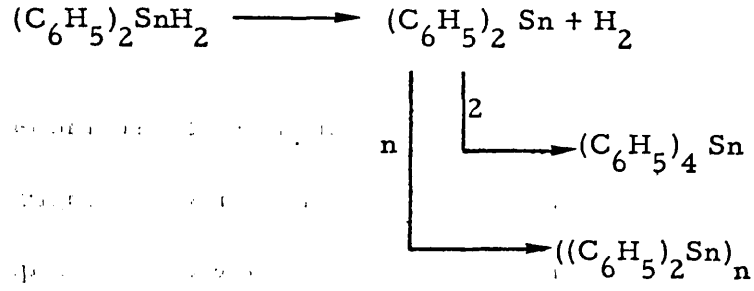

The decomposition was also found to be catalysed by vacuum grease as a bright yellow colour was found around the "quick fit" joints of the apparatus and vacuum line. The preparation was done in an atmosphere of nitrogen to avoid decomposition by air.

A solution of di-phenyl tin dichloride in dry ether was added dropwise from a pressure equilibriating funnel to an ether slurry of $LiAlH_4$, over a period of an hour. This was stirred continuously for a further 30 minutes, maintaining the temperature throughout, at 0°C. At the end of the experiment the excess of $LiAlH_4$ was destroyed by the dropwise addition of ice water. The flask containing the ether mixture of hydride was then taken into a nitrogen filled dry bag, the ether layer was separated from water and washed a few times with ice water. The flask was then connected to a vacuum line for several hours to remove ether. The vacuum was broken with nitrogen when a "constant" volume was left in the flask. The hydride was transferred to an N.M.R.

tube after filtering through a fine filter fitted to a syringe in a millipore, to avoid any solid impurities which may have arisen from the partial decomposition. A few drops of T.M.S. were added as an internal reference. This was also done in the nitrogen filled dry bag. The n.m.r. tube was then connected to a vacuum line, where it was degassed and sealed under vacuum.

Partially Deuterated Hydride was prepared in order to study isotope effects and study of line shapes of protons coupled to deuterium. In order to obtain strong signals, it was necessary that a proper amount of -HD species should be present in the hydride mixture. This was done by suppressing the formation of di hydride by using a reducing mixture which contains more deuterating agent than the hydrogenating one. According to the isotope effects on reaction rates, deuteration is a slower process than the hydrogenation and it was found, after using the $LiAlH_4$ and $LiAlD_4$ in different proportions that to get a reasonable amount of -HD species in the hydride mixture, these reducing agents should be used in a 1:5 ratio. The rest of the procedure for the preparation of partially deuterated hydride is the same as pure hydride.

When the sample was not being used it was kept in the dark in a refrigerator as it was thought that light may have some catalytic effect on the decomposition.

The spectra were initially obtained using the Varian Associates EM-360 spectrometer, to identify the compound

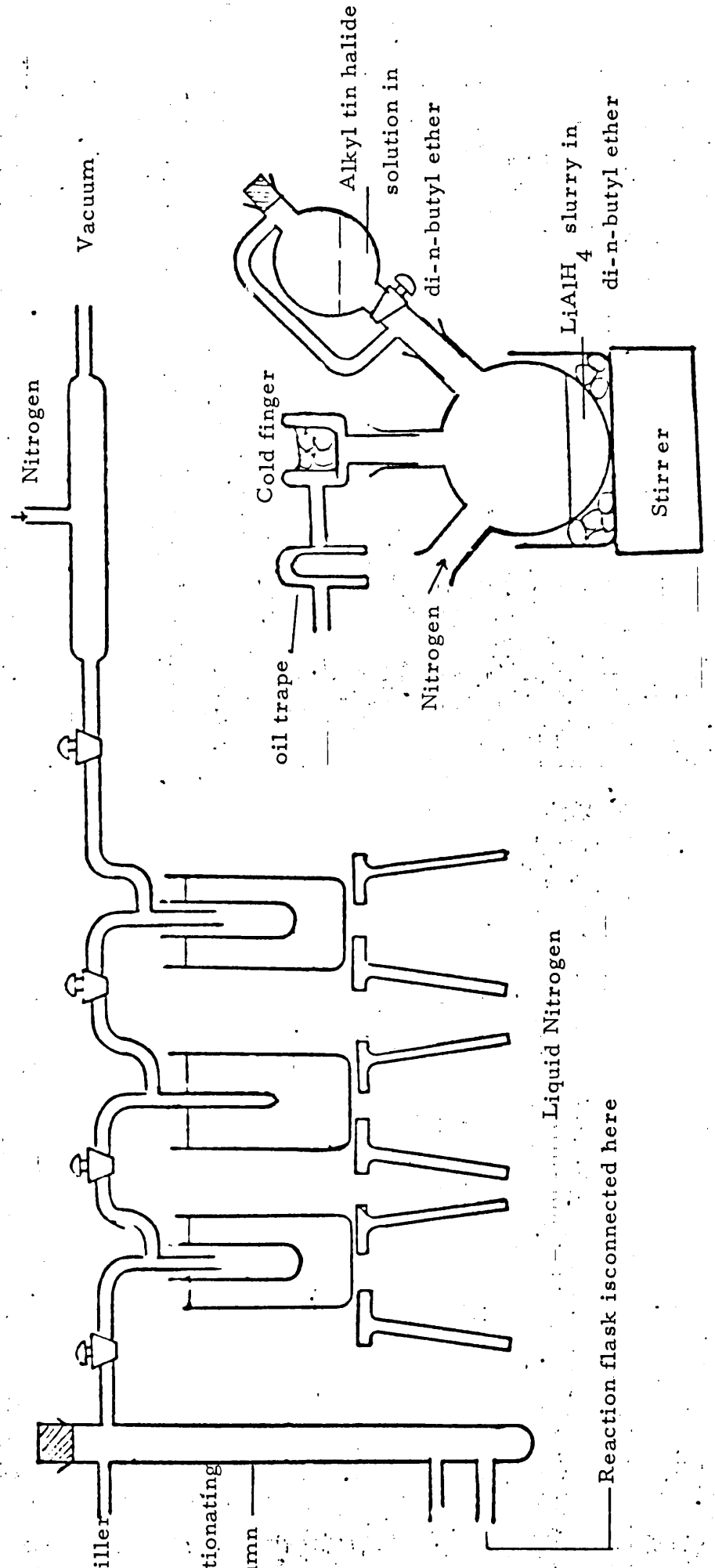

Fig.II.IV. General features of the apparatus used to prepare methyl stannanes.

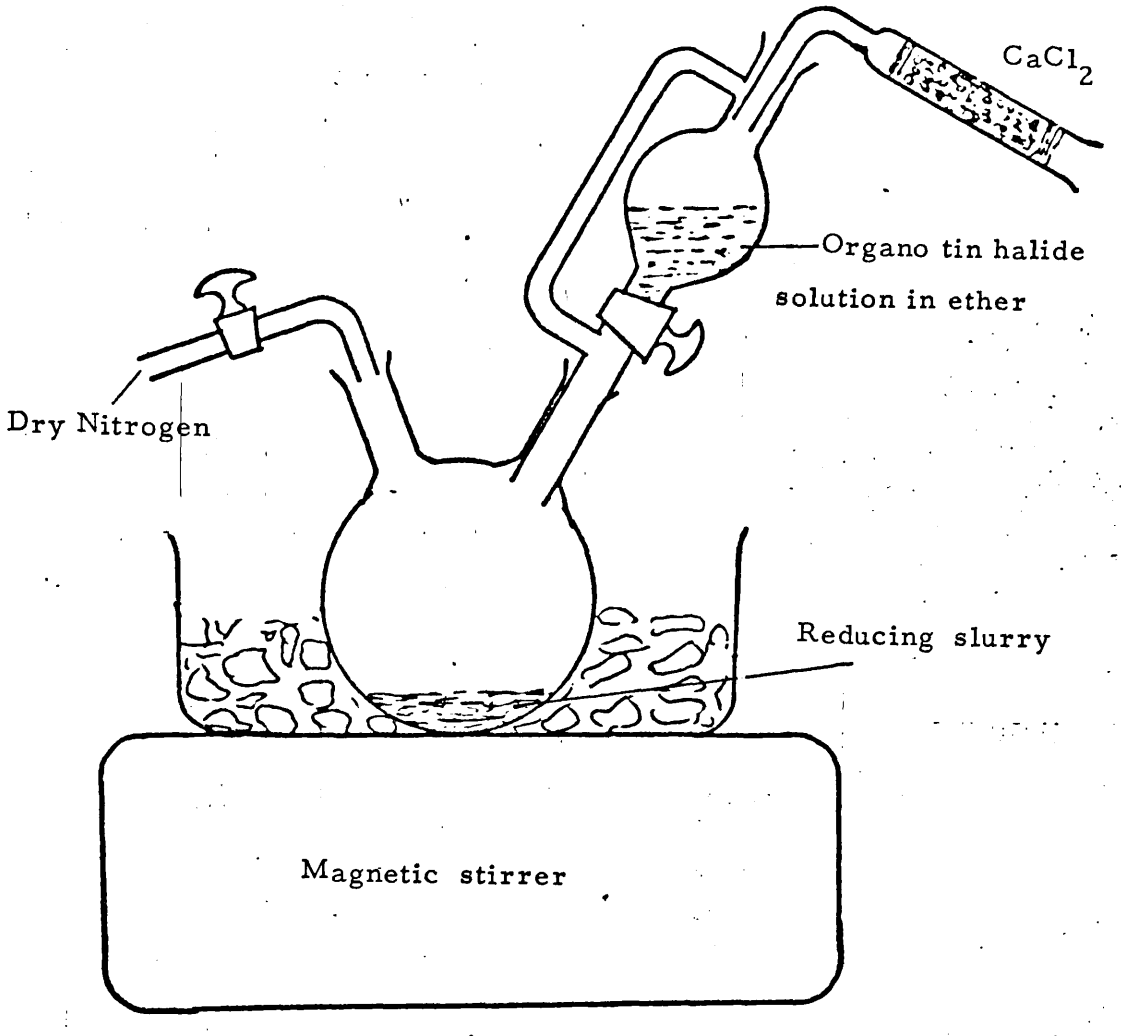

Fig. II. V. The apparatus used for the preparation of high b.pt. hydrides.

and to check the impurities, solvent in particular.

II. 1.2 Tri-phenyl Tin Hydride

$(C_6H_5)_3SnH$, was purchased from Cambrian Chemicals Limited. The hydride was used without further purification, the sample was filtered, degassed and sealed under vacuum. This hydride has a reported b.pt.of 168-172°/0.5 mm. In air it decomposes to form hexa phenyl di tin.

$$(C_6H_5)SnH \longrightarrow (C_6H_5)_3\,Sn\,Sn\,(C_6H_5)_3 + H_2$$

II. 1.3 Phenyl Tin Tri-Hydride[97]

$C_6H_5SnH_3$ was prepared by the method of Neumann and Niermann[95] as reported by Amberger et al.[5] The hydride has a reported b.pt.of 57-64°/106 mm. The reduction of an aqueous potassium hydroxide solution of phenyl tin trichloride was carried out with sodium borohydride at 0°C, with continuous stirring of the reactants. Phenyl tin hydride comes out as a heavy colourless oily liquid at the bottom of the flask, it was separated from water by a separating funnel and was washed twice with ice water. After the addition of a few drops of T.M.S., the sample was degassed, sealed under vacuum and checked for impurities in the EM-360 in the usual way.

II. 1.4 Dicyclohexyl Tin Dihydride

$(C_6H_{11})_2SnH_2$ was prepared by the same procedure as diphenyl tin dihydride. Dicyclohexyl tin dibromide was purchased from Ventron Alpha Products. In this case, the reaction

mixture was left overnight, which seemed to improve the yield. This hydride is a solid and has not been reported before. It was dissolved in benzene which also acts as an internal reference.

II.2. Methyl Stannanes[100],[101]

$MeSnH_3$, b.pt.1.4°, Me_2SnH_2, b.pt.35°, and Me_3SnH, b.pt.59°, are low boiling point hydrides and are conveniently prepared by reducing the appropriate methyl tin chloride with $LiAlH_4$ using some high b.pt.ether as solvent. The hydride is then distilled over by a vacuum line. The general method of preparation was changed slightly from the reported methods to speed the preparation.

Lithium aluminium hydride was placed in a three necked round bottomed flask, and a small volume of di-n-butyl ether (b.pt.138° - 143°C) was added to make a slurry. Dimethyl tin dichloride was dissolved in the above mentioned ether and slowly added by means of pressure equalising funnel, over a period of an hour into the reaction flask which was kept cool in an ice plus rock salt mixture (temp. ca. -10°). It was found that the reaction carried out at about -10°C, gave a better yield and proceeded faster than at the reported temperature of -78°C (cardice + acetone). The reaction was done under an atmosphere of nitrogen and a cold finger fitted to the reaction flask was used to prevent any gaseous products being swept over with the nitrogen.

The mixture was stirred constantly from the first addition until the reaction had ended. When the reaction was complete the flask was transferred to the bottom of the fractionating column containing ethylene glycol solution in water (3:2) which was kept at -13° by passing it through a chiller. A total of three traps were arranged to collect the products. The first one was at -25°, using carbon tetrachloride and liquid nitrogen slush bath. Another change of temperature was made here. In the reported method, the first trap should be at -78°C, but it took several hours to collect any significant amount of product because the rate of distillation at this temperature was so low. This change of temperature increased the chances of ether distillation with the hydride, but this problem was overcome by cooling down the reaction flask in ice at the bottom of the fractionating column. The vacuum was maintained at 1.0 mm by controlled bleeding of nitrogen into the vacuum line.

The remaining two traps were kept at liquid nitrogen temperature (-197°C). All the products were collected in the n.m.r. tube at the second trap. The tube also contained a small quantity of benzene to use as a reference.

For the preparation of partially deuterated hydride, a 1:3 ratio of the $LiAlH_4$ and $LiAlD_4$ seemed to produce a suitable amount of -HD species to obtain reasonably strong n.m.r. signals.

The sample was degassed and sealed under vacuum in the usual way. The product appeared to contain small

traces of ether, which could not be avoided when the reported procedure was followed exactly.

N.M.R. tubes containing samples were stored in the dark and at reduced temperature. Such tubes should be handled carefully as the pressure developed due to production of hydrogen can lead to an explosion.

II. 7.6 Tri-n-Butyl Tin Hydride and Tri-n-Butyl Tin Deuteride

$(n\text{-}Bu)_3SnH$ and $(n\text{-}Bu)_3SnD$ were purchased from Cambrian Chemicals Limited. No impurities were revealed by the n.m.r. spectrum and the samples were prepared in the usual way without further purification. The reported b.pt. is 76° -81°/0.7- 0.9 mm.

II. 7.7 Di-Ethyl Tin di Hydride and Tri-Ethyl Tin Hydride [98, 99]

$(C_2H_5)_2SnH$ and $(C_2H_5)_3SnH$ have reported b.pts. of $99^{\circ}C$/760 mm and $142^{\circ}C$/760 mm respectively. Both were prepared following the method of Finholt et al.[101] (the same as diphenyl tin dihydride).

Note: Diethyl stannane decomposes explosively in a stream of oxygen.

II. 7.8 Di-benzyl Tin dihydride

$(C_6H_5CH_2)_2SnH_2$ was prepared by the reaction between Lithium aluminium hydride and di-benzyl tin chloride in diethyl ether solution. The apparatus and general procedure was essentially the same as that used in the preparation of di-phenyl tin dihydride. The reaction was found to give poor yield.

Section II. 8 Sample preparation for relaxation time measurement.

The intermolecular contributions become of great importance when paramagnetic species (e.g. oxygen in this case) are present in the sample, since γ_e is 657 times larger than γ_H and can change T_1 drastically. Oxygen was removed by degassing the sample as usual. Furthermore, these molecules were studied as 10% dilute solutions in an inert solvent to minimise the intermolecular relaxation contributions. The requirement of a magnetically inert solvent merely means that it should contain neither fluorine nor proton substituents and in practice it is usual to approximate to this requirement by using a deuterated substance which has the added convenience of providing a lock signal for the spectrometer. All samples were studied in 5 m.m. O.D. N.M.R. tubes. A 180°-τ-90^{0} pulse sequence was employed for both the ^{1}H and ^{13}C measurements. The relaxation rates ($1/T_1$) are obtained from the slope of semilog plot of longitudinal magnetization (least squares fits) versus τ, the time measured from the initial 180° pulse. A considerable delay time ($\simeq 5\ T_1$) was given before the next cycle of measurements. These measurements were carried out on two different spectrometers.

II. 8.1 Varian CFT-20 spectrometer operating at 80 MHz for proton and 20 MHz for carbon (located at Varian, Walton on Thames).

II. 8.2 Brucker HX 90E spectrometer operating at 90 MHz for protons and 22.63 MHz for ^{13}C, coupled to a Nicolet 1080 computer and a Kennedy magnetic tape store (located at P.C.M.U. Harwell)

CHAPTER III

PROTON N.M.R. SPECTRA OF TIN HYDRIDES

Section III. 1 Main features of proton spectra:

III. 1. 1 Introduction

The proton N. M. R. spectra of $RnSnH_{4-n}$ and Ar_nSnH_{4-3} (where n = 1, 2, 3) have been studied. A certain amount of work has already been done in this field.[1-9] Several authors have inferred a correlation between the chemical shift and the nature of the substituent. When measurements have been reported previously, comparisons are made; the spectra of di-cyclohexyl tin dihydride and di-benzyl tin hydride are reported for the first time.

A strong signal in the proton N. M. R. spectrum of proton(s) bound to non-magnetic tin (abundance 84. 2%) is flanked by two pairs of small satellite signals which are symmetrically distributed about the central resonance, one pair due to ^{117}Sn (abundance 6. 67%, $I = \frac{1}{2}$) and the other due to ^{119}Sn (abundance 8. 68%, $I = \frac{1}{2}$). The much weaker satellites arising from the ^{115}Sn (abundance 0. 35%, $I = \frac{1}{2}$) were not readily observable.

III. 1. 2 Results

Chemical shifts and tin-proton coupling constants for protons directly bonded to tin are given in table III. 1. A typical phenyl stannane spectrum consists of a complex multiplet from the phenyl ring(s) and a single line from the hydride proton(s). This line, however, is noticeably broadened (ca. 0.6 Hz) in phenyl stannane

TABLE III.1 Proton Chemical shifts and $^1J(Sn\text{-}H)$ coupling in some alkyl- and aryl stannanes

Compounds	δ (Sn-H) p.p.m.	$J(^{119}Sn\text{-}H) \pm 1Hz$	$J(^{117}Sn\text{-}H) \pm 1Hz$	Conditions	Reference/Footnote
SnH_4	3.89	1933	1842	under pressure in CCl_4 at ca -20°	3
	3.85	1931	1846	-50°C (C_5H_{10})	9
CH_3SnH_3	4.15	1853	1770	10% benzene + T.M.S.	This work ξ
	4.14	1852	1770	C_5H_{12}	4
$(CH_3)_2SnH_2$	4.41	1796	1717	10% benzene 25°C	This work ξ
	4.45	1797	1717	C_5H_{12}	9
$(CH_3)_3SnH$	4.68	1744	1664	10% benzene	This work ξ
	4.73	1744	1664	C_5H_{12}	
	4.61	1755	1677	?	9
$(C_2H_5)_3SnH$	5.12	1612	1540	10% benzene 27°C	This work †
	5.00	1611	1540	C_5H_{10}	9
$(n\text{-}C_3H_7)_3SnH$	4.52	1607	1537	10% benzene	This work †
	4.79	1605	1533	neat	9
$(n\text{-}C_4H_9)_3SnH$	4.76	1612	1539	10% benzene	This work †
	2.07	1722	1650	CS_2	3
	4.78	1609	1532	Not specified	9
	4.80	1609	1524	Not specified	8
$C_6H_5SnH_3$	5.08	1923	1838	10% T.M.S. -15°C	This work †
	5.02	1921	1836	Et_2O	5

Continued ...

TABLE III.1 - Continued

Compounds	δ (Sn-H) p.p.m.	J(^{119}Sn-H) ± 1Hz	J(^{117}Sn-H) ± 1Hz	Conditions	Reference/Footnote
$(C_6H_5)_2SnH_2$	6.10	1928	1843	10% T.M.S. 27°C	This work #
	6.02	1927.8	1842	Et_2O	5
$(C_6H_5)_3SnH$	6.83	1934	1850	10% T.M.S.	This work #
	6.84	1935.8	1850.8	Et_2O	5
$(C_6H_{11})_2SnH_2$	4.86	1592	1521	Conc. solution in benzene	This work ξ *
$(C_6H_5CH_2)SnH_2$	5.21	1796 ± 2	1720 ± 2	10% T.M.S.	This work ξ *

* reported for the first time.

measured from 10Hz scan.

ξ measured from 20Hz scan.

† measured from 50Hz scan.

and this could arise from unresolved splittings from the phenyl protons. As can be seen from Table III. 1 the chemical shift of the hydride proton(s) moves downfield by about 0.8 p.p.m. with the substitution of each phenyl ring in the molecule. Indeed in the case of the tri-phenyl tin hydride the hydride proton appears only just clear from the phenyl feature. Some samples of di-phenyl tin dihydride were studied with a small amount of di-ethyl ether in them (ca. 10%), but this did not affect the chemical shifts and coupling constants.

In methyl stannanes the hydride feature is a multiplet due to spin-spin coupling with the methyl protons. The shift lies between 4 and 5 p.p.m. and with increasing methyl substitution a downfield shift of ca. 0.3 p.p.m. is observed. The hydride ^{119}Sn and ^{117}Sn satellites are well separated but the methyl satellites overlap. In the preparation of these samples di-n-butyl ether was used as a solvent and it was found to be present (ca. 3%) in a few samples as an impurity. The proton n.m.r. parameters observed, however, showed no dependence on these levels of ether contamination.

Heteronuclear double resonance studies on the methyl satellites are clearly more favourable on sensitivity grounds than those on the hydride satellites. However, they are less favourable on account of overlapping ^{117}Sn and ^{119}Sn features. Figure III. I, shows the spectra where one component of a satellite triplet has been

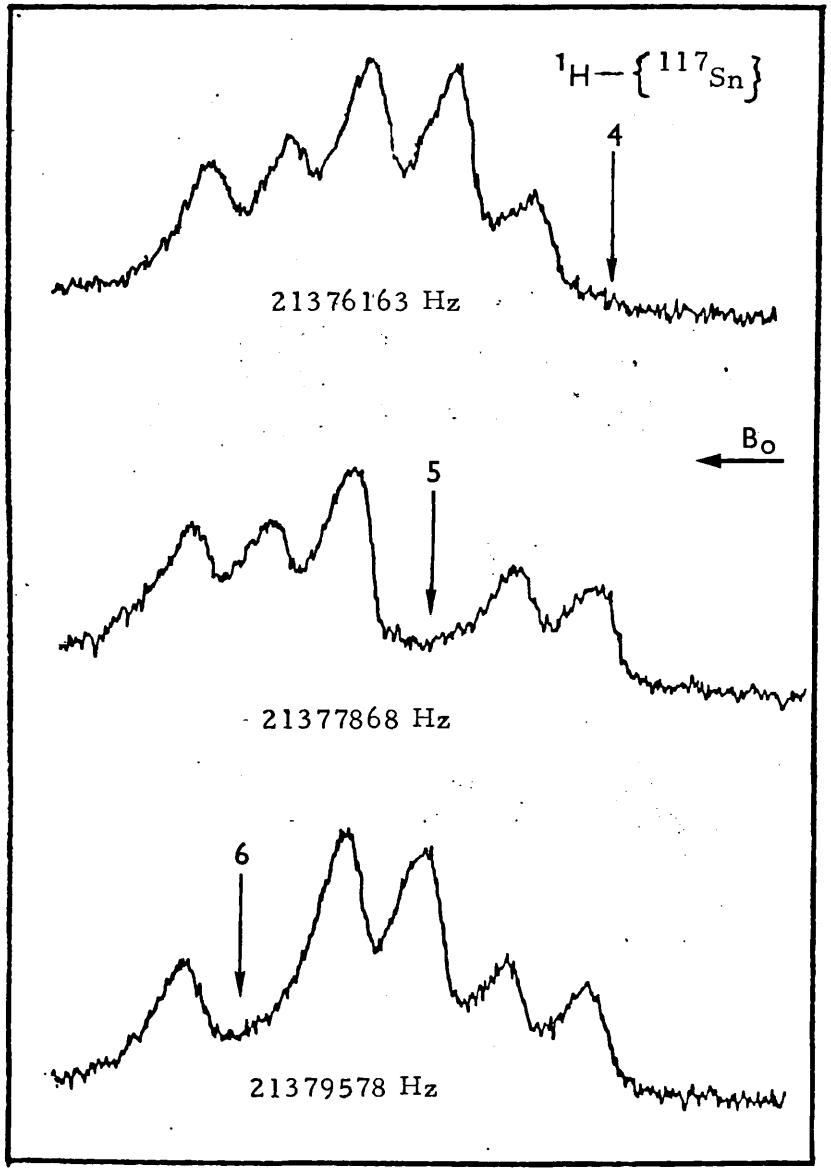

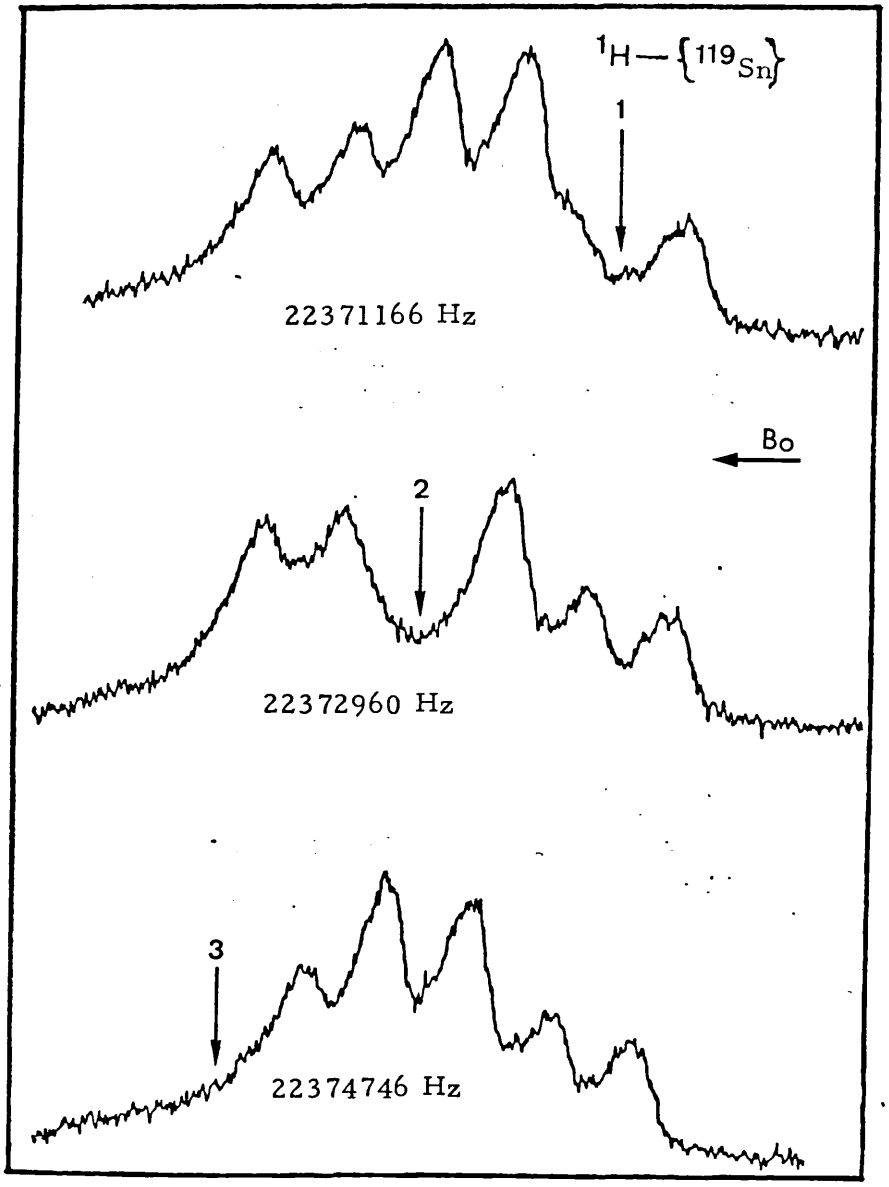

Fig. III. I. $^{1}H-\{Sn\}$ double resonance spectra of the ^{117}Sn and ^{119}Sn methyl satellites at highfield.

"removed" by decoupling. The results of these experiments are shown in Table III.2. They confirm that $^{1}J(Sn-H)$ and $^{3}J(H-H)$ are indeed opposite in sign. The experiment was not pursued; all the other double resonance experiments were observed at the hydride satellites. Other experiments involving simultaneous decoupling of one tin nucleus whilst performing more selective double resonance experiments on the other have been carried out on tetra-ethyl tin but it is a fact that although the experiments are feasible, in practical cases it is more convenient overall to observe the hydride satellites.

TABLE III.2

High field ^{1}H lines	Associated ^{119}Sn frequencies ± 10 Hz	Associated ^{117}Sn frequencies ± 10 Hz
1	(1166	-
2	22,37 (2960	-
3	(4746	-
4		(6163
5		(7868
6		21,37 (9578

Values of two bond $^{2}J(^{119}Sn-CH_3)$, $^{2}J(^{117}Sn-CH_3)$ and three bond $^{3}J(HCSnH)$ spin spin coupling constants have also been determined and are presented in Table III.3, and for the purpose of comparison reported[4] values are also included in the table (in brackets)

TABLE III.3

Compounds	$^{3}J(HCSnH)$ Hz	$^{2}J(^{119}Sn\text{-}CH_3)$	$J(CH_3\text{-}^{119}Sn) \pm 0.5$	Conditions/Footnote	Reference
CH_3SnH_3	2.72 ±0.02Hz	60 ≠	60 ≠	10% benzene, 10°C	This work
	(2.70)			*	4
$(CH_3)_2SnH$	2.65 ± 0.02Hz	60.3 ±0.5Hz	58.0	10% benzene, 27°C	This work
	(2.55)	(58.0)	(55.5)	*	4
$(CH_3)_3SnH$	2.34 ± 0.02Hz	59.2 ± 0.5Hz	56.3 ± 0.05	10% benzene, 27°C	This work
	(2.37)	(56.5)	(54.5)	*	4
$(C_6H_5CH_2)_2SnH_2$	1.85 ± 0.02	65 ≠	65 ≠	10% T.M.S. 25°C	This work

≠ represents an average value

* observed at 40°C as 9% solution in neopentane

These values shown for the two bond couplings are in good agreement considering that changes in solvent may affect these values by up to 0.5% [9] and also that they may be temperature dependent.

The three bond coupling values probably agree within experimental error, the present values are thought to be accurate to $\pm$ 0.02 Hz having been measured from spectra expanded to 10 or 20 Hz over 50 cm.

Section III.2 Deuterated species

III.2.1 Deuterated di-methyl tin di-hydride

The compounds present in the n.m.r. tube were

1) $Me_2Sn H_2$

2) Me_2SnHD

and 3) Me_2SnD_2

Let us now consider each compound and its effect on the n.m.r. spectra. The main features of the first species is that of an A_2X_6 system and consists of as expected a simple septet, components with binomial distribution 1: 6:15:20:15:6:1, for the two hydride protons coupled to six equivalent methyl protons, chemically shifted 4.41 p.p.m. from T.M.S. The methyl peak is split by the two equivalent hydrides producing three lines in the intensity ratio 1:2:1 at 0.20 p.p.m.

The proton hydride spectrum of Me_2SnHD in the presence of Me_2SnH_2 is shown in Fig. III.II. The signal is a septet due to coupling with the methyl protons and the further splitting arises

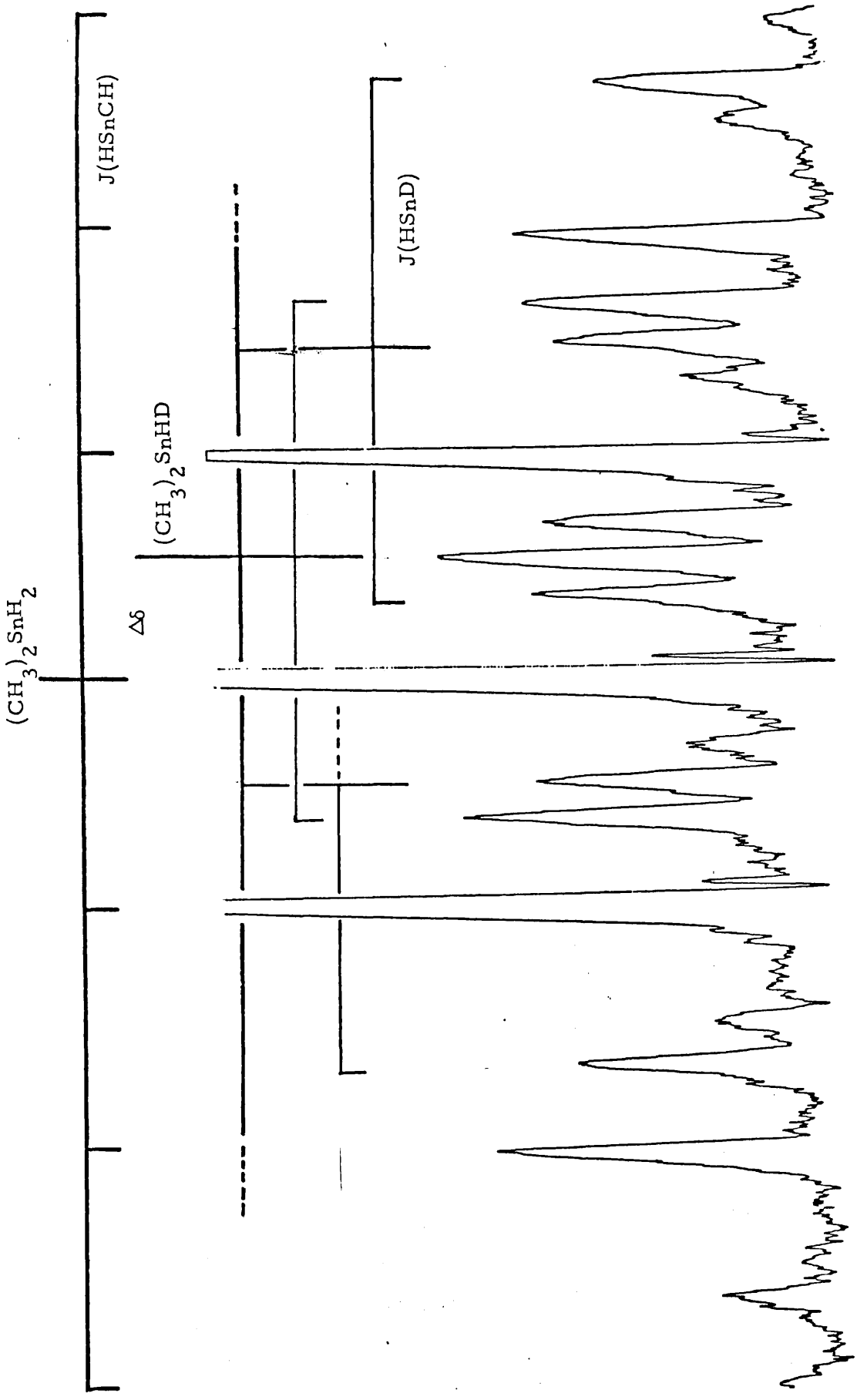

Fig. III. II. Proton spectrum of di-methyl tin hydride and its deuterated species

(central feature)

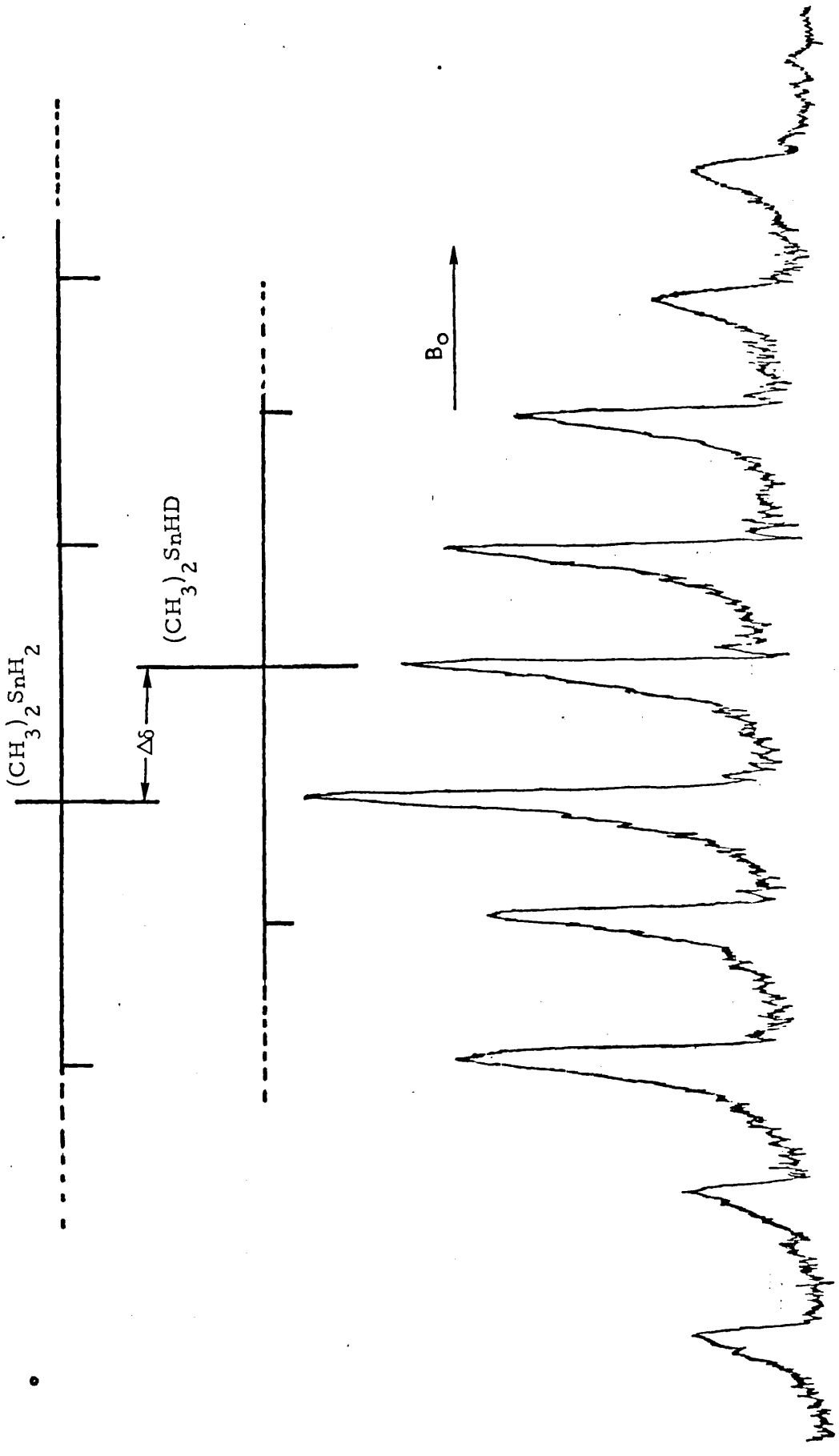

Fig. III. III. Proton spectrum of the central feature of di-methyl tin hydride and its deuterated species

(deuterium decoupled)

from coupling to the deuterium (I = 1) nucleus. The spacings of the lines which are equal correspond experimentally to $^2J(HD)$ are simply related[10] to that between two protons in equivalent positions J(HH) by a factor consisting of the ratio of gyromagnetic constants of deuteron and protons, $^2J(HH)$ was calculated from the measured values of $^2J(HD)$ by taking

$$J(HH) = J(HD) \times 6.513$$

the results are reported in Table III.4. (see page 80).

^1H-$\{^2H\}$ heteronuclear double resonance was performed by irradiation at 9211875 Hz in order to decouple ^2H from the spin system. This resulted in the collapse of the triplets as shown in Figure III.III. The spacings and intensities of this deuterium decoupled septet are symmetrical about the mid point of the band which corresponds to the origin of the multiplet produced by two equivalent methyl groups. The hydride resonance is shifted 0.0236 ± 0.002 p.p.m. upfield from that of the undeuterated hydride.

Figure III. V shows the methyl region of the spectrum and Figure III. VI, with deuterium decoupling. The non-decoupled spectrum consists of a 1:2:1 triplet for $(CH_3)_2SnH_2$ caused by a coupling of 2.65 ± 0.02 Hz to the two hydride protons; a doublet of 1:1:1 triplets for $(CH_3)_2SnHD$ caused by a coupling of 2.65 ± 0.02 Hz to the hydride proton and 0.42 ± 0.01 Hz to the deuterium; a 1:2:3:2:1 quintet for $(CH_3)_2SnD_2$ caused by a coupling of 0.42 ± 0.01 Hz to the two deuterons. The three bond isotope shifts from $(CH_3)_2SnH_2$ are 0.0046 p.p.m. and 0.009 p.p.m. for $(CH_3)_2SnD_2$ respectively.

Satellite spectra (see Fig. III. XI (a, b) and III. X (a, b)) were carefully examined and compared with the central feature to study the isotope effect on coupling constant; the data are presented in Table V.1. It was found that the peaks from the deuterated species are not at the same relative position as they are in the central feature. Rather they appear to be displaced towards the central hydride feature. in both satellites. To simplify the spectra deuterium decoupling was employed as shown in Figure III. XII and it was found that the coupling constant $^1J(Sn\text{-}H)$ in Me_2SnHD was 0.6Hz smaller than that in Me_2SnH_2, as a result of a geminal deuterium isotope effect.

INDOR:

Figure III. VII illustrates the ^{119}Sn INDOR spectrum of Me_2SnD_2 in the presence of Me_2SnHD and Me_2SnH_2 in the same tube. The spectrum was obtained by monitoring the high field methyl satellite, and sweeping through the ^{119}Sn spectrum. The trace obtained is similar to the ^{119}Sn spectrum of Me_2SnD_2 recorded by the pulse

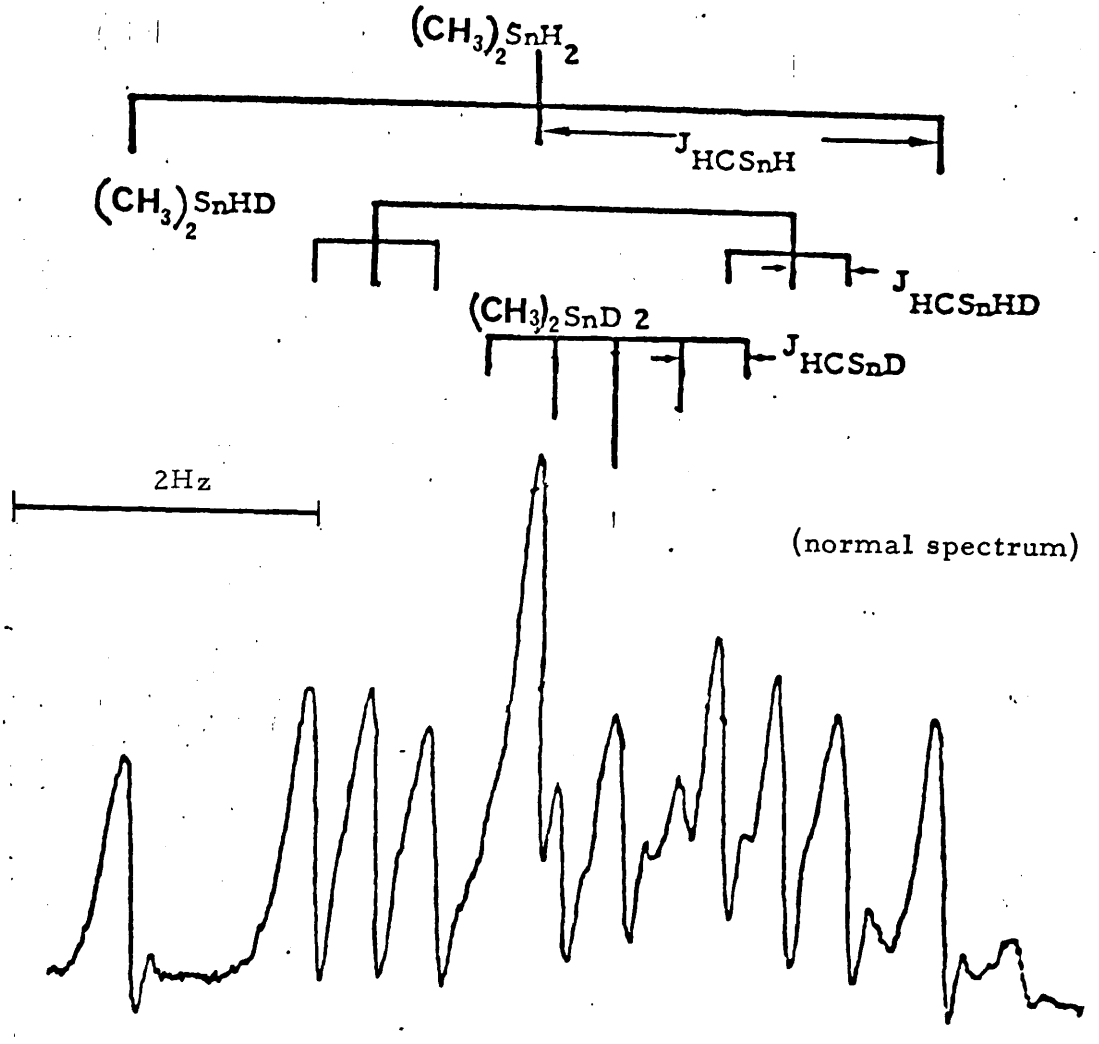

Fig. III. V. The proton spectrum at 60 MHz of molecules: $(CH_3)_2SnH_2$ $(CH_3)_2SnHD$, and $(CH_3)_2SnD_2$ (methyl region).

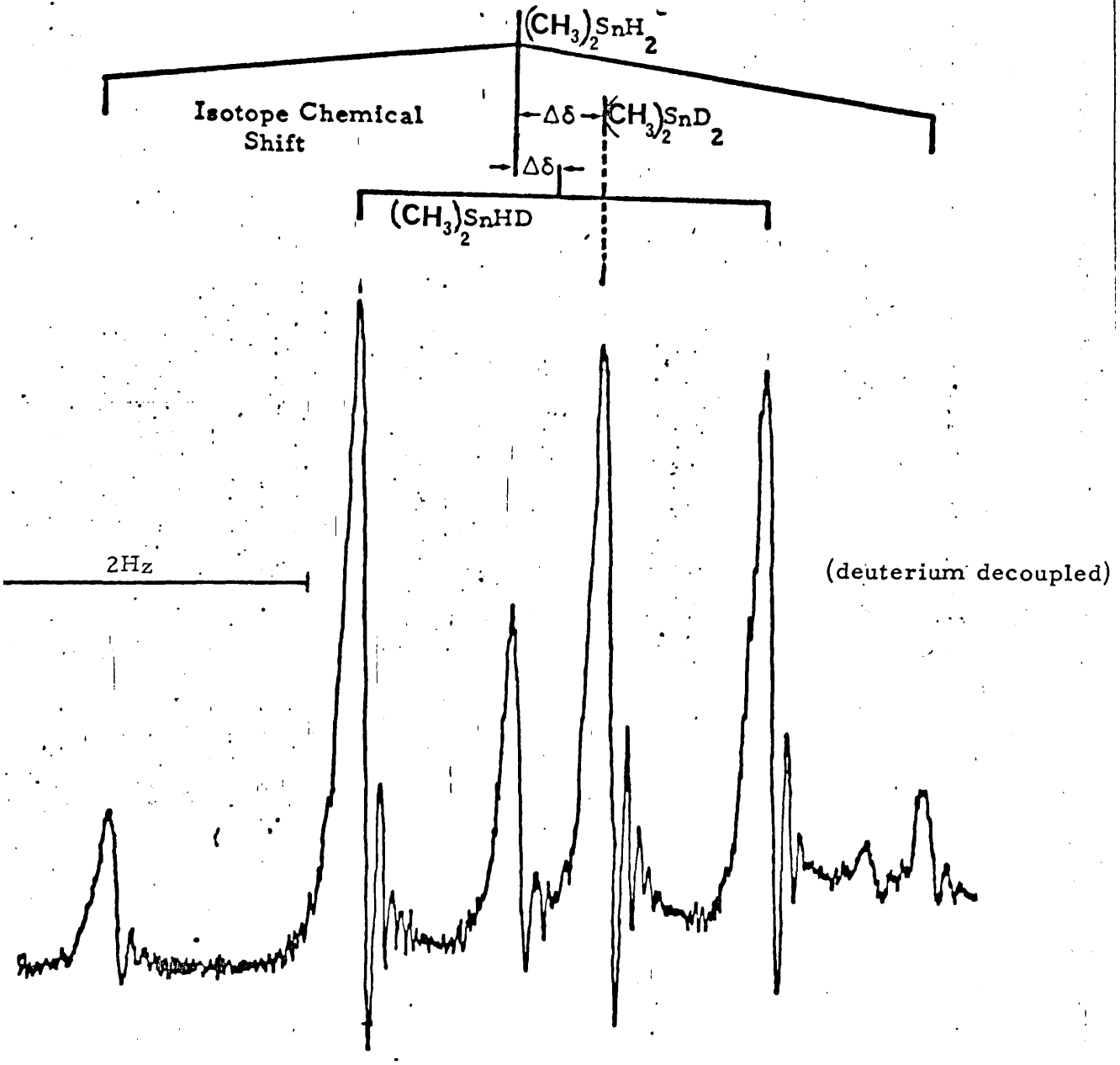

Fig. III. VI. Deuterium decoupled proton spectrum (methyl region) of $(CH)_3SnH2$, $(CH_3)SnHD$ and $(CH_3)_2SnD_2$.

Fig. III. XI. High field ^{119}Sn satellite spectra of deuterated di-methyl tin hydride in the presence of undeuterated parent hydride.

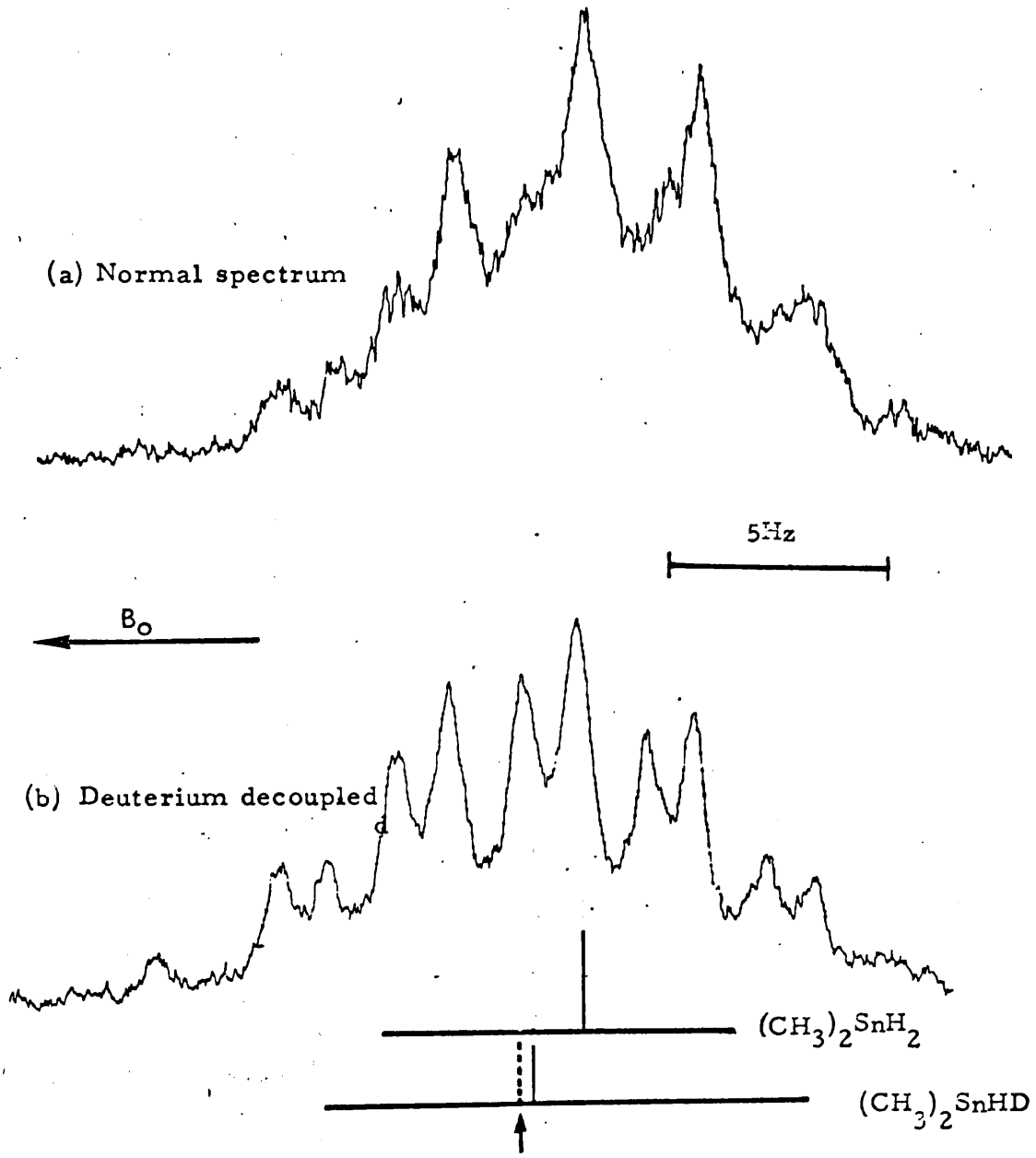

The arrow marks the position of the centre of the centre of the septet (of triplets) if there were no isotopic effect on the coupling constant.

Fig. III. XII. Low field ^{119}Sn satellite spectra of deuterated di-methyl tin hydride in the presence of undeuterated parent hydride.

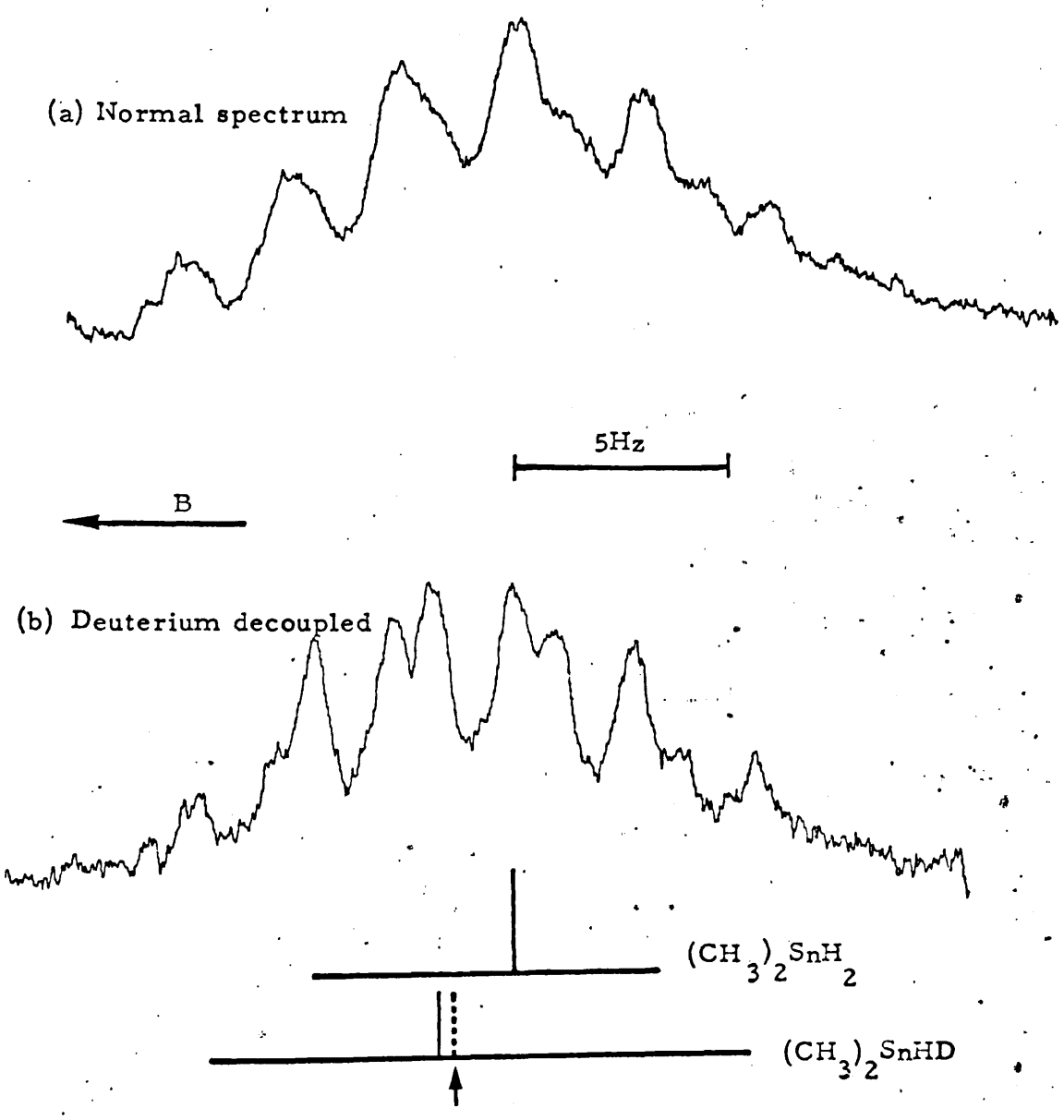

The arrow marks the position of the centre of the septet (of triplets) if there were no isotopic effect on the coupling constant.

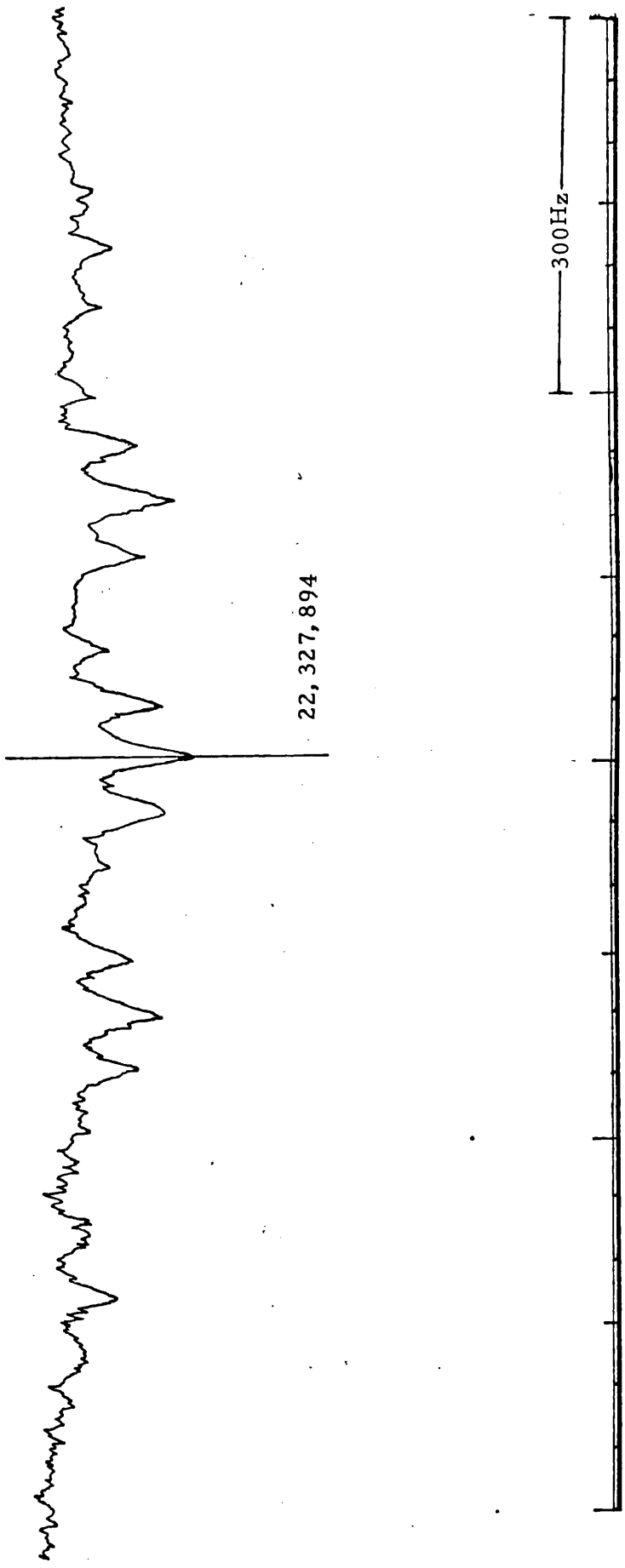

Fig. III. VII. ^{119} SnINDOR spectrum of $(CH_3)_2SnD_2$ observing upfield methyl satellite

method (see IV.4.3). The spectrum can be interpretted as a quintet of septets. Twenty of the expected thirty five lines are observed, the rest being covered by noise. The corresponding coupling constants were measured (see table III.5) and compared with the values obtained from the proton and F.T. spectra and they are in good agreement within the experimental errors.

TABLE III.5

Coupling constants	INDOR	F.T. spectra	Proton spectra
$J(^{119}Sn - D)$	274.5 ± 1 Hz	274.4 ± 1	-
$J(^{119}Sn - CH_3)$	59.0 ± 1 Hz	61 ± 1	60 ± 1 Hz

The centre of the multiplet was located at 22.372894 MHz. This value was compared with the ^{119}Sn resonance frequency obtained from the high field methyl satellite of Me_2SnH_2 for reference see Table III.2. The difference between the two frequencies gives the deuterium isotope effect on the tin resonance frequency due to the introduction of two deuterium atoms on tin. The value of the isotope shift obtained by this method (Me_2SnD_2 ca. 3 p.p.m. to high field) is in good agreement with the value obtained by the direct method.

III.2.2 Deuterated di-phenyl tin di-hydride

Figure III.VIII (a) shows the proton spectrum of the central hydride feature of a sample containing a mixture of $(C_6H_5)_2SnH_2$, $(C_6H_5)_2SnHD$ and $(C_6H_5)_2SnD_2$. The corresponding chemical shifts and coupling constants are listed in Table III.1.

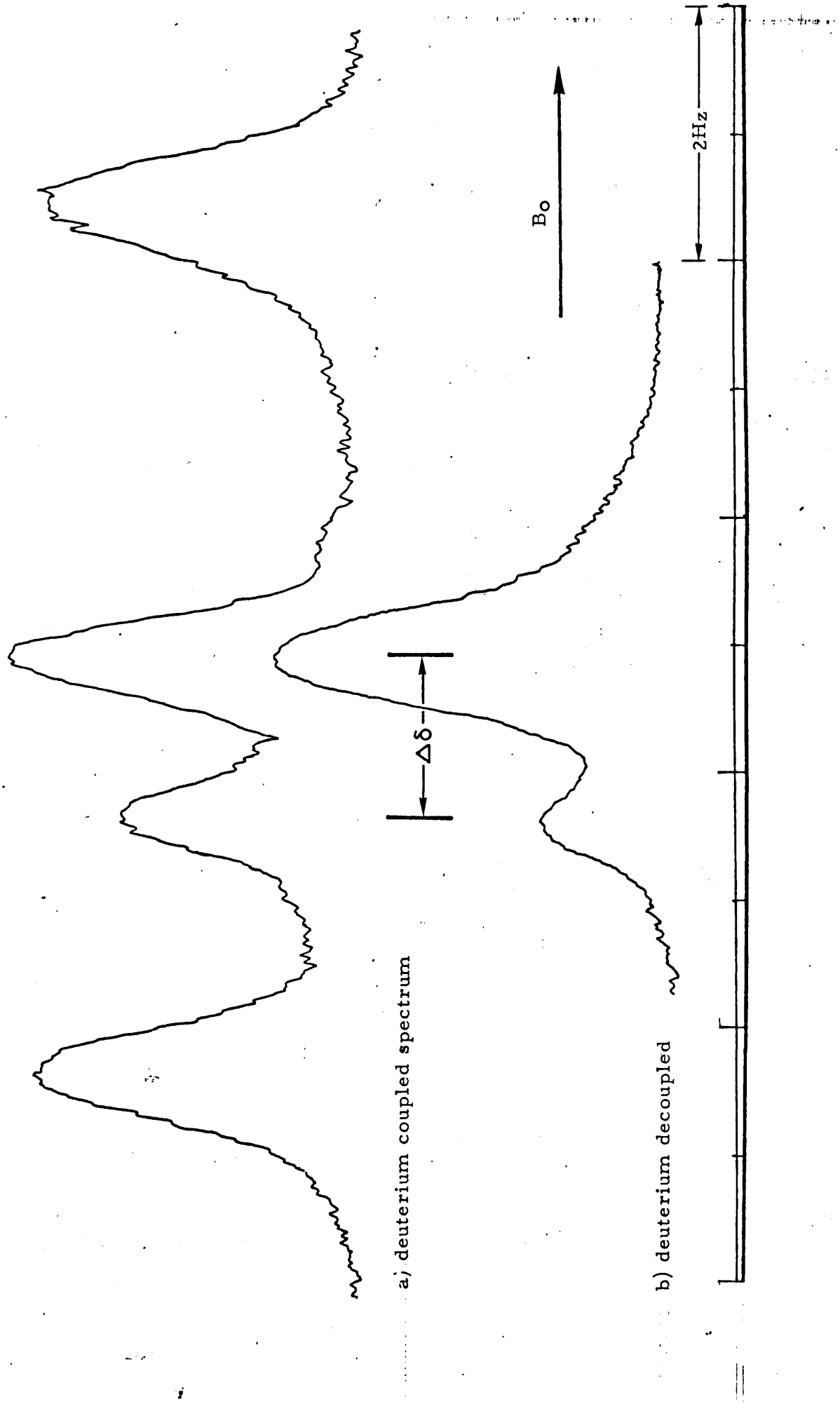

Fig. III. VIII. Proton spectrum of deuterated diphenyl tin hydride with trace of undeuterated material.

The proton magnetic resonance spectra of the monosubstituted material consists of a deuterium coupled 1:1:1 triplet shifted 0.021 p.p.m. upfield from the single peak corresponding to the parent compound. The HD coupling constant is presented in Table III.4. The di-deuterated compound would have no peaks in this region of the spectrum.

Deuterium decoupling experiments were performed and the optimum frequencies (Table III.6) were determined (± 1 Hz) for both the central and satellite features. Figure III.VIII (b) illustrates the ^{2}H decoupled spectrum of the central feature.

TABLE III.6

Feature	Optimum frequency ± 1 Hz.	Distance from the centre (Hz)
Upfield ^{119}Sn	9,211,810	-146
" ^{117}Sn	9,211,815	-141
Central	9,211,956	0
Low field ^{117}Sn	9,212,097	+ 141
" " ^{119}Sn	9,212,105	+ 149

These values confirm of course that Sn-H and Sn-D couplings have the same sign. The values indicated for $^{1}J(^{119}Sn\text{-}D)$ 295 Hz and $^{1}J\ (^{117}Sn\text{-}D)$, 282 Hz agree within experimental error with values of 296 Hz and 283 Hz respectively calculated from Sn-H values by taking $\gamma H/\gamma D = 6.513$. Measurements on satellite spectra showed a decrease of 0.65 ± 0.06 Hz in the ^{1}J (Sn-H) value on deuterium substitution. These isotope effects will be discussed in Section III.3.2.

III. 2. 3 Deuterated mono-phenyl tin tri-hydride

The 'H spectra of the stannane and three of its deuterated species i.e. $C_6H_5SnH_3$, $C_6H_5SnH_2D$, $C_6H_5SnHD_2$ and $C_6H_5SnD_3$ all present together as a mixture were recorded on a Varian Associates HA100 spectrometer on a 50 Hz scan at -15°C. Figure III. IX(a), exhibits clearly the singlet of the parent molecule, the 1:1:1 deuterium coupled triplet of the mono-substituted compound and the 1:2:3:2:1 deuterium-coupled multiplet of $C_6H_5SnHD_2$ superimposed upon the triplet. The spacings of these multiplets correspond to $^2J(H\,D)$' Table III. 4 and give the geminal H, D coupling constants. The difference between the singlet and the centre of triplet gives the isotope shift due to the introduction of one deuterium on tin. $(21.2 \pm 1.6) \times 10^{-3}$ p.p.m. Similarly, the isotope shift due to the introduction of two deuterons on tin can be obtained by measuring the frequency difference between the singlet and the origin of the quintet $(42.5 \pm 1.7) \times 10^{-3}$ p.p.m. The satellite lines appear on either side of a central peak. However, closer inspection and comparison with the central feature again reveals that the satellites are not identical in appearance to each other nor to the central feature. In the central feature, the triplet and quintet lines are distinctly separated from the singlet but in the satellites they are seen to overlap. Further comparison of the low and high field satellites (see Fig. III. IX(b)) indicates that the outer component of the low field satellites (triplet from species $C_6H_5SnH_2D$) has moved just underneath the hydride singlet, causing the increased intensity. While in the

Fig. III. IX. 100 MHz spectrum of mono-phenyl tin hydride and its deuterated species, showing main features of the spectrum.

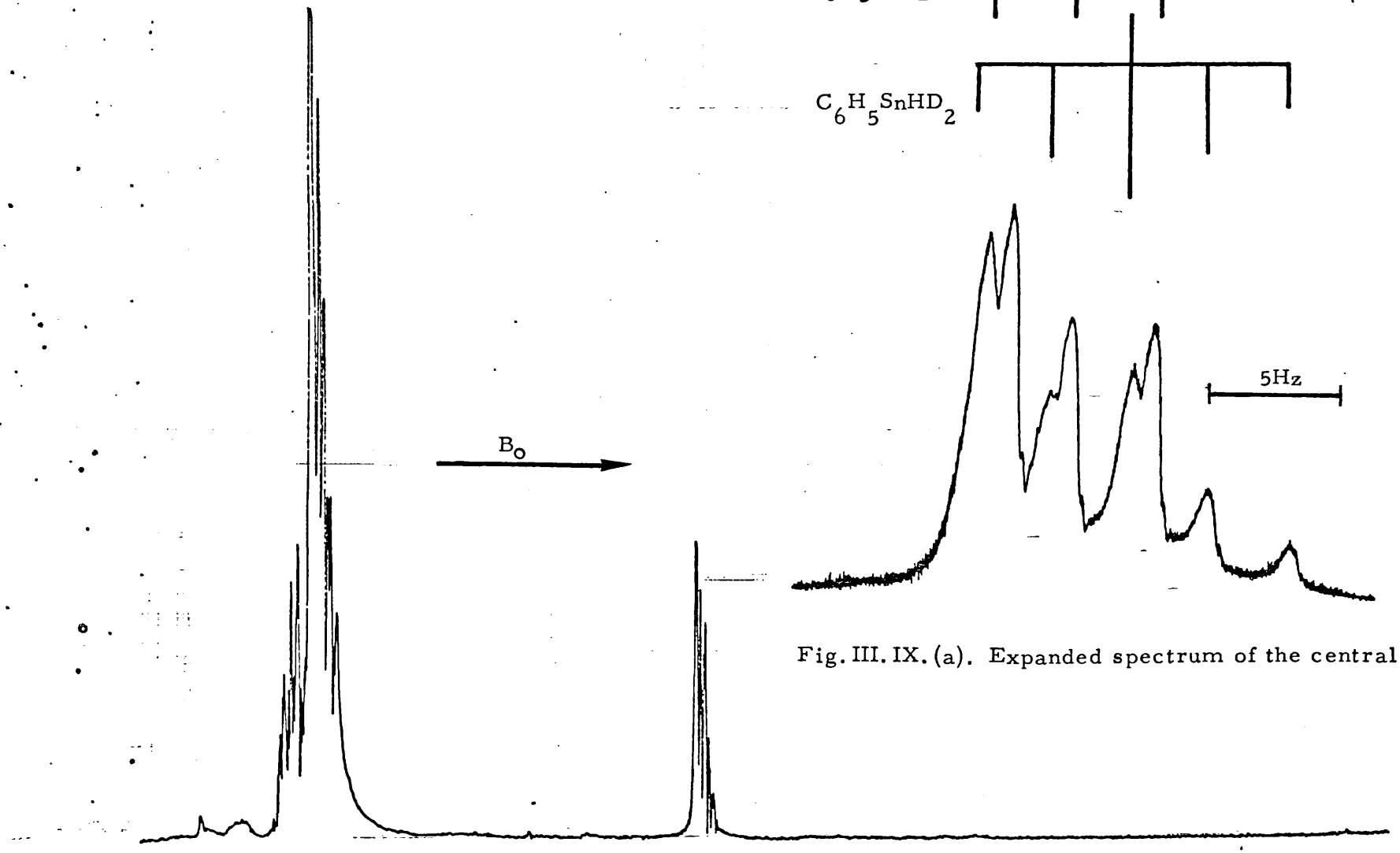

Fig. III. IX. (a). Expanded spectrum of the central feature.

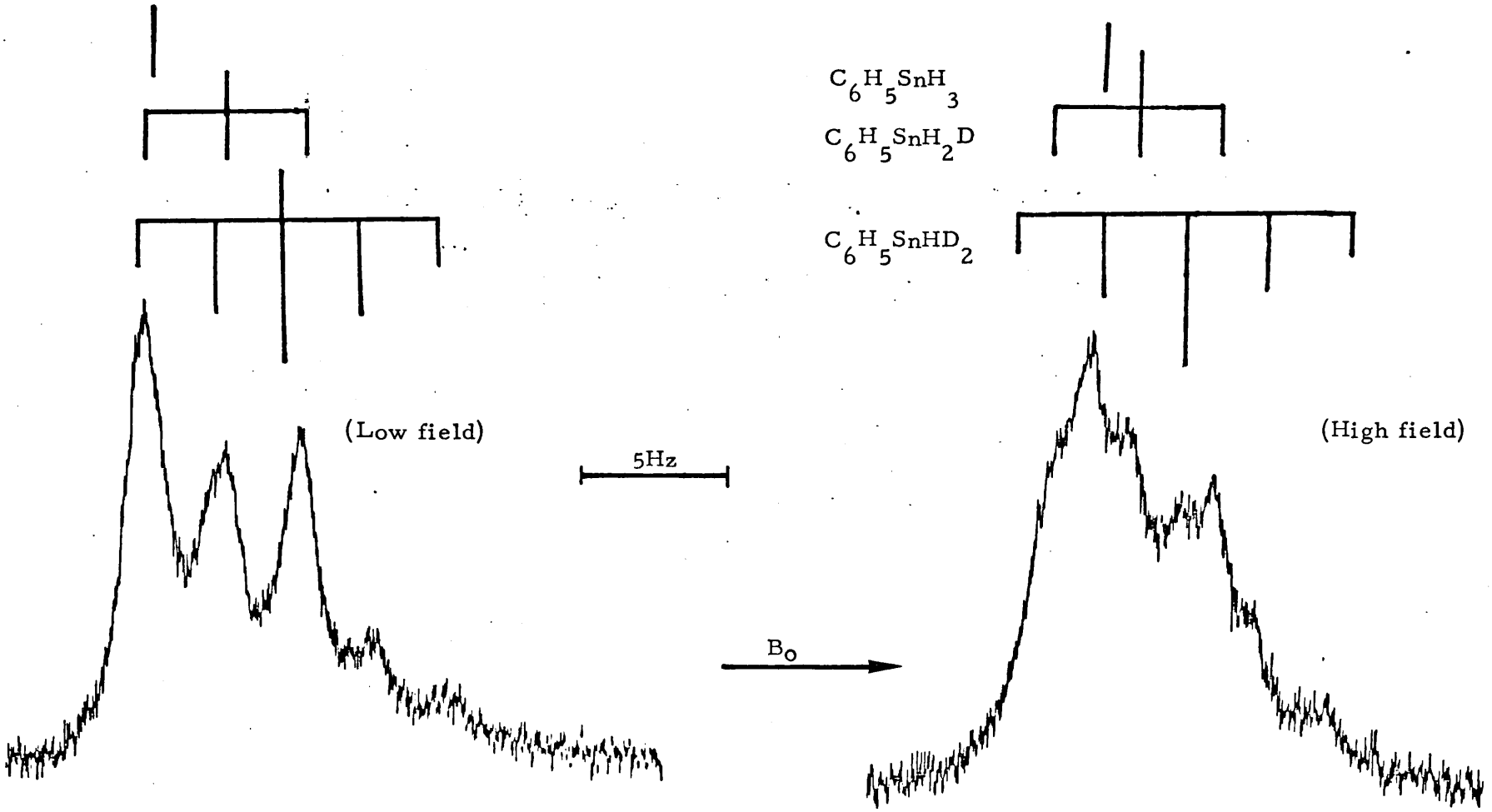

Fig. III. IX. (b) Expanded 100 MHz ^{119}Sn low and high field satellite spectra of mono-phenyl tin hydride and its deuterated species showing isotope effect on the coupling constant.

case of the upfield satellites, the presence of a shoulder on the low field side of the hydride singlet showed on measurement that the centre of the triplet had shifted slightly downfield as compared to its position in the central feature. The features are caused by an isotopic effect on the coupling constant. There is no observable isotopic shift on ^1H as a result of substitution of ^{119}Sn (or ^{117}Sn) for non magnetic tin species.

In the central feature the triplet and the quintet (from $C_6H_5SnD_2H$ species) are observed to be separated but in the satellites they are seen to overlap. On measurement a decrease of 0.65 ± 0.06 Hz and 1.30 ± 0.05 Hz was found in the $^1J(Sn-H)$ coupling constants of $C_6H_5SnH_2D$ and $C_6H_5SnHD_2$ species respectively (the effect is additive for the second deuterium).

III.2.4 Deuterated di-benzyl tin di-hydride

The proton n.m.r. spectrum of the hydride region of a $(C_6H_5CH_2)_2SnH_2$, $(C_6H_5CH_2)_2SnHD$ and $(C_6H_5CH_2)_2SnD_2$ mixture is shown in Fig. III.X(a). On the HA60 spectrometer, the H_2, and HD features could not be seen separately as was observed in other cases. Examination of the overlapping multiplets showed some additional lines in the high field side when compared with the spectrum of the undeuterated compound (Fig. III.X(b) and the lines were also found to be broader than in the parent compound. From this observation it became obvious that the value of the isotope shift at 60 MHz

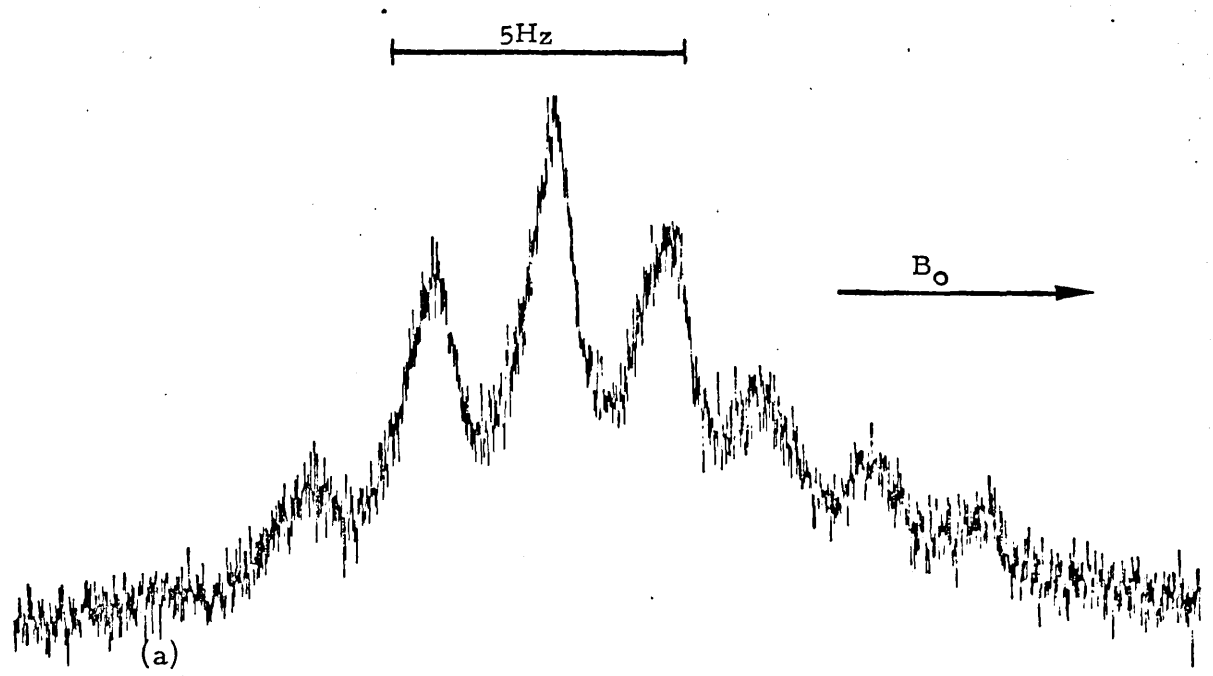

Fig. III. X. 60 MHz proton spectrum of di-benzyl tin hydride and its deuterated species (central feature).

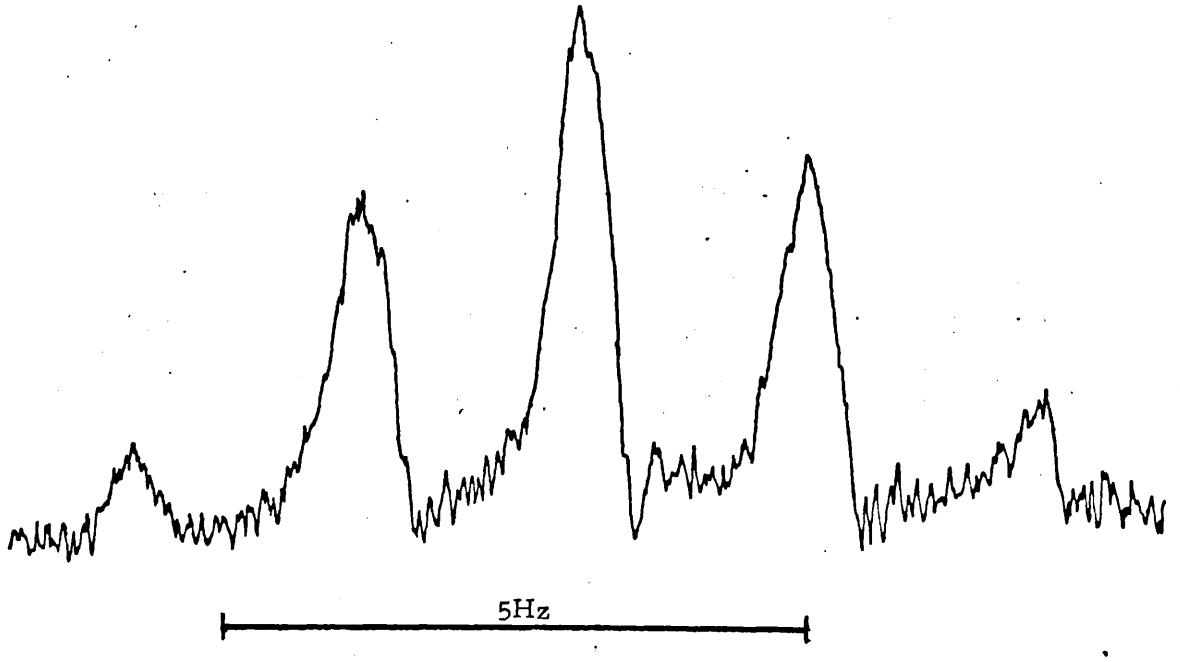

Fig. III. X.(b) The protn spectrum of di-benzyl tin hydrides showing the central feature.

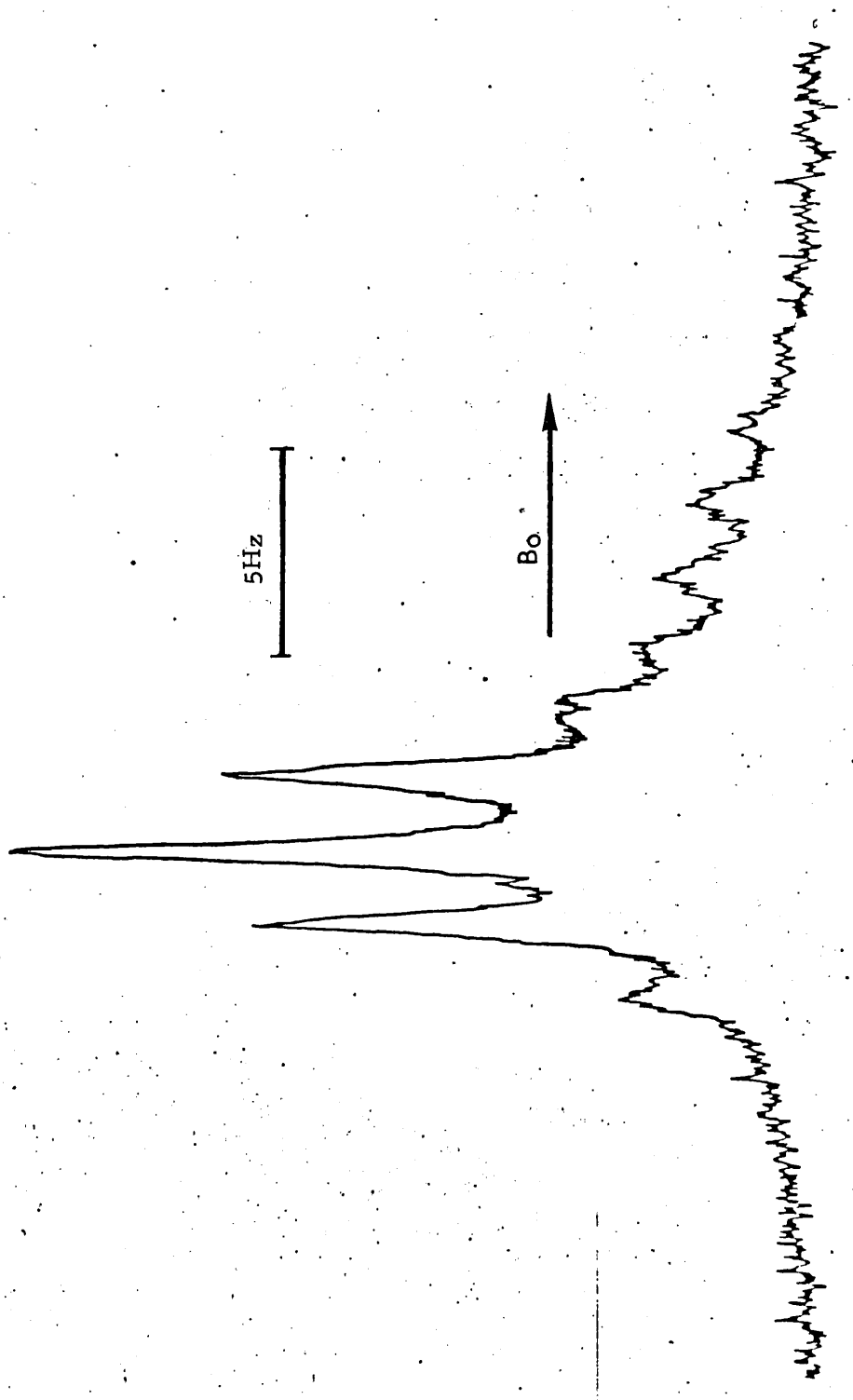

Fig. III. XI. 220 MHz spectrum of di-benzyl tin hydride and its deuterated species showing the central feature.

is approximately equal to the methine and hydride proton spin spin coupling. This central hydride feature was then recorded at 220 MHz and Figure III. XIII shows an excellent example where measurements can be done accurately for a 220 MHz spectrum but not for that obtained at 60 MHz. The hydride spectrum of $(C_6H_5CH_2)_2SnHD$ can now be seen as a separate multiplet moved upfield. The isotope shift measured at 220 MHz was found to be 6.65 Hz. This corresponds to 1.81 Hz at 60 MHz which being close to the value of 1.85 Hz found for $^3J(HC-Sn-H)$ confirms the accidental overlap in the 60 MHz spectra.

Comparison of the line widths of both multiplets shows that the components of the quintet from the deuterated sample are broader than the hydride quintet. which presumably arises from overlapping of triplet components arising from $^2J(HD)$ spin spin coupling and from broadening due to the quadrupole moment of the deuteron. Low and high field satellite spectra were obtained at 220 MHz but on account of the low S/N ratio, small changes in the coupling due to isotopic substitution could not be measured. The methine satellites were not studied thoroughly on account of their low intensity. The separation between the two sets of satellites was found to be roughly 65Hz (Table III. 3).

TABLE III.4

Spin spin coupling constants in some partially deuterated stannanes

Compound	^2J H-Sn-D (Hz)	$^2J^*$ H-Sn-H (Hz)	^3J D-Sn-CH (Hz)	$^3J^*$ H-Sn-CH (Hz)	Conditions
Me_2SnHD	3.10 ± 0.05	20.18	0.42 ± 0.05	2.73	in the same mixture
Me_2SnD_2	-	-	0.42 ± 0.02	2.73	
$(C_6H_5SnHD$	3.34 ± 0.02	21.74	-	-	27°C
$C_6H_5SnH_2D$	2.75 ± 0.05	17.9	-	-	-15°C
$C_6H_5SnHD_2$	2.70 ± 0.05	17.57	-	-	-15°C
$(C_6H_2CH_2)_2SnHD$	2.0#	13.0	0.28**	1.85≠	27°C 10% T.M.S.

* value was obtained from the corresponding H-D coupling constants multiplied by the ratio of $\gamma H/\gamma D = 6.51$

≠ actual value

** calculated from ^3JH-Sn-CH

\# multiplets overlap on approximate value

Section III. 3 Discussion

Table III. 1 summarizes the chemical shifts and coupling constants of a number of organo tin hydrides. The n. m. r. parameters on phenyl stannanes are in excellent agreement with the values found by Amberger et al[5]. The δ value of 4. 76 p. p. m. in di-methyl tin dihydride reported by Flitcroft et al[4] is only in modest agreement both with the value of 4. 41 p. p. m. reported here and with the value of 4. 45 reported by Maddox et al.[9] The only wide discrepancy exists between the chemical shift of 4. 76 observed for tri-n-butyl tin hydride and a value of 2. 07 reported by Potter et al[3]. But our value is in good agreement with the value of 4. 78 published by J. C. Maire[8] and Maddox et al[9], other δ values are in good agreement with the published values, see Table III.1.

Chemical shifts of the hydride proton(s) in these hydrides lie at ca 3. 9 -7 p. p. m. on the low field side of T. M. S. The position of Sn-H proton(s) varies with the number and nature of alkyl and aryl substituent and as the stannane is successively substituted a diamagnetic shielding of the remaining proton(s) is observed. On comparing any series it is found that

$$\delta\ (HSnR_3) \nearrow (H_2SnR_2) \nearrow (H_3SnR) \nearrow (SnH_4)$$

In order to compare the effect of different substituents among the mono-, di- and tri-stannanes, the data can be conveniently represented in terms of chemical shifts measured in p. p. m. taking the SnH_4 resonance as reference. The shifts are listed in Table III. 5, and plotted against the number of substituents in Figure III. XIV.

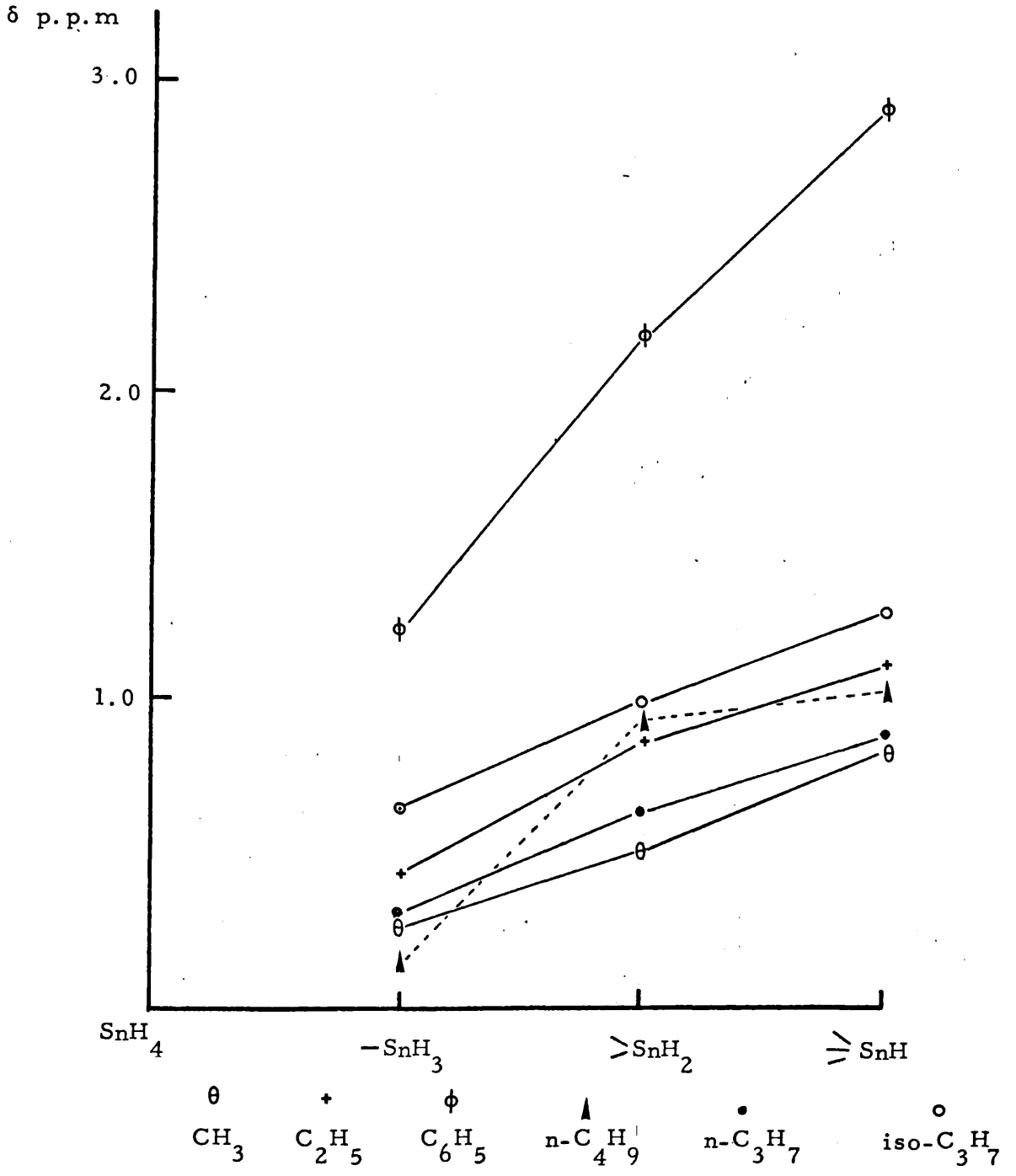

Fig. III.XIV. Aplot of the δ values of the hydride proton(s) versus number of substituents (taking SnH_4 resonance as reference).

TABLE III.5

Changes in chemical shifts of proton(s) in SnH_4 on different substituted groups

Number of tin bound proton(s)	n-C_4H_4-	CH_3-	n-C_3H_7-	C_2H_5-	iso-C_3H_7-	C_6H_5-
3	0.13	0.24	0.28	0.45	0.65	1.23
2	0.88	0.5	0.63	0.86	1.04	2.21
1	0.87	0.81	0.9	1.11	1.29	2.95

(All values are positive and in p.p.m.)

From these values an effective shielding constant for a substituted group can be calculated with the formula given by Shoolery[72]

$$\delta = \delta SnH_4 - \sum_i \delta_{i\ eff}$$

where $\delta_{i\ eff.}$ is the effective shielding constant of the ith group and is an average value of shifts caused by successive substitution of the group(s) on SnH_4. Table III.6 represents values for the effective shielding constants for the above mentioned substituted stannanes obtained by least squares analysis.

TABLE III.6

Substituted group	CH_3-	C_2H_5-	n-C_3H_7-	iso-C_3H_7-	n-C_4H_9	C_6H_5-
effective shielding	0.28 ± 0.02	0.33 ± 0.06	0.31 ± 0.04	0.32 ± 0.38	-	0.85 ± 0.07

It can be seen that the dependence of δ on the number of substituents is to good approximation linear for methyl, ethyl, n-propyl and phenyl stannanes. In the case of iso-propyl and n-butyl the relationship is distinctively non-linear as can be seen from the plot III.XIV. It is noteworthy that the substituent effects for the alkyl substituents are broadly comparable (about 0.3 p.p.m.) in contrast to the approximately three times greater value found for phenyl. It is interesting to note that the value of 0.62 p.p.m. calculated for benzyl from the one piece of data for $(C_6H_5CH_2)SnH_2$ (Table III.1) is intermediate.

So far the discussion has been concerned with the possibility of a correlation between the chemical shifts and the nature of the substituent on stannane. An inductive contribution to the shifts might be expected to increase regularly with the number of substituents. However, significant non linearities are observed presumably caused by other factors, e.g. magnetic anisotropy.

The coupling constants in tin hydrides $^1J(^{119}Sn\text{-}H)$ and $^1J(^{117}Sn\text{-}H)$ are in the range of 2,000 Hz. This is exceptionally large when compared for instance to the value of 202.5 Hz found for $^1J(^{29}Si\text{-}H)$ in SiH_4[73] even allowing for the fact that γ (^{119}Sn) is 1.876 times greater than γ (^{29}Si). Buckingham and Schneider[74] have explained this in terms of contact interaction which is large for large values of nuclear charge. In the case of atoms with hybridized bonding orbitals, as is in the present case, the contact contribution is proportional

to the percentage s -character of the orbital used in forming the bond. The s - character depends on the relative electronegativities of the substituents and has the tendency to concentrate in the orbitals of atom which connect the less electronegative groups.[75] The trends observed are then reasonable. Progressive substitution of alkyl groups for hydrogen in SnH_4 has resulted in a reduction of Sn-H spin-spin coupling constants. The change is not strictly linear but is comparable among the series. It must not be overlooked that changes in the coupling constants in phenyl stannanes are only about 0.5% .

It might be concluded from this slight difference of spin-spin coupling constants in the phenyl series that the phenyl substitution of a stannane proton does not produce any significant changes of the distribution of electron density around the remaining Sn-H bond(s).

Some authors[4,5] have tried to find out some correlation between the coupling constants and the number of substituents. Flitcroft and Kaez[4] plotted $^1J(^{119}Sn\text{-}H)$ as a function of number of substituents, n, for the methyl series and it was found that the effect of increasing substitution is not strictly additive and the plot deviates strongly from the extrapolated straight line. A similar plot[5] was a straight line for the three phenyl stannanes, while stannane appeared inconsistent with the plot. There has been no suggestion in the literature of any underlying relationship between

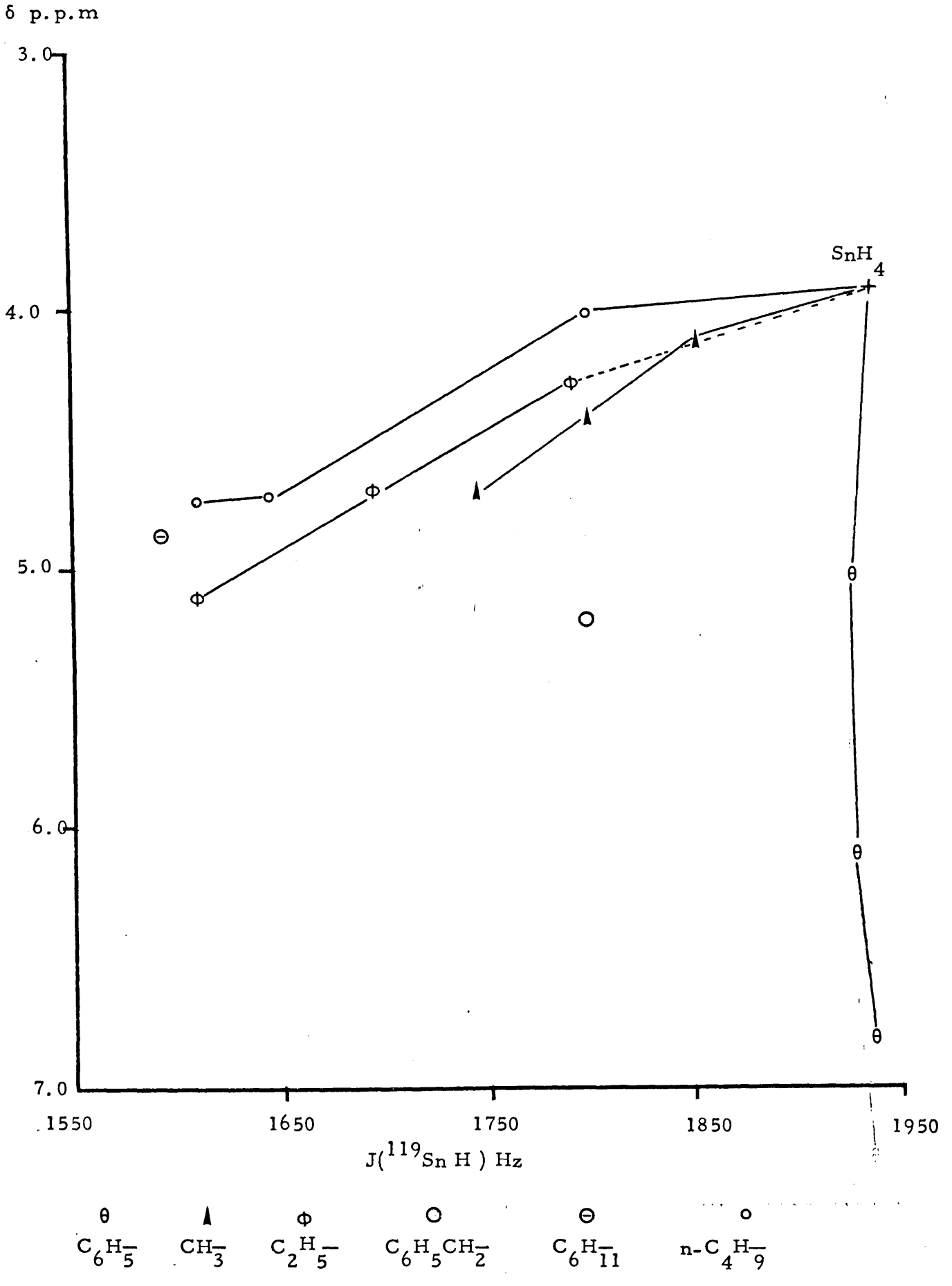

Fig. III.XV. A plot of coupling constants versus chemical shifts in some stannanes . Starting from the upright at SnH_4 each of the points within the series going down to the lower left represents increasing number of substituents.

the chemical shift and coupling constant for the tin proton moiety as the number and type of substituent is varied.

Figure III.XV shows the chemical shifts of stannanes relative to T.M.S. graphed vs $^{1}J(^{119}Sn\text{-}H)$, starting from upper right at SnH_4. The figure shows that each of the points within the series going down to the lower left represents increasing number of alkyl groups such as $RSnH_2$, R_2SnH_2 and R_3SnH and it is evident that the farther downfield the resonance of hydride proton appears the smaller is the coupling constant. The most striking feature is the consistency of the coupling constants in phenyl stannanes. It is interesting to note that the value for benzyl stannane is found to lie between that of the phenyl and methyl series. (Discussion of isotopic effects and band shape analysis in the proton spectra of deuterated hydrides is considered separately in Chapter V. and X respectively.)

CHAPTER IV

^{119}Sn SPECTRA

Section IV. 1 Introduction and review of previous work

Of all elements tin has the largest number of isotopes. Of these ten isotopes, three nuclei have non zero spin.

Properties of magnetic tin isotopes

Isotope	Spin	Natural abundance	Sensitivity relative to ^1H	Sensitivity relative to ^{13}C	Resonance frequency in MHz (1.41 T)	γ rad $T^{-1} S^{-1}$
^{115}Sn	$\frac{1}{2}$	0.35%	0.035 (1.23×10^{-4})	2.2 (0.70)	19.49	-8.691×10^7
^{117}Sn	$\frac{1}{2}$	7.67%	0.045 (3.45×10^{-4})	2.83 (19.6)	21.37	-9.530×10^7
^{119}Sn	$\frac{1}{2}$	8.58%	0.052 (4.46×10^{-4})	3.27 (25.3)	22.37	-9.971×10^7

values in parenthesis include corrections for natural abundance calculated as in ref. (16)

^{115}Sn is not readily observable due to very low abundance. ^{119}Sn and ^{117}Sn have similar magnetic moments. However, ^{119}Sn is slightly more sensitive to detection and since it is also more abundant magnetic isotope ^{119}Sn has therefore been studied more. The sensitivity is only approximately 5% of that of a proton in the same magnetic field strength for equal numbers of nuclei. The approximate shift range is 2,000 ppm. A more meaningful comparison perhaps is to carbon-13 in natural abundance.[16] It transpires that ^{119}Sn is intrinsically twenty five times more favourable than ^{13}C in natural abundance.

The first direct observation of ^{119}Sn resonance was reported by Burke and Lauterbur.[17] The spectra of mixtures of $SnCl_4$, $SnBr_4$ and SnI_4 were examined. All the twelve mixed tin (IV) halides formed due to random halogen exchange were found in the expected concentrations. They also found the lifetime of these various compounds. The spectra

were obtained on a Varian V4300B spectrometer, operating at 8.5MHz by the field sweep method. Depending on the relaxation times, the resonances were recorded as rapid passage signals, slow passage dispersion mode or absorption mode signals; high R.F. power levels were used.

Hunter and Reeves[18] reported chemical shifts for compounds of the group IV elements silicon and tin. They measured chemical shifts of ^{119}Sn in a series of alkyl tin compounds and investigated the concentration and solvent dependence of chemical shifts for simple methyl tin bromides and chlorides. Measurements were carried out on a modified Varian HA60 and in most cases an absorption signal was presented. Calibration was done by the side band technique. The protons were decoupled at high power levels using an N.M.R. specialties S.D. decoupler.

The other early measurements carried out by the direct method were by White[19] and Considine[20], employing large samples, using suitable frequency and rapid sweep rates at high R.F. power levels. The spectra were poorly resolved with low signal to noise ratio.

McFarlane[21] and co-workers obtained tin-119 chemical shifts in 59 organo tin compounds by using the method of heteronuclear double resonance $^{1}H-\{^{119}Sn\}$, in which a ^{119}Sn satellite line in the proton spectrum of the compound is observed, whilst the sample is irradiated at the same time with an r.f. at the ^{119}Sn resonance frequency. In favourable cases where spectra

were not complicated ^{119}Sn line positions were determined to $\pm$ 0.5 Hz ^{1}H spectra were obtained on a JEOL-C60H spectrometer. The ^{119}Sn resonance frequency was derived from a FS30 Schlumberger frequency synthesizer.

Zuckerman et al.[22] have reported the ^{119}Sn chemical shift values of another 37 organotin compounds, which were obtained in a very similar way to that of McFarlane .

Banney and Wells[23] extended the INDOR method applications to ^{13}C, ^{199}Hg and ^{207}Pb nuclei in natural abundance to obtain chemical shifts. They investigated Me_4Sn, Me_2Hg, Me_4Pb and some alcohols for ^{13}C spectra .

The recent advances in Fourier Transform spectroscopy have resulted in renewed interest in the studies of less receptive and less abundant nuclides. The F.T. approach is more applicable to routine spectral determinations including samples of complex mixtures for which complicated proton spectra could preclude INDOR experiments. On the basis of available data, it appears that the F.T. method provides spectra that are at least as good in terms of line width and signal-to-noise ratio as the best INDOR spectra reported for the most favourable cases. The nuclear Overhauser effect (NOE) arising from proton irradiation is expected to be of no help in improving the sensitivity of ^{119}Sn spectra. The effect relies on a dipolar relaxation mechanism between tin and the irradiated protons and is not normally expected to be very important in this case. Since ^{119}Sn has a negative magnetogyric ratio, the NOE is negative in sign.

The maximum NOE effect would be achieved when the tin relaxes totally via proton intramolecular dipole-dipole relaxation and is given by (see section I.5.3).

$$\eta_{max} = 1 + \frac{\gamma_{1_H}}{2\gamma_{119_{Sn}}}$$

the calculated value is -0.34 which means that the signal is inverted and 1/3 the original size. In practice it is very unlikely that the signal will go negative in this way because in the hydrides spin rotation is expected to be a dominant mechanism at least at room temperature, on account of facile molecular rotation, giving a relatively small nuclear Overhauser reduction.

Section IV.2 Experimental

The spectra were obtained on a "pulse F.T. HA60" spectrometer operating at 22.3 M Hz described in Section II. In most of the cases the sample (neat liquid) was in a 5 m.m. O.D. N.M.R. tube placed in a 12 m.m. N.M.R. tube filled with water to lock the signal. In some cases where a reasonable amount of sample was available, 12 m.m. sample tubes were used with a few drops of T.M.S. in it to lock the signal. A fast analog-to-digital converter sampled up to 8192 points on each free induction decay and typically 4,000 such transients would be accumulated to improve the S/N ratio. All experiments were normally carried out with a pulse length of 100 μS duration and an acquisition time of 0.8192s and the frequency spectra have a pulse repetition rate of normally one second.

The radio frequency carrier is at the extreme left of the chart and the frequency increases towards the right. After Fourier transformation the spectrum was displayed on the oscilloscope to adjust the phase before recording the spectrum. At the end, the computer printed out a parameter list of

N.T. number of transients, the number of accumulation desired to store can be from 1 to

D.P. Data points, the number of data points that are used during the acquisition.

W.P. Width of plot

C.T. Completed transients

E.P. End of plot, refers to the end of presentation

V.S. Vertical scale, refers to the size of the spectrum

Y.Y. The Y-axis displacement of the spectral width (range of frequencies)

T.H. Threshold, is a vertical parameter value above which the computer will calculate the number, intensity, position and frequency for various lines.

R.F. radio frequency on the frequency synthesizer.

All spectra were recorded without proton decoupling except Me_2SnD_2 where methyl proton decoupling was achieved.

At least two sets of measurements and usually more in the case of high boiling point compounds were made on each

sample, multiplet features were expanded and most of the shifts are believed to be accurate to within about ± 2 p.p.m.

Section IV.3 ^{119}Sn chemical shifts.

Chemical shifts should be reported as parts per million (p.p.m.) relative to a suitable reference compound and for tin our choice is Me_4Sn. This molecule has the advantages that it is 1) available as a neat liquid 2) can readily be observed in one pulse 3) out of the multiplet signal of 13 lines, 11 clearly observable after 10 pulses, the central high intensity line can easily be recognised. 4) since Me_4Sn is also the end member of methyl series.

The question of the sign convention to be used for chemical shifts is not yet resolved and both possibilities are in current use and have something to be said for them. We have given here shifts to higher field than the reference as negative numbers.

The observed resonance frequency of ^{119}Sn (ν_{obs}) was standardized according to the formula given by McFarlane[62]

$$\nu_{T.M.S.} = \nu_{obs} \left(1 \pm \frac{f \pm 60\delta}{60 \times 10^6} \right)$$

where $\nu_{T.M.S.}$ is the ^{119}Sn nuclear resonance frequency at the field at which the protons of T.M.S. reference display their signal at 60 MHz, f is the modulation frequency, δ is the shift of the proton lock signal from T.M.S. (δ scale is used). Signs depend upon which side band was used to lock the internal stabilization signal, positive for the low field and negative for upfield side band.

Section IV.4 Results

Table IV.1 presents the chemical shifts that were observed in this study. All spectra are described separately and a general discussion of results is given at the end.

IV. 4.1 Tri-methyl tin hydride

The spectrum of Me_3SnH shown in Fig. IV.1, resulted from the accumulation of 4,000 F.I.D s; the experiment took approximately $1\frac{1}{2}$ hours. First order analysis is applicable since the $\Delta\nu/J$ ratio is large. By definition it is an A M_9X spin system and the spectrum consists of a doublet (1:1) of ten lines separated by $J_{H_3C-^{119}Sn}$ and the intensities are roughly in the ratio of coefficients in the binomial expansion. The outer two lines are not clearly observable due to the noisy base line. Values of coupling constants involved were measured and were compared with the values obtained from the proton spectra listed in Table III. I. They were found to be in good agreement. The difference of frequencies between Me_4Sn and the centre of the doublet gave the chemical shift value. This value was found to be 9 p.p.m lower than the reported value in reference (11), which may be attributed to the difference of conditions when spectra were recorded, since these shifts are expected to be both solvent and temperature dependent.

IV. 4.2 Di-methyl tin dihydride.

The ^{119}Sn spectrum is shown in Fig. IV.II and was the result of 1,000 pulses accumulated in half an hour. The spectrum can be analysed as a 1:2:1 triplet due to the hydride protons with

TABLE IV.1

No.	Compound	$\nu(^{119}Sn)\pm 10$Hz	$\delta(^{119}Sn)$ (p.p.m.)	$^1J(^{119}Sn\text{-}H)\pm 1$ Hz	Conditions	Reference
1	Me_3SnH	22,370,298	-113	1743	neat liquid(27°C)	this work
			-104		in benzene "	11
2	Me_2SnH_2	22,367,703	-229	1797	neat liquid "	this work
			-224		10% in C_6H_{12}-(-20°)	11
3	Me_2SnH_2	22,367,726	-228	1797	) all present	
	Me_2SnHD	22,367,703	-229		) in the same	this work
	Me_2SnD_2	22,367,681	-230	274.4(±0.3)	) mixture (27°)	
4	Me_2SnD_2	22,367,658	-231	275	neat liquid (27°C)	this work
5	$(C_6H_5)_3SnH$	22,369,515	-148	1938	" " "	" "
6	$(C_6H_5)_2SnH_2$	22,367,390	-243	1926	" " "	" "
			-234		20% in T.M.S. (30°)	11
7	$C_6H_5SnH_3$	22,365,668	-320	1920	neat liquid (-15°)	this work
8	(n-But)$_3$SnH	22,370,701	-95	1611	neat liquid	this work
			-91		in CCl_4	11
9	(n-Propyl)$_3$SnH	22,370,835	-89	1602	neat liquid	this work
10	Et_3SnH	22,371,394	-64	1610	neat liquid	this work
			-40		50% in benzene	11
11	Me_4Sn	22,372,826	0		neat liquid	

All δ values are relative to Me_4Sn, negative signs indicate upfield shifts and are reproducible to ± 2 p.p.m.

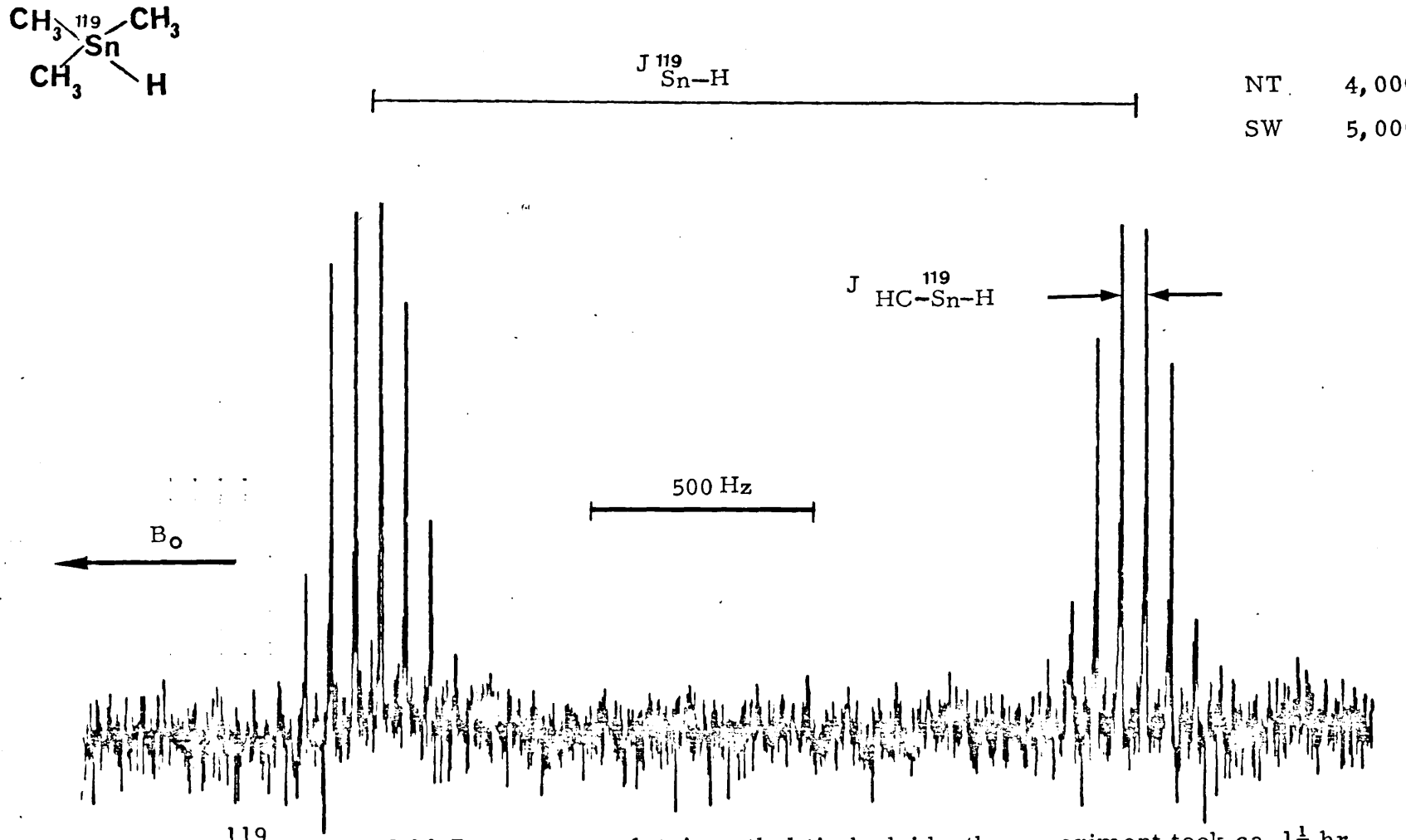

Fig. IV. I. 22. 37 MHz ^{119}Sn F. T. N. M. R spectrum of tri-methyl tin hydride, the experiment took ca. 1½ hr.

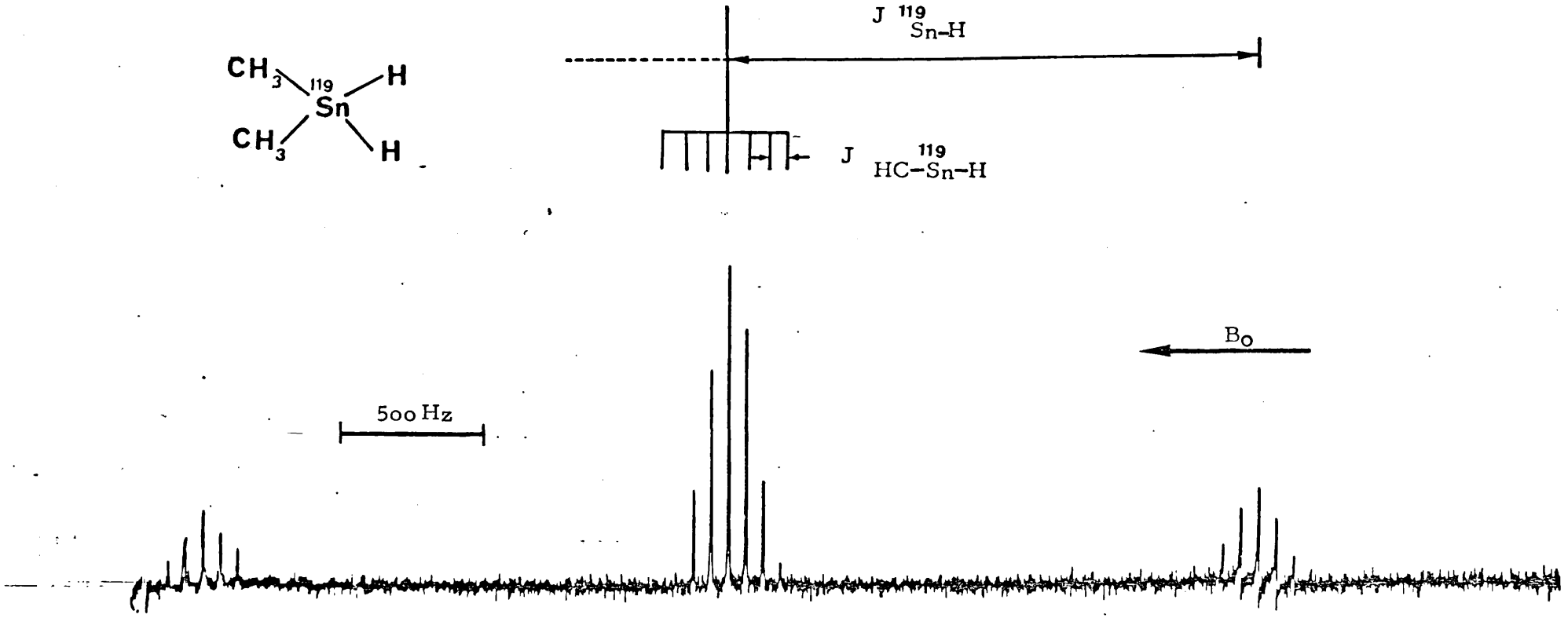

Fig. IV. II. The ^{119}Sn F. T spectrum of dimethyl tin dihydride (neat liquid), resulting from 1,000 transients

further mutiplicity produced by the six equivalent protons of two groups (septets). On measurement the values of $^{2}J(^{119}Sn-H)$ and $J\ (CH_3-^{119}Sn)$ were found to be in good agreement with those obtained from proton spectra (see Table III.1.). The δ value reported here is 4.4 p.p.m. less than the reported[11] value.

IV. 4.3 Deuterated dimethyl tin hydride $(CH_3)_2SnD_2$)

Initially the spectrum was obtained on a 5KHz band width, later it was expanded for accurate measurements, Figure IV.III (a) shows such an expanded spectrum (plot width now 1365 Hz). One thousand F.I.D's were accumulated.

The general features of the spectrum show a pentet (1:2:3:2:1) due to spin-spin interaction between ^{119}Sn and the two equivalent directly bonded deuterons. Each line is further split into a septet whose components are of binomial relative intensity with spacing equal to $^{2}J_{(CH_3-Sn^{119})}$. Out of a total of 35 lines 28 can clearly be counted.

Heteronuclear double resonance was done by irradiating methyl protons at the proton resonance frequency. To carry out $^{119}Sn-\{^{1}H\}$ heteronuclear double resonance experiments the field had to be locked to some nucleus other than proton. For this purpose, the sample tube was put in a 12 mm O.D.N.M.R. tube containing C_6F_6 to lock the signal to fluorine. Complete removal of methyl proton spin-spin coupling was achieved when the sample was irradiated at a proton resonance frequency of 59, 995, 717 Hz. The resulting decoupled spectrum was a 1:2:3:2:1 quintet. The

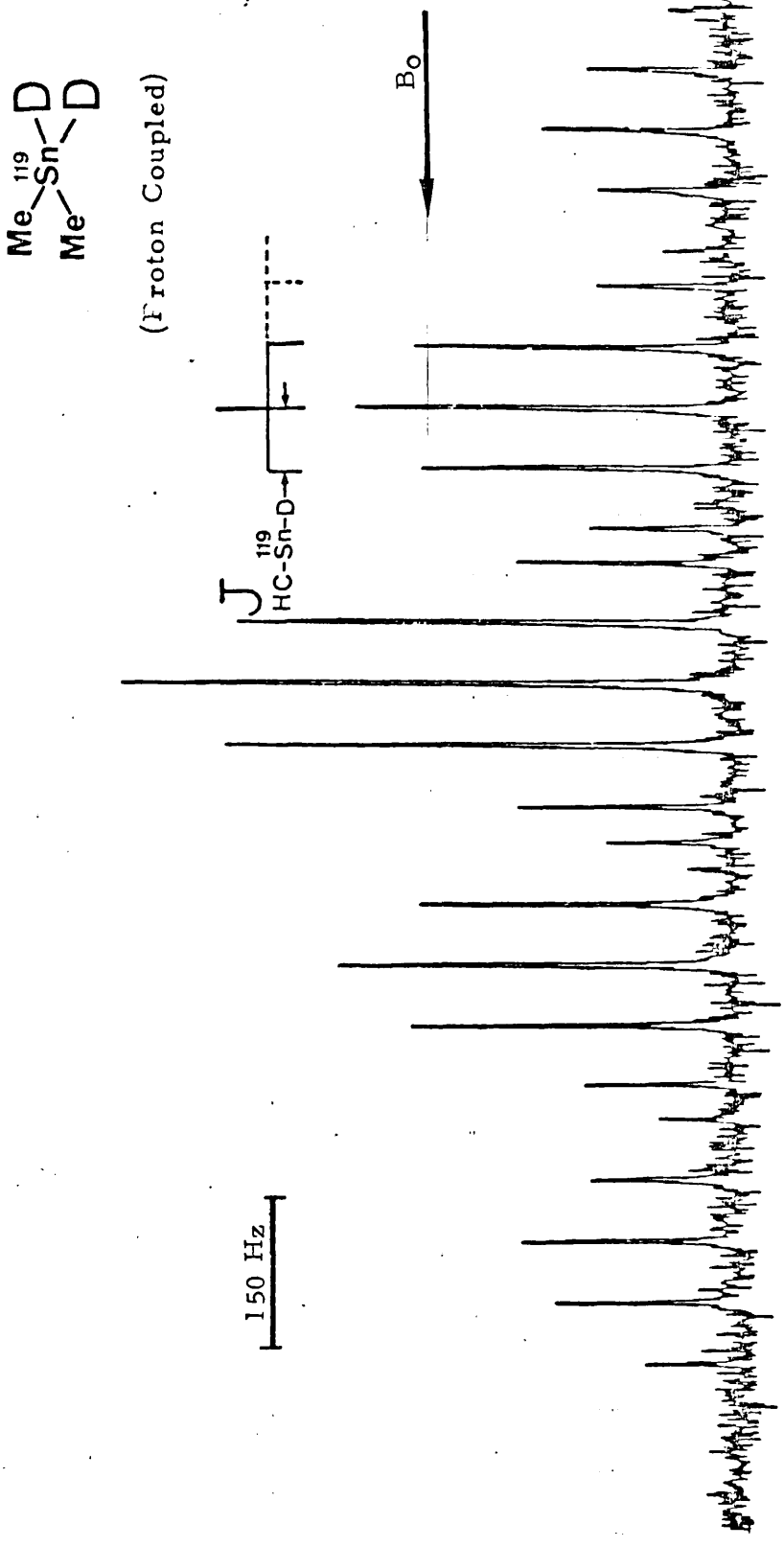

Fig. IV. III. (a). 22.37 MHz ^{119}Sn spectrum of deuterated di-methyl tin hydride.

The FIDs from 1000 pulses were accumulated to obtain this spectrum.

Fig. IV. III. (b). 22.37 MHz ^{119}Sn-[^{1}H] FT N.M.R spectrum of deuterated di-methyl tin hydride.

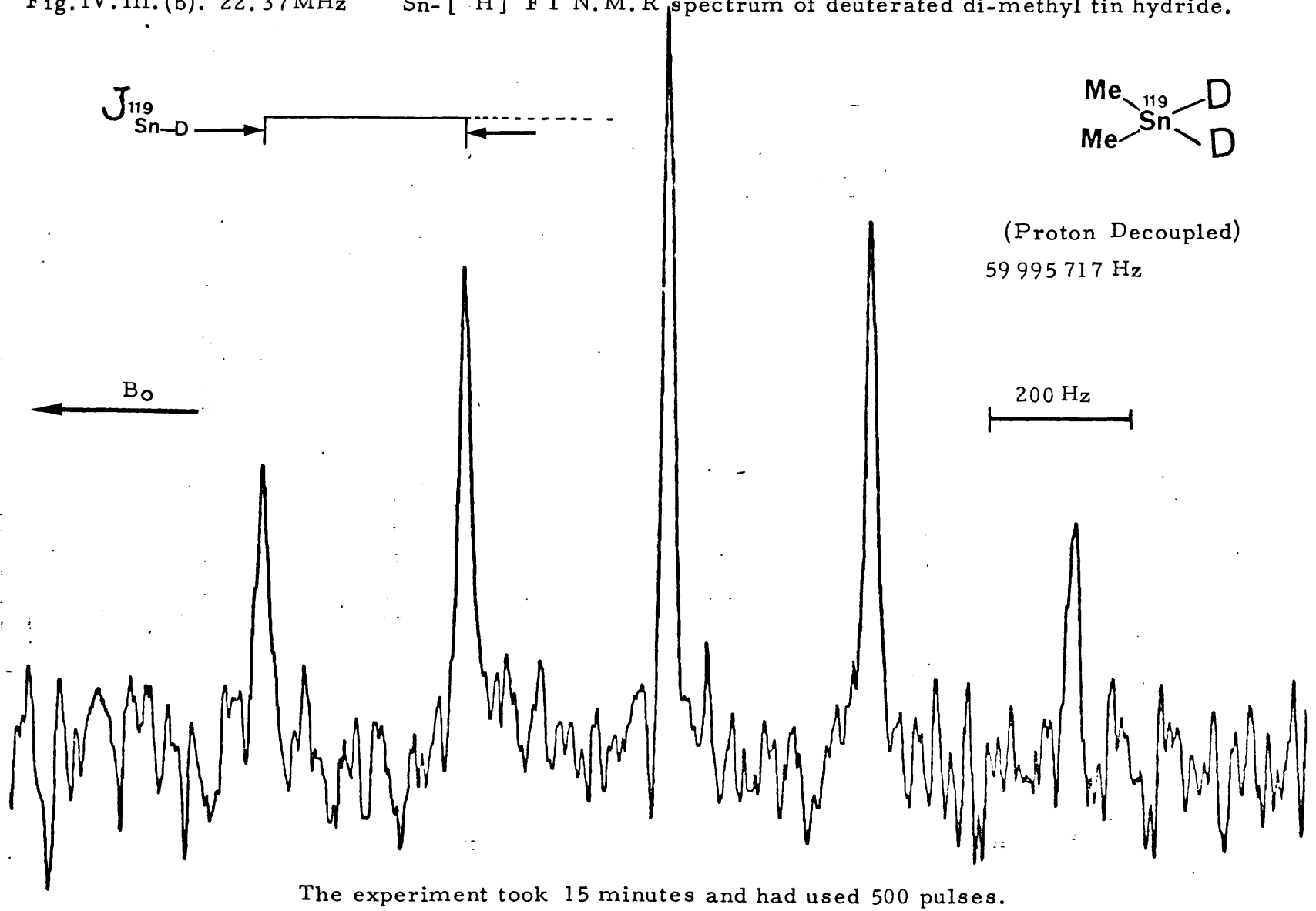

The experiment took 15 minutes and had used 500 pulses.

spectrum shown in Figure V.III (b) resulted after 500 transients and took only 15 minutes. The quintet is shifted ca. 2 p.p.m. upfield from the ^{119}Sn shift of the parent hydride (Table V.1) due to an isotope effect. The measured value for ^{1}J (^{119}Sn-D) of 274.4 $\pm$ 0.3 Hz (see Table V.1) is in agreement with the value of 274.5 $\pm$ 1 Hz obtained by the INDOR experiment (see Table III.5) and with a value of 274.4 $\pm$0.1Hz obtained from the deuterium spectrum. This latter spectrum was measured at Queen Mary College, London, on a Brucker HFX-90 spectrometer operating at 13.8 MHz for deuterium. The 5 m.m. sample tube was placed in a 10 m.m. tube which contained C_6F_6 for locking purposes. The spectrum width was 500 Hz and consisted of 2048 data points. Clearly the deuterium spectrum provides the best digital resolution (0.244 Hz) and this combined with a spectral line width of approximately 0.3 Hz means that this provides the most accurate value of $^{1}J(^{119}Sn$-D).

IV.4.4. Deuterated di-methyl tin mono hydride (Me_2SnHD)

Figure IV.IV shows the ^{119}Sn spectrum of a mixture containing Me_2SnH_2, Me_2SnHD and Me_2SnD_2 in the same 5 m.m. O.D. N.M.R. tube. The spectrum resulted from 21,000 transients accumulated in total time of ca.7 hrs. Out of the total 126 lines (Me_2SnH_2 21 + Me_2SnHD.70 + Me_2SnD_2 35) 91 lines were clearly counted and assigned to their corresponding multiplets.

The spectrum was divided into four regions and each one was then expanded for measurements and the spectrum can be interpretted as a doublet of triplets of septets. The doublet of triplets arises due to J (^{119}Sn-HD) spin-spin coupling, further

Fig. IV. IV.

^{119}Sn spectrum of

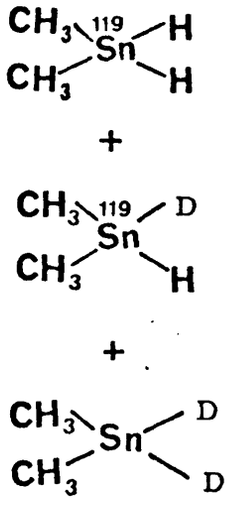

The spectrum was recorded using 21,000 pulses .

splitting in the triplets is caused by the spin-spin interaction of protons on the two methyl groups $J(^{119}Sn\text{-}CH_3)$.

IV.4.5 Tri-phenyl tin hydride $(C_6H_5)_3SnH$

This hydride has a comparatively high boiling point and was available in a reasonable amount, therefore a 12 m.m. sample was used to record the spectrum. To record the spectrum shown in Fig.IV.V. 10,000 pulses were used. The spectrum is a doublet of multiplets showing unresolved spin-spin coupling between ^{119}Sn and phenyl protons.

The value of 1938 $\pm$ 1 Hz for $^1J(^{119}Sn\text{-}H)$ obtained here is listed in Table IV.1 and agrees with the one obtained from proton spectra (see Table III.1) within the experimental error.

IV.4.6 Di-phenyl tin dihydride $(C_6H_5)_2SnH_2$.

The spectrum is shown in Figure IV.VI and was obtained after pulsing for 10 hrs. The spectrum consists of a (1:2:1) triplet of multiplets. The multiplet structure was expanded. The main splitting of the feature is a triplet due to ^{119}Sn spin-spin coupling with the two protons of benzene in ortho position, and there is further unresolved splittings due to coupling with meta and para protons on the ring. However, a value of 1926 $\pm$1Hz measured from the full scale spectrum was found in agreement with the previously determined value from proton spectra (see page 55). The chemical shift was measured from the centre of the triplet and the value of -243 p.p.m. so obtained (see Table IV.1)was10 p.p.m. higher than the reported[11] value of -233.6 p.p.m.

Fig. IV. V.

^{119}Sn spectrum of

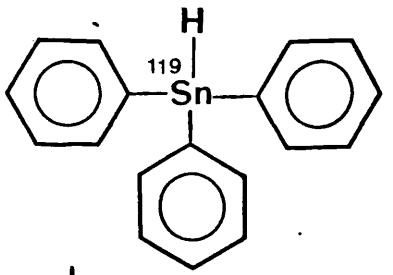

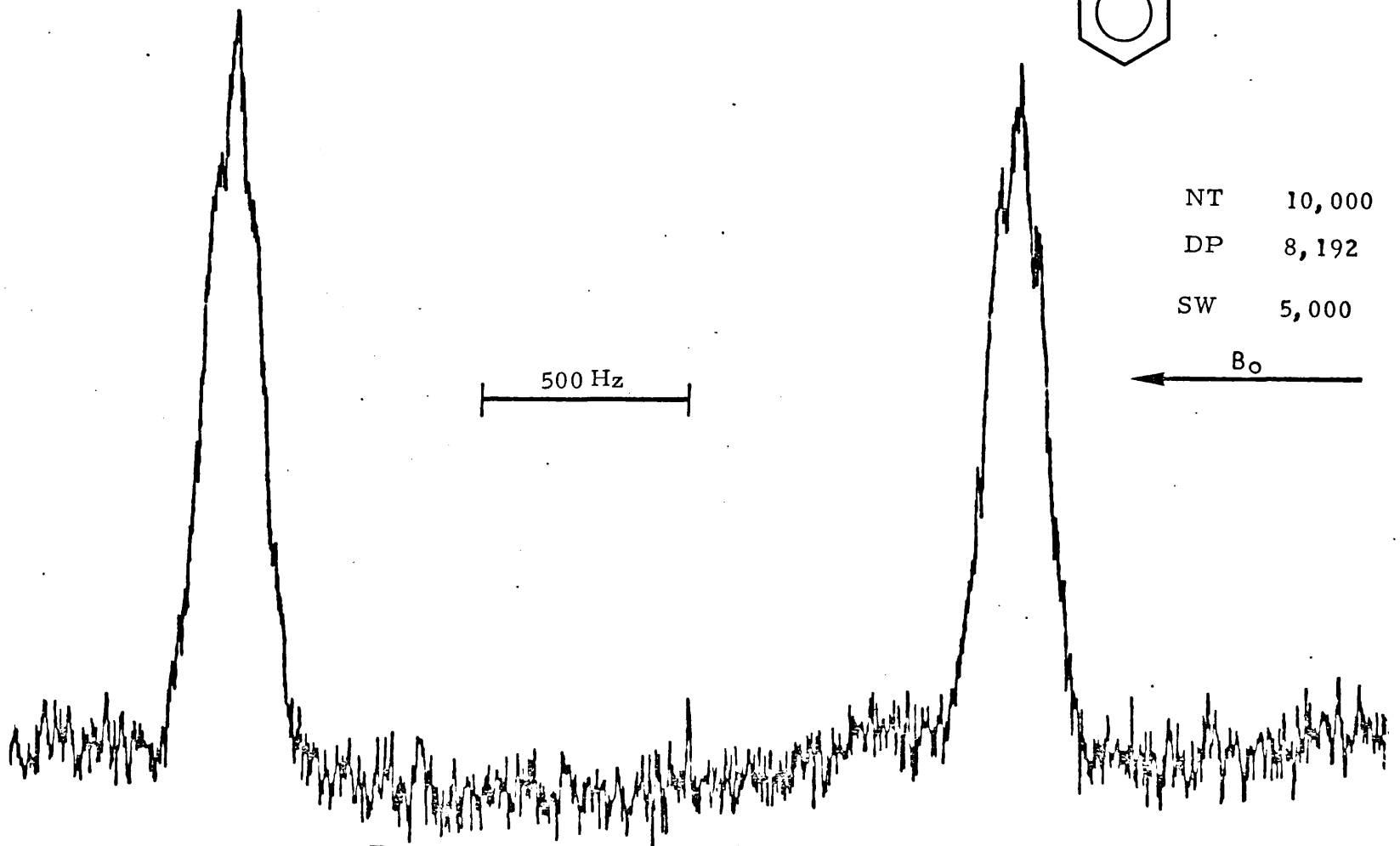

The experiment took ca. 5 hr

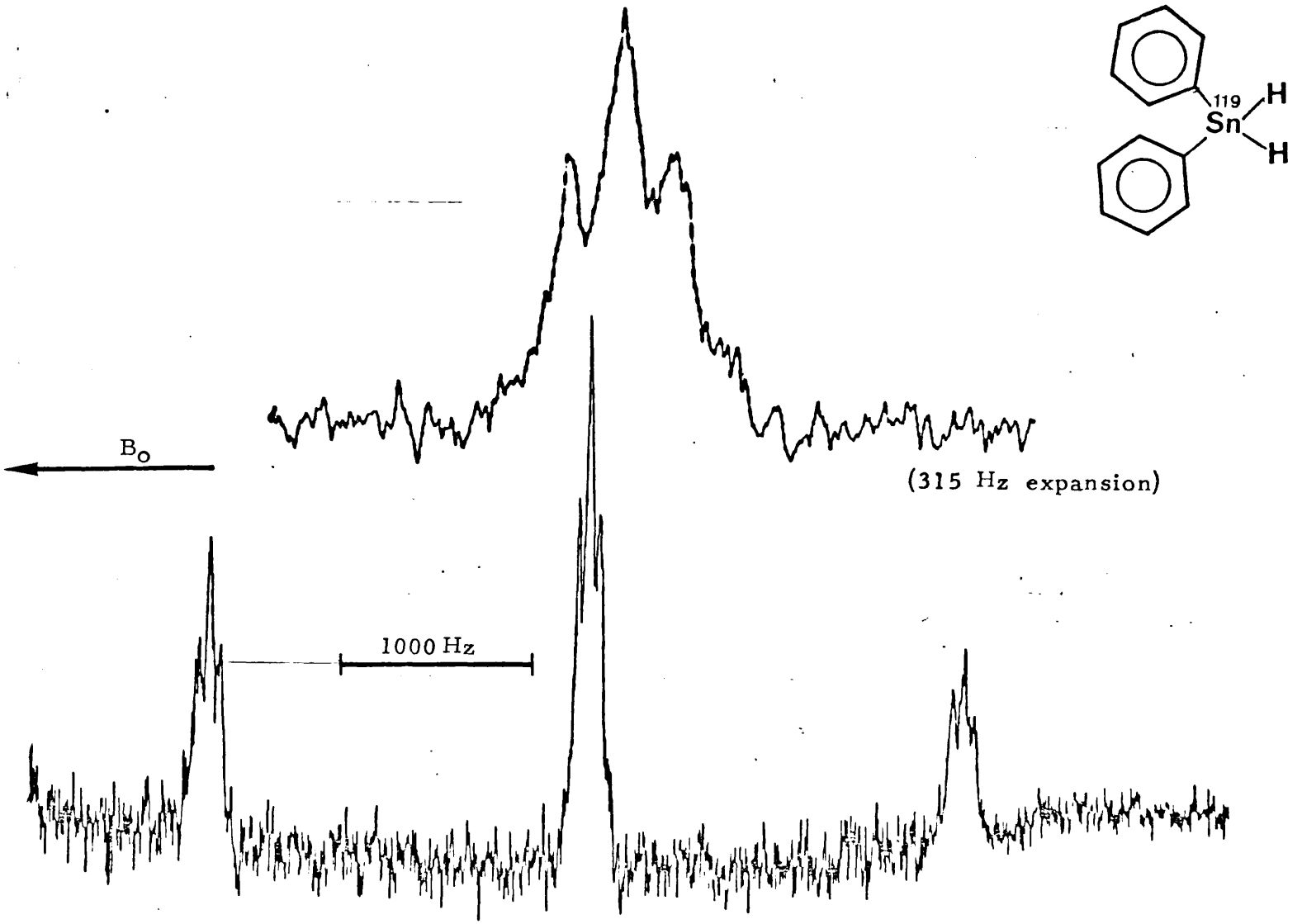

Fig. IV. VI. ^{119}Sn spectrum of the central atom of diphenyl tin dihydride . The spectrum resulted from 25,000 free induction decays.

IV.4.7 Mono-phenyl tin trihydride($C_6H_5SnH_3$)

This hydride has a low boiling point and decomposes at room temperature, therefore spectra were recorded at -15°C. The spectrum obtained was "folded" due to the multiplicity of the signal (a quartet) and the large value of the coupling constant involved (total about 6,000 Hz) as compared to the bandwidth. After recognising the features of the resulting folded quartet (by comparing the intensities and distance) the value of $^1J(^{119}Sn\text{-}H)$ was obtained. One of the high intensity multiplet components of the quartet was expanded and Fig. IV.VII shows an 80 Hz expansion of a 5000 Hz spectral width. The feature can be explained as a triplet due to spin-spin interaction between ^{119}Sn and the two ortho protons on the benzene ring. The value of the coupling constant is 21.5 ± 0.5 Hz. The quartet structure could be explained on a first order basis by equal coupling constants of 4.5 ± 0.5 Hz between tin and the meta and para protons. The phenyl region in the proton spectrum is rather featureless and has not been analysed. Speculative spectral simulations could be attempted with a view to assessing the relevance of a first order analysis in this case. The chemical shift is reported for the first time and is listed in Table IV.1.

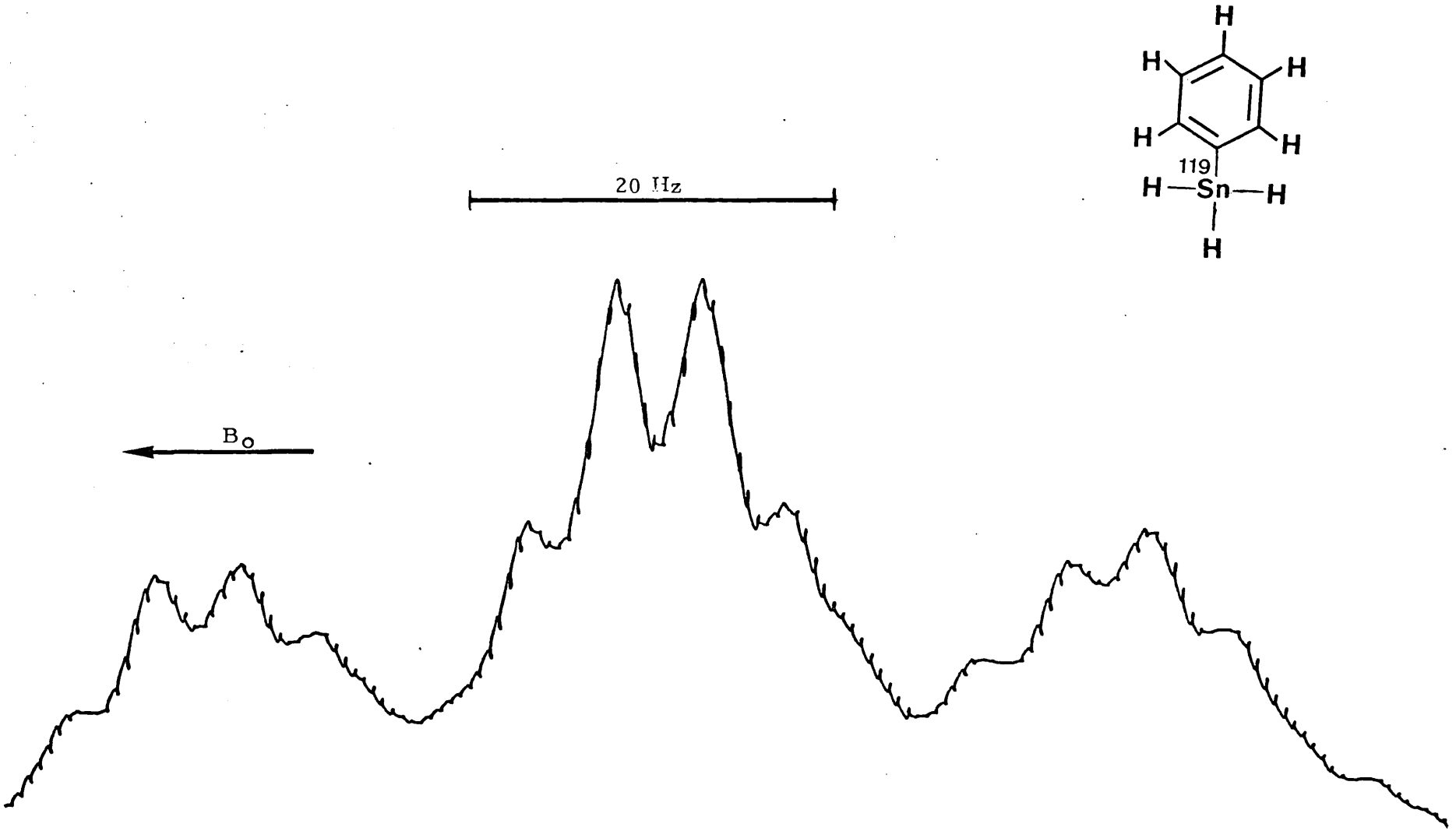

Fig. IV. VII. ^{119}Sn N. M. R spectrum of mono-phenyl tin hydride at -15°C. The figure shows one of the four lines of the main spectrum.

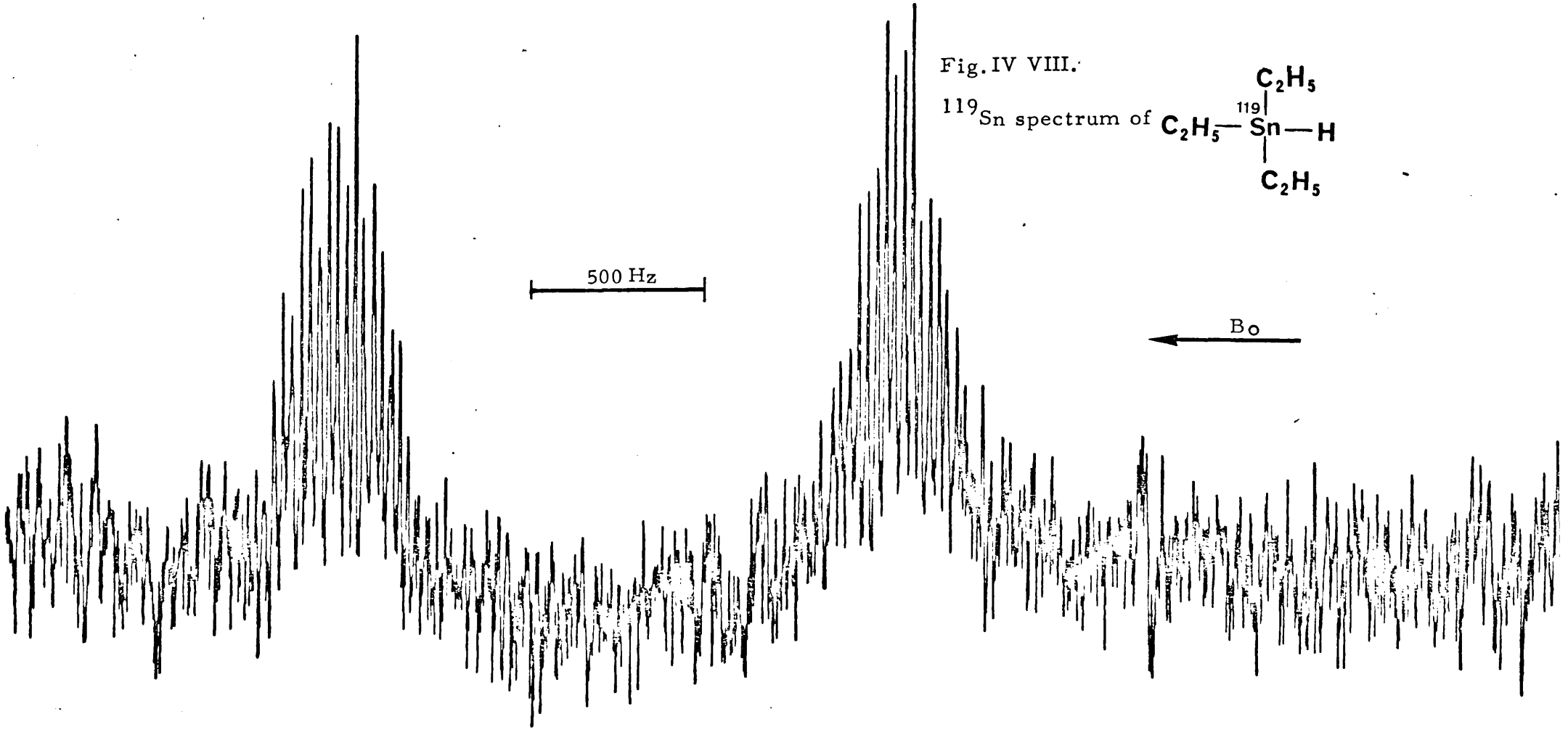

Fig. IV VIII.

^{119}Sn spectrum of $(C_2H_5)_3{}^{119}Sn{-}H$

The spectrum was obtained from the accumulation of 9,000 F.I.Ds, and took ca. 3 hr.

Fig. IV. IX. ^{119}Sn spectrum of (n-Propyl)$_3$Sn–H neat liquid at 25°C

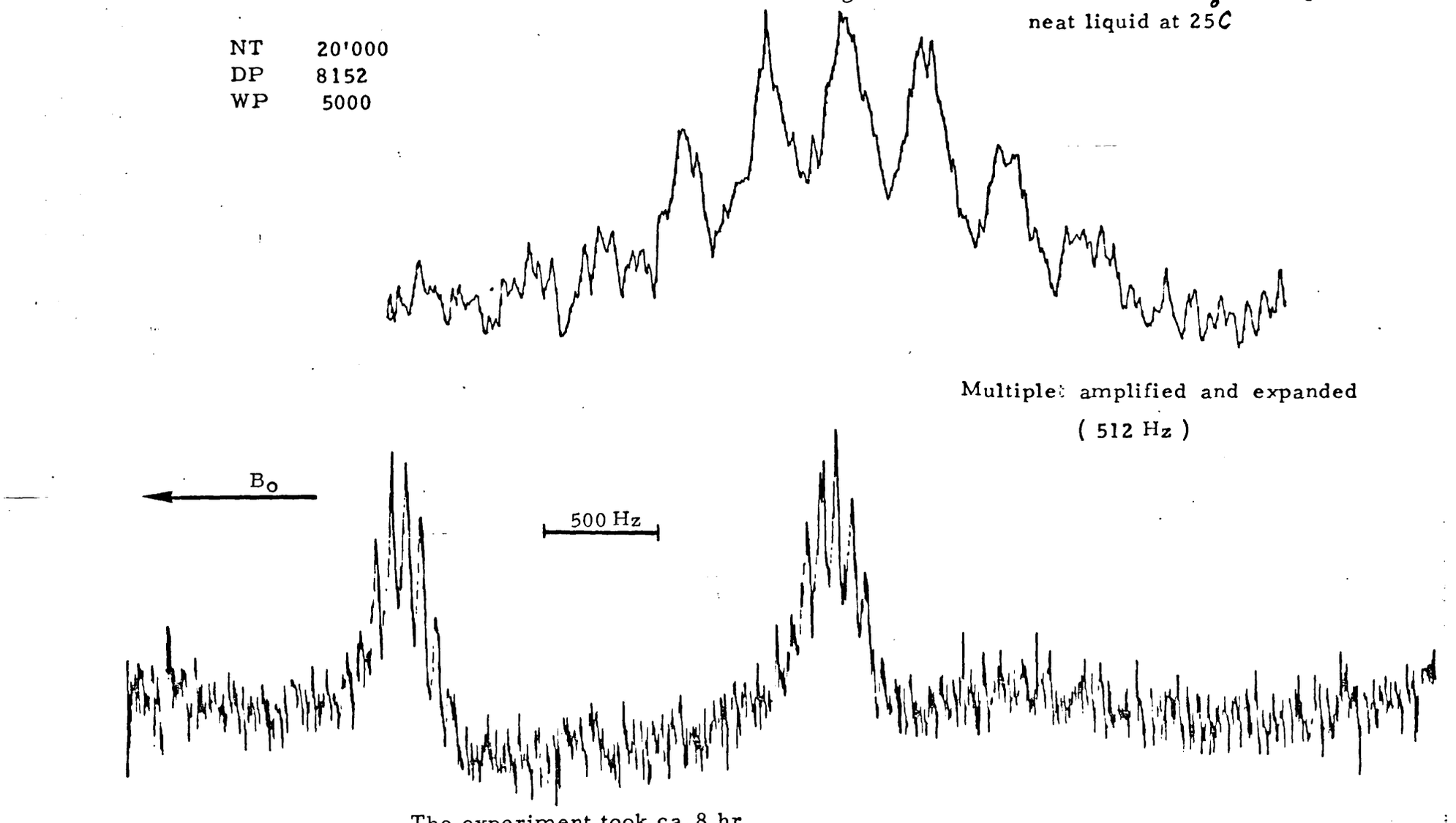

The experiment took ca. 8 hr

IV.4.8 Tri-ethyl tin hydride $(C_2H_5)_3SnH$

Figure V.VIII displays the spectrum of Et_3SnH as a doublet of multiplets. The spectrum took about 3 hours and was the result of 9000 pulses. The value of chemical shift obtained in this case (Table IV.1) is 24 p.p.m. less than the reported[11] value, this large difference may be due to solvent effects since the reported value was obtained from a 50% solution in cyclohexane.

IV.4.9 Tri-n-propyl tin hydride $(n\text{-}C_3H_7)_3SnH$

The expected doublet of complex multiplets is shown in Figure IV.IX. No attempt was made to interpret the multiplet structure. However, the chemical shift was calculated and $^1J(^{119}Sn\text{-}H)$ was found to be in good agreement with the ^1H spectra value (see Table III.1).

IV.4.10 Discussion

The major contributions to the shielding of a nucleus are generally divided into a) diamagnetic effects b) paramagnetic effects c) long range effects, and d) solvent effects. It has been generally accepted, based on a number of calculations[63] for a number of heavy atoms that the paramagnetic term dominates and the long range terms are usually ignored in case of tin shifts because the overall range is so large. The paramagnetic term to the shielding will be (see Section I.3.1).

$$\sigma^p_{local} = \frac{\mu_o}{4\pi} \frac{e^2h^2}{2m^2\Delta E} \left[\langle r^{-3} \rangle_p Q_p + \langle r^{-3} \rangle_d Q_d \right]$$

It is not clear whether substituent effects principally alter the mean excitation energy (ΔE) or $\langle r^{-3} \rangle$ or Q. The value of Q depends on the bond order and charge density related to the effective nuclear charge of the tin atom. Increasing substituent electronegativity therefore may be held responsible for an increase in the value of Q and therefore to shift the resonance to high frequency assuming that in the same/ similar series the mean excitation energy, ΔE, and the hybridization of the tin atom remains constant.

There have been numerous attempts to correlate ^{119}Sn chemical shifts with the number of substituents R_nSnX_{4-n} (where $R = CH_3$-, C_2H_5-, C_4H_7-, C_6H_5-; X = Cl, Br, OR, SR, SeR) but a non-linear dependence was reported.[18,21,22,24]

Figure IV.X shows a non linear plot redrawn from the data of McFarlane et al[21] for the phenyl tin chlorides. Whereas, Fig.IV.XI shows δ plotted versus the number of substituents both for phenyl and methyl stannanes. Least squares analysis yields the following data (Tables IV. 2,3,4).

TABLE IV.2 Methyl series

n	1	2	3	4
experimental	-346	-229	-113	0
fit	-345.1	-229.7	-114.3	0.9
error	0.9	-0.7	1.1	0.9

Standard deviation = 1.024

TABLE IV.3 Phenyl series

n	1	2	3	4
experimental	-320	-243	-148	-
fit	-323.0	-237.0	-151.0	(-65.0)
error	-3.0	6.0	-3.0	-

Standard deviation = 3.67

TABLE IV.4 Ethyl series

n	1	2	3	4
experimental	-282	-231	-64	-6.7
fit	-294	-195.57	-96.28	3.01
error	-12.86	35.43	-32.28	9.71

Standard deviation = 25.28

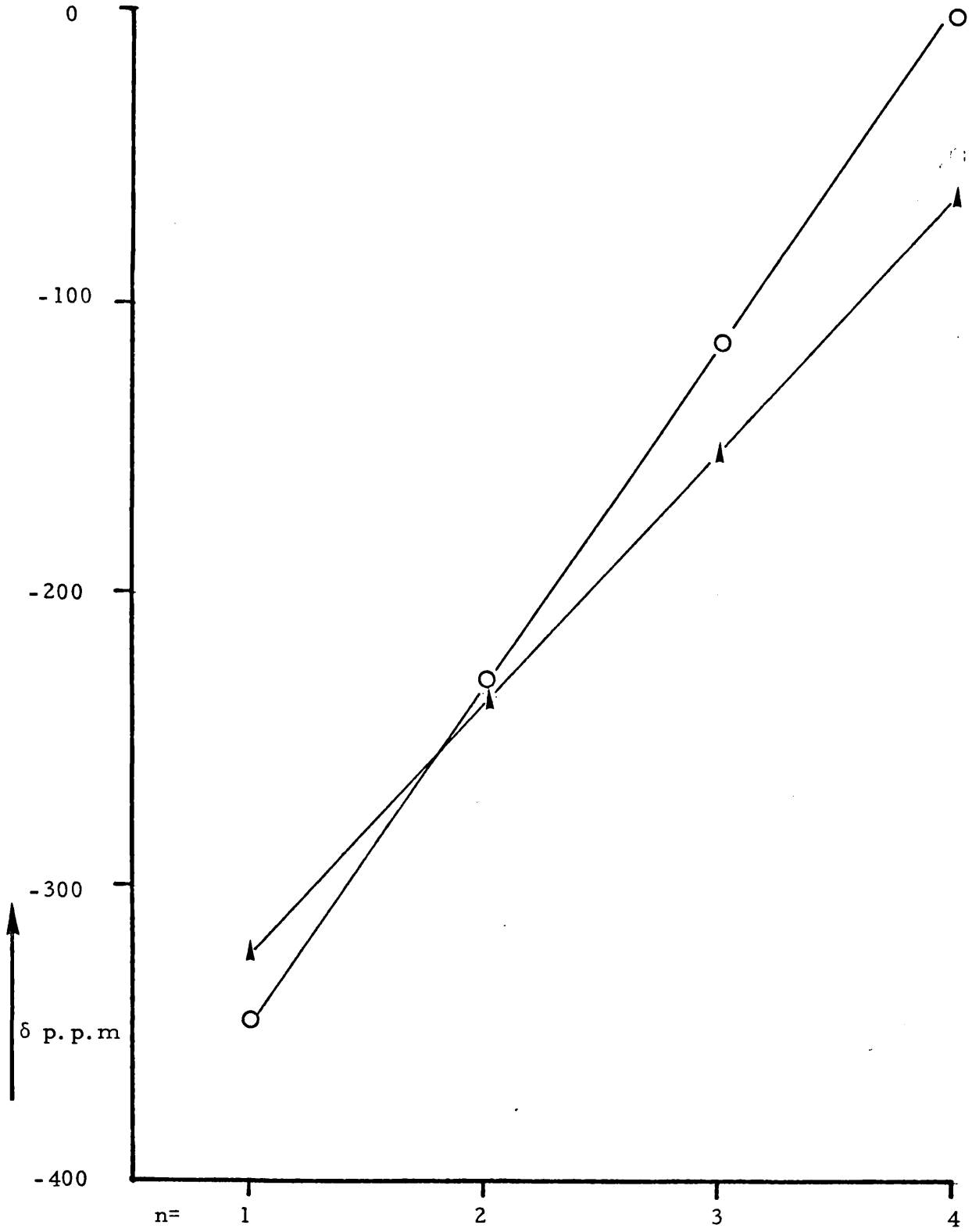

Fig. IV.XI. ^{119}Sn chemical shift as a function of n (number of substituents) for the phenyl and methyl stannanes.

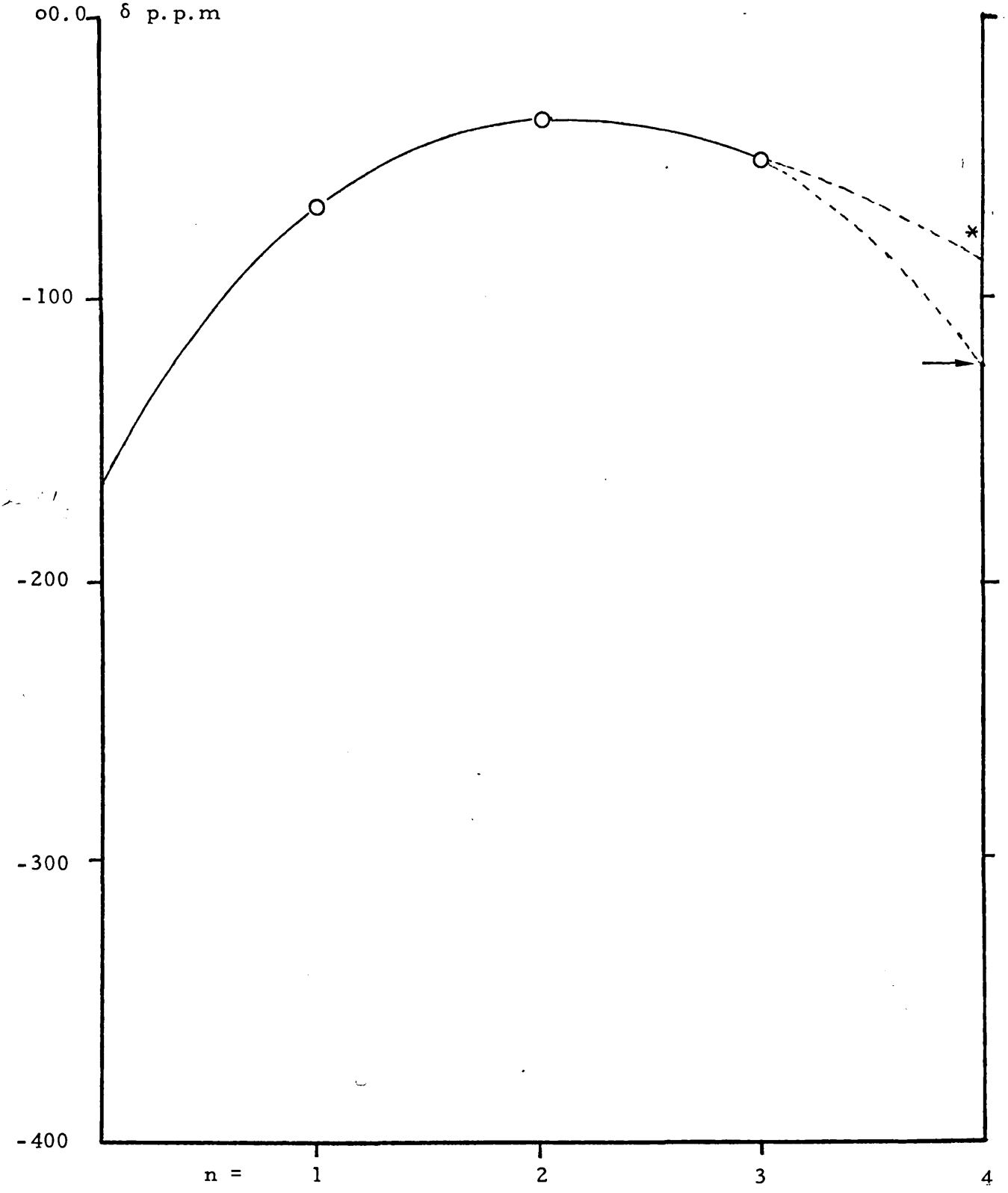

Fig. IV. X. ^{119}Sn chemical shifts in $Ph_{4-n}SnCl_n$ plotted as a function of number of substituents n . The arrow marks the estimated value of Ph_4Sn (-120 ± 20 p.p.m) as in reference 21 and * marks another extrapo--lation which gives a value of -85 p.p.m close to a value of -65 p.p.m predited from a similar plot of phenyl stannanes (fig. III. XI).

The intercepts are significantly different and each should point to the shift value for SnH_4 if the relationships are totally valid. However, the tin shift of $^{119}SnH_4$ has not yet been reported as yet and may well have a quite different value. The dependence of $^1J(^{119}Sn\text{-}H)$ on the number of substituents discussed in section III. 3 indicates that SnH_4 does not lie on the straight line which is indicated by the substituted hydrides.

The tin shift for $(C_6H_5)_4Sn$ has not been reported but it is inviting to make a prediction from the best straight line of -65.0 ± 3.7 p.p.m. This should be compared to the value of 120 ± 20 predicted by McFarlane[58] from a study of phenyl tin chlorides. Figure IV. XI shows this data on the same scale as Figure III. X and indicates the way the data was extrapolated to obtain a value for $(C_6H_5)_4Sn$. Also shown is an extrapolation to the value predicted by the present work and which is consistent with the rest of the curve.

CHAPTER V

ISOTOPE EFFECTS

Section V.1 Introduction

The term isotope shift is used to describe the shielding changes occurring upon isotopic substitution. The effect was predicted for hydrogen by Ramsey[26] on theoretical grounds. The subject has been reviewed in detail by Batiz and Bernheim[27]. Although this review appeared in 1967 and although there are not many more experimental observations of isotope effects the review remains as the standard one in the area. Theoretical understanding was thin and remains today in a rather unsatisfactory state. Isotopic substitution alters the dynamic steady state of a molecule and shifts may be caused by small changes in bond lengths or bond angles.

It has been found in almost all cases that substitution of a heavy isotope shifts the n.m.r. signal to a higher magnetic field[14]. Exceptions to this general trend are the proton shift in cis-CHF=CDF[13] deuterated ammonium ions[14], nitrobenzenes[25], the Tl^{205} shift in $(CD_3)_2Tl\,NO_3$[15] and the ^{13}C chemical shift in $(CD_3)_2CO$,[64] where the shifts are downfield from the non-deuterated species. Primary and secondary effects may be distinguished; the primary refers to a change in the resonance of a nucleus at the site of isotopic substitution and secondary refers to the changes in the remainder of the molecule.[33,34]

An analogous effect on the reduced spin spin coupling constant is also possible. The effect is referred to as a primary effect when one of the two coupled nuclei, A and X, is changed.

A secondary effect results in a change in the coupling constant J_{AX}, where neither A nor X nucleus is substituted.[25,40]

V.2 Results and discussion

V.2.1 Deuterium isotope effects in proton spectra:

The results of ^{2}H isotope effects on proton spectra described in Section III.2 are summarized in Table V.1, the measurements are given in parts per million and are positive (upfield shift with respect to the undeuterated molecule). The table demonstrates that the

1) geminal and vicinal substitution of proton by a deuteron has caused an ^{1}H upfield chemical shift that is additive with increasing deuterium substitution.

2) The geminal (two-bond) isotope effect is $\sqsubset 21 - 29.7\sqsupset \times 10^{-3}$ p.p.m. upfield per deuterium in a variety of deuterated organo tin hydrides.

3) For vicinal (three bond) substitution the isotope effect on the methyl protons also resulted in an upfield shift of ca $\sqsubset 4.6\sqsupset \times 10^{-3}$ p.p.m. per deuterium substitution, which is only 1/5 of that produced by the geminal substitution.

4) There is a significant decrease of ca. 0.6 Hz in the observed $^{1}J(Sn^{119}\text{-}H)$ on substituting a proton by deuterium in almost all the cases and an "additivity rule" is also applicable since the decrease in the coupling constant is doubled in $C_6H_5SnD_2H$ as compared to $C_6H_5SnDH_2$.

The effects of deuterium substitution on both proton and

TABLE V.1

Deuterium isotope effect - effects on proton chemical shifts and J(Sn^{119}-H) spin-spin coupling constants in proton spectra

Compounds	Feature	$\Delta\delta'H \times 10^3$ (p.p.m.)	$\Delta\delta'H/D$	ΔJ (Sn^{119}-H) Hz
$C_6H_5SnH_2D$	central hydride	21.2 ± 1.6	-	-0.70 + 0.05
$C_6H_5SnHD_2$	"	42.5 ± 1.7	21.25	-1.30 ± 0.05
$(C_6H_5)_2SnHD$	"	21.0 ± 1.5	-	-0.65 ± 0.06
$(CH_3)_2SnHD$	"	23.6 ± 1.8	-	-0.64 ± 0.06
"	methyl	4.6 ± 0.1	-	-
$(CH_3)_2SnD_2$	"	9.0 ± 1.7	4.5	-
$(C_6H_5CH_2)_2SnHD$	central hydride	29.7 ± 1.6	-	-

$\Delta\delta$ = chemical shift difference taking the parent hydride as an internal standard. All values are positive (up field shift)

shift per deuteron

$\Delta J = {}'J^*$ (Sn^{119}-H)-$'J(Sn^{119}$-H) where J* is gem.coupling constant in partially deuterated sample.

fluorine spectra have been reported in a number of compounds.[28-32] The magnitude of the shift is generally dependent on how remote the isotopic substitution is from the nucleus under observation and is approximately proportional to the number of atoms that have been isotopically substituted. The isotope shift in the proton resonance is 0.035 p.p.m. for both HTeD[59] and HSeD and 0.04 p.p.m. for HD[60]. The typical value of a geminal deuterium isotope effect on the ^{19}F chemical shift is 0.60 p.p.m. (in n- C_3F_7D). Dreeskamp[7] found that $(CH_3)_2SnHD$ had an 'H isotope shift of 0.023 $\pm$ 0.001 p.p.m. for δ (Sn-H) and 0.005 $\pm$ 0.008 p.p.m. for δ (C-H), in agreement with the values reported here see Table V.1. But the results on ΔJ (for definition see Table V.1) found in this work (Table V.1) for $(CH_3)_2SnHD$ and $(C_6H_5)_2HD$ (ca. 0.6 Hz) are larger than the 0.3 Hz reported by Dreeskamp[7] and furthermore it was not stated under what conditions the values were obtained. The data reported here are felt to be more reliable since the measurements of both shifts and coupling constants were carried out in at least three different samples for the same molecule and spectra were run at a scale expansion of 0.2 Hz/cm for $(C_6H_5)_2SnHD$, 0.4 Hz/cm for $(CH_3)_2SnHD$, 1 Hz/cm for $C_6H_5SnHD_2$ and $C_6H_5SnH_2D$. Deuterium decoupling was used to improve the accuracy of the measurements except for the last two molecules where spectra were recorded on a Varian HA-100 with no facilities for heteronuclear decoupling.

V.2.2 Deuterium isotope effects in Sn^{119} spectra

By means of Fourier Transform N.M.R. spectroscopy ^{119}Sn chemical shifts and values of the coupling constants $^1J(Sn^{119}-H)$ and $^1J(Sn^{119}-D)$ have been measured (see Chapter IV). The observed isotope effects are listed in Table V.2. The isotope effects were measured relative to $(CH_3)_2Sn^{119}H_2$ as internal standard thereby eliminating solvent and temperature effects on the isotope effect. Measurements on a sample of pure $(CH_3)_2SnD_2$ are shown in the first row of Table V.2 the shift figures shown in parenthesis were calculated by comparison with a separate sample of pure $(CH_3)_2SnH_2$. The value reported indicates the general reproducibility of shifts derived in this way and also emphasises the need for making comparison in the same sample.

In the Table V.2 the changes in ^{119}Sn chemical shifts brought about by substitution of a proton by a deuteron are ca. 1 p.p.m. upfield (as is usually the case for the substitution of a heavier isotope), which is roughly the same magnitude as these observed for ^{19}F upon deuterium substitution for proton in some organic molecules containing ^{19}F.[27] However, these values are lower than those produced with ^{19}F-N.M.R. (ca. 2.5 p.p.m. for HF),[51] or with ^{31}P-N.M.R. (ca. 2.4 p.p.m. for $C_6H_5PD_2$, 1.30 for (iso-$C_3H_7)_2PD$).[35]

This difference in the shielding value (chemical shift) is of theoretical interest. Qualitatively it may be seen that the direction of the shift indicates a "greater electron donating power for deuterium than for proton".[61]

TABLE V.2

Deuterium isotope substitution effects on ^{119}Sn shifts and $'J(^{119}Sn\text{-}H)$ spin-spin coupling constants

Compound	$\Delta\delta\ ^{119}Sn$ (p.p.m.)	$\Delta\delta$ per ^{2}D (p.p.m.)	$'J(^{119}Sn\text{-}D)$ Hz	$'J^{*}(^{119}Sn\text{-}H)$ Hz	ΔJ Hz	$\frac{'J(^{119}Sn\text{-}H)}{'J(^{119}Sn\text{-}D)}$	Conditions
$(CH_3)_2{}^{119}SnD_2$	(2.50 ± 0.1)	(1.25)	274.5 ± 0.3	1789 ± 2	-8	6.55 ± 0.02	neat liquid at 27°C
$(CH_3)_2{}^{119}SnD_2$	2.12 ± 0.1	1.06	274.4 ± 0.5	1788 ± 3	-9	6.55 ± 0.02	in the same n.m.r. tube; 27°C
$(CH_3)_2{}^{119}SnHD$	1.0 ± 0.1	-	275.0 ± 0.5	1792 ± 3	-5	6.53 ± 0.02	in the same n.m.r. tube; 27°C

$$*J(^{119}Sn\text{-}H) = \left(\frac{\gamma_H}{\gamma_D}\right) 'J(^{119}Sn\text{-}D)$$

$\Delta\delta = \delta\ (CH_3)_2Sn^{119}H_2 - \delta(CH_3)_2SnD_2$ and all chemical shift differences are positive (up field shift)

$\Delta J = 'J^{*}\ (Sn^{119}\text{-}H) - J(^{119}Sn\text{-}H)$

γ_H/γ_D	"normal"	6.5137

The negative isotope effect $\Delta J = [{}^1J(Sn^{119}\text{-}D)\times\frac{\gamma_H}{\gamma_D}]-[{}^1J(Sn^{119}\text{-}H)]$ on the coupling constant ${}^1J(Sn^{119}\text{-}H)$ has been observed. The values of ${}^1J(Sn^{119}\text{-}D)$ listed in Table V.2 have been converted into ${}^1J^*(Sn^{119}\text{-}H)$ by assuming the validity of the following equation

$$J(HH) = \frac{\gamma_H}{\gamma_D} = 6.5137\ J(HD)$$

The values of ${}^1J(Sn^{119}\text{-}H)$ seem to be significantly greater than $6.5137 \times {}^1J(Sn^{119}\text{-}D)$. In the measurements of Borisenko et al, primary isotope effects (up to -5.0 ± 0.8 Hz) have been discovered for ${}^1J({}^{31}P\text{-}H)$ in both three and four coordinated phosphorous compounds. Recently Sergeyev et al [40] have reported the results of their theoretical calculations on ${}^1J({}^{13}C\text{-}H)$ at various ${}^{13}C\text{-}H$ distances in methane, changes of ca. 2Hz per 0.01 Å were predicted.

CHAPTER VI

RELAXATION

Section VI. 1 Introduction to Nuclear Relaxation

F. Bloch[108] at Stanford and F. M. Purcell[109] at Harvard discovered for the first time the phenomenon of nuclear magnetic resonance in bulk matter. F. Bloch[110] established his phenomenological equations. Then in 1948, N. Bloembergen[111] established theoretical expressions for relaxation times on a stochastic basis. These investigations were followed by several workers [112–115]. This early work was compiled into a book by Abragam[116] which still serves as the basis of the beginning of establishment of general formulae of relaxation.

If a collection of spin $I = \frac{1}{2}$ nuclei is placed in a static magnetic field B_o and this collection is at thermal equilibrium with the surroundings (lattice), then according to Boltzmann's distribution law, the ratio of the populations in these two states is

$$\frac{N_{upper}}{N_{lower}} = e^{-\Delta E/kT} = e^{-\gamma h B_o/kT}$$

ΔE for protons $\lesssim 5 \times 10^{-19}$ erg in 15000 Gauss

$T \lesssim 300$ Abs. (room temperature)

$$\therefore \quad \frac{N_{upper}}{N_{lower}} \lesssim e^{(-1.2 \times 10^{-5})}$$

$$\lesssim 1 - 1.2 \times 10^{-5}$$

which shows that there is a slight excess of nuclei in the low energy state (about 0.001%). It is this very small but finite excess of nuclei in the lower energy state that gives rise to net

absorption of energy in the radio frequency region. As the absorption of energy depends on the finite population difference between lower and upper states, this absorption will tend to equalise the population. If there is no energy transfer mechanism from the spin, the phenomenon of absorption would disappear altogether by saturation. In fact the upper state is able to lose energy without emitting radiation and the ways in which it does are known as relaxation processes. These characterise the return to equilibrium of the spin level populations following some perturbation.

In liquids, spins are not only submitted to the action of B_o and the r.f. field but also the action of neighbouring spins. Molecules in the sample are moving around very rapidly, giving rise to fluctuating electric or magnetic fields at the nucleus being observed. These local magnetic fields fluctuate according to the molecular motion and the frequency or variation of the interaction caused by such motion is referred to as modulation and is characterised by a correlation time, τ_c , which thus sets a time scale to the random fluctuations.

For any random motion there is a spectrum of frequencies of fluctuations but the variation and analysis of the intensity of the fluctuations and their frequency distribution depends on the exact type of motion concerned.

These different interactions permit the coupling of nuclear spins with the lattice, and allow the spin system to be in thermal equilibrium with the lattice. The study of these mechanisms responsible for relaxation is of fundamental importance in N.M.R.

VI.I.1 Longitudinal and Transverse Relaxation Times

It is not a single nuclear moment which we study but rather an ensemble containing a large number of identical nuclei. When a magnetic field B_o is applied, the magnetic moments start precessing around it and a net macroscopic magnetization M is oriented along the z axis. A finite period of time is required for M to grow to reach its equilibrium value M_o. It is called the longitudinal relaxation time, because it is a measure of the rate at which the magnetization M_z of the nuclear spin system approaches to its equilibrium value. In a sample a magnetic nucleus is subjected to fluctuating electric and magnetic fields. Each precessing nucleus has a magnetic vector component perpendicular to the main field. If two nuclei are very close this small rotating magnetic field is exactly what is required to induce a transition in the neighbouring nucleus. This natural exchange of spins shortens the life time of an individual precessing nuclei and they get out of phase with each other and thus it corresponds to the decay of the transverse components M_x and M_y of the magnetisation. Energy is transferred between spins in the system and the time constant is called T_2, the

spin-spin relaxation time or transverse relaxation time. It should be noted that it does not contribute to the maintenance of the required excess of nuclei in the lower state. The natural width of a line is inversely proportional to the average time the system spends in the excited state. Both T_1 and T_2 contribute to the width of a spectral line.

VI. I.2 The Bloch Equations

The macroscopic magnetisation M of a sample depends on the population difference of α and β spin states. The Z component of M can be written as

$$M_z = \gamma \hbar n$$

As the population difference n decays exponentially to equilibrium because of spin lattice relaxation, the rate of change can be expressed classically as

$$\frac{dn}{dt} = -\frac{n}{T_1}$$

or

$$\frac{dM_z}{dt} = -\frac{M_z}{T_1}$$

(since M_z is proportional to n)

This z component of magnetization tends to approach a steady state value M_o, we may express the relaxation of the z component towards its equilibrium value as

$$\frac{dM_z}{dt} = -\frac{M_z - M_o}{T_1}$$

Although, the M_x and M_y components decay exponentially with time is generally different

$$\frac{dM_x}{dt} = -\frac{M_x}{T_2}$$

and

$$\frac{dM_y}{dt} = -\frac{M_y}{T_2}$$

In a homogeneous static magnetic field $\underline{B}$ the equation of motion of the magnetic moment is

$$\frac{d\underline{M}}{dt} = \gamma \underline{M} \times \underline{B}$$

$$= \gamma (M_y B_z - M_z B_y)\, \underline{i} - \gamma (M_z B_x - B_z M_x)\, \underline{j}$$

$$- \gamma (M_x B_y - B_x M_y)\, \underline{k}$$

But the total magnetic field is a sum of the static field B_o along the Z axis and the magnetic vector of r.f. field B_1. B_1 is a rotating magnetic field in the x y plane at an angular velocity ω. Thus its components

$$B_x = B_1 \cos \omega t$$

$$B_y = -B_1 \sin \omega t$$

$$B_z = B_o .$$

Now the equation of the establishment of the resultant magnetic moment and accounting for relaxation as Bloch assumed, M_x and M_y decay back to their equilibrium value of zero, while M_z goes back to its equilibrium value M_o.

The final Bloch equations are then

$$\frac{dM_x}{dt} = \gamma (M_y B_o - M_z B_1 \sin\omega t) - \frac{M_x}{T_2}$$

$$\frac{dM_y}{dt} = \gamma (M_z B_1 \cos\omega t - M_x B_o) - \frac{M_y}{T_2}$$

$$\frac{dM_z}{dt} = \gamma (M_x B_1 \sin\omega t + M_y B_1 \cos\omega t) - \frac{M_z - M_o}{T}$$

In treating these equations, it becomes very helpful to refer the motion of magnetization in changed from fixed axes to a set of axes rotating at Larmor frequency about the z axis. In a rotating frame both B_o and B_1 are fixed.

The projection of M onthe x,y plane is resolved into two components u and v, along and perpendicular to B_1 respectively and in and out of phase with B_1.

Under "slow passage" conditions

$$u = M_o \frac{\gamma B_1 T_2^2 (\omega_o - \omega)}{1 + T_2^2(\omega_o - \omega)^2 + \gamma^2 B_1^2 T_1 T_2}$$

$$v = -M_o \frac{\gamma B_1 T_2}{1 + T_2^2(\omega_o - \omega)^2 + \gamma^2 B_1^2 T_1 T_2}$$

$$M = M_o \frac{1 + T_2^2(\omega_o - \omega)^2}{1 + T_2^2(\omega_o - \omega)^2 + \gamma^2 B_1^2 T_1 T_2}$$

When

$$\gamma^2 B_1^2 T_1 T \ll 1$$

The absorption signal

$$v = \frac{\gamma B_1 T_2}{1 + T_2^2 (\omega_o - \omega)^2}$$

In these conditions of non-saturation, the passage of spin from lower to higher energy state on the application of r.f. field being largely compensated by the inverse factor of relaxation. The shape of the absorption line is a Lorentzian. At the centre when the condition of resonance is exactly fulfilled,

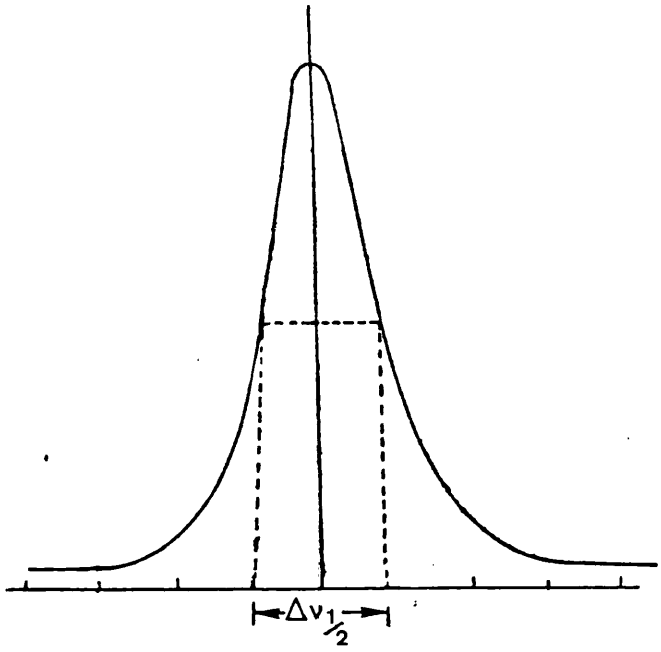

$(\omega_o \pm \omega) =$ zero and the signal height is proportional to $\gamma_1 B_1 T_2$, which means the line width must be inversely proportional to T_2

$$\text{or} \quad \delta\omega = \frac{2}{T_2}$$

$$\delta\nu = \frac{1}{\pi T_2} = \Delta\nu_{1/2}$$

Section VI. 2. The Correlation Function.

In the study of turbulent motion and other problems in which the quantity of interest is a stationary random function of space and time coordinates, the statistical description can be expressed in terms of correlation functions. They are the probability distribution for the quantity for all points in space-time.

In a fluid due to motion of molecules, the position of a molecule is a variable function y (t) whose value depends on low probability

$$P\ (y,\ t)$$

The mean position at instant t can be obtained by integrating over the space

$$\overline{y}\ (t) = \int P\ (y, t)\ dy$$

Defined in the same way is the same function

$$P\ (y_1,\ t_1,\ y_2,\ t_2)$$

the probability that at time t_i , $y = y_1$ and at t_2 $y = y_2$. This probability is equal to one if $y_1 = y_2$ (no movement) and zero if there is no relationship between the position. The average value of the fluctuating field f (y) at position y in the lattice at time t is given by

$$\overline{f}(t) = \int P\ (y, t)\ \ f\ (y)\ dy$$

Now what we want to know is the correlation which exists between the values of the randomly variable functions f (y) at two instants t_1 and t_2. This is represented by the correlation function

$$G(t_1, t_2) = \overline{f(t_1)\ f^*(t_2)}$$

(f^* is the complex conjugate of f and the bar denotes the average behaviour of an ensemble of nuclei).

or

$$G(t_1\ t_2) = \iint P(y_1, t_1; y_2, t_2)\ f(y_1)\ f^* y_2\ dy_1\ dy_2$$

The form of autocorrelation depends on the physical model chosen to describe the movements in solution. We shall suppose that we deal with a stationary random process which does not depend at all upon the origin in time but only on the difference of time, i.e.

$$\tau = t_2 - t_1$$

and the function of autocorrelation becomes

$$G(\tau) = \iint (y_1\ y_2\ \tau)\ f(y_1)\ f^*(y_2)\ dy_1\ dy_2$$

The correlation function $G(\tau)$ can be related to a correlation time τ_c which is a measure of the length of time over which significant correlation persists. In the situation where reorientations may be taken as isotropic, B.P.P. have shown that $G(\tau)$ can be described by a unique exponential

$$G(\tau) = G(0) \exp\left(-|\tau| / \tau_c\right)$$

If the orientations are anisotropic the autocorrelation function is expressed as a function of three diffusion constants D_x D_y and D_z and is no longer a simple exponential.

By the Fourier Transformation of G (τ) we can determine the motional frequencies and their intensities

$$J(\omega) = \int_{-\infty}^{+\infty} G(\tau) \exp(-i\omega\tau) d\tau$$

and the inverse transform gives

$$G(\tau) = \frac{1}{2\pi} \int_{-\infty}^{+\infty} J(\omega) \exp(i\omega t) d\omega$$

Section VI.3. The Spectral Density Function and Correlation time

Figure VI shows a plot of variation of spectral density function J (ω) of the random fluctuations against the frequency (ω) where ω_o is the nuclear resonance frequency and it will be seen that relative magnitudes of ω_o and $1/\tau_c$ determine the efficiency of spin lattice relaxation.

The dotted line is plotted for $\omega_o \tau_c \approx 10^{-3}$

The solid line is for $\omega_o \tau_c \approx 1$

and dashed line for $\omega_o \tau_c \approx 10^3$

The area under these curves is equal, since the energy associated with molecular motion is constant. Changes in τ_c merely modify the distribution of power in the frequency spectrum.

When the value of τ_c is long, low motional frequencies have a very high probability and higher frequencies will

Fig. VI.

Plot of spectral density $J(\omega)$ versus frequency (ω),

Horizontal scale is logarithmic.

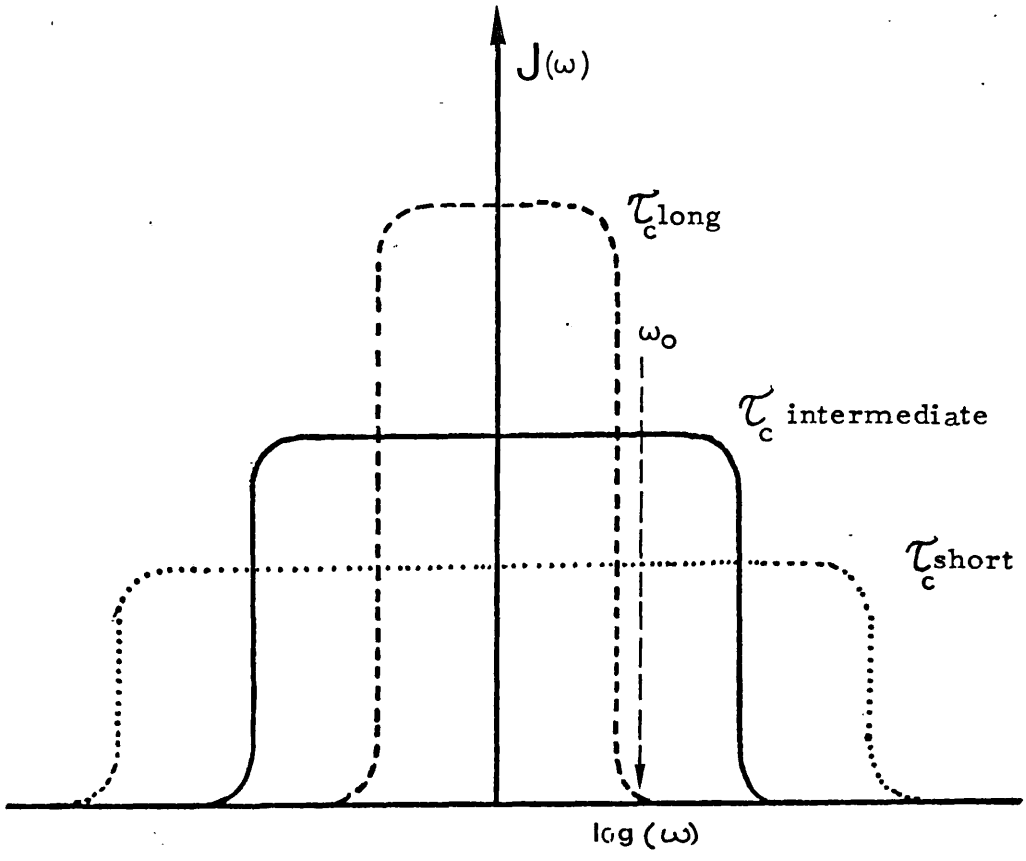

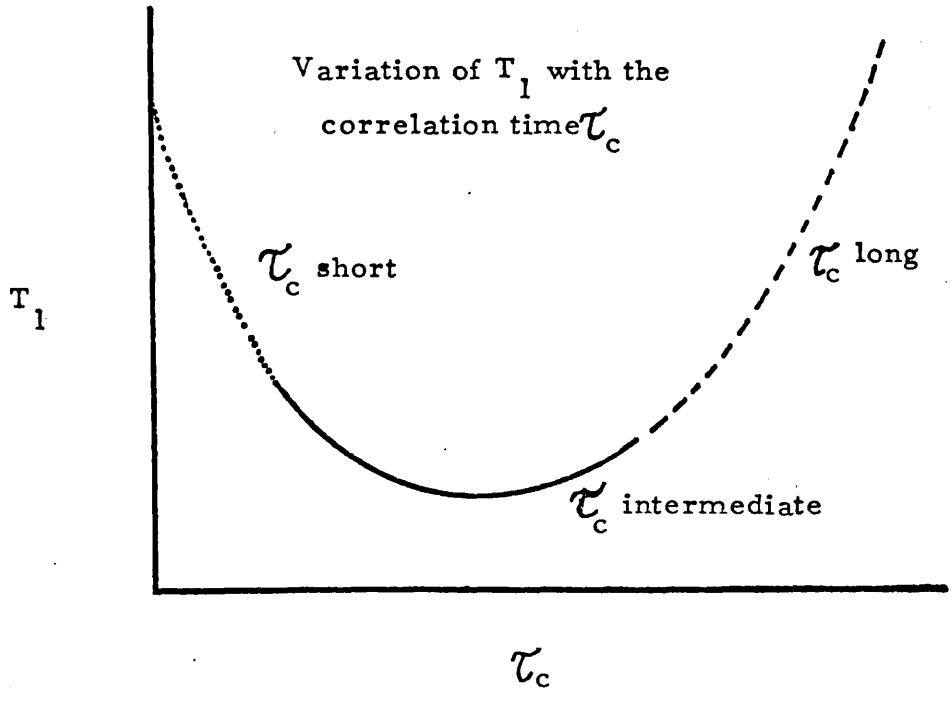

be almost totally absent. The spectral density J (ω) will be very small near the Larmor frequency ω_o; spin lattice relaxation will be inefficient and T_1 will be long. As τ_c becomes smaller, the spectral density function moves out to higher frequencies, and T_1 becomes shorter. In the intermediate region where $\omega_o \tau_c \simeq 1$, the motional components at ω_o will be the largest. When τ_c is very short, the spectral density moves to higher frequencies such that J (ω) is very small near the Larmor frequency-relaxation is inefficient and T_1 becomes longer.

A plot of variation of T_1 with the correlation time τ_c is shown in Figure VI. With increasing temperature, τ_c becomes shorter (more rapid molecular motion). Depending on the region of τ_c, T_1 may increase or decrease. In the normal situation in liquids where $\omega_o \tau_c \ll 1$ and T_1 is seen to increase with temperature.

Section VI. 4. Extreme Narrowing

In a liquid the fluctuating field usually varies rapidly compared to the precessional frequency of the nucleus under observation. Typical values for a small molecule are ca. 10^{-12} s for τ_c and 10^8 rads^{-1} for ω_o so that

$$\omega_o \tau_c \ll 1$$

which is the so-called case of extreme narrowing. This corresponds to the short τ_c situation in Figure VI.

Section VI. 5 . 1 The Density Matrix Operator

The mathematical development of B.P.P.[111] theory is based on Bloch's phenomenological equations and the system is described in terms of populations of its energy levels. A quantum mechanical treatment of spins in a lattice, based on the approximation of the equation of motion of the density matrix was developed by Bloch and Wangsness[117,118] and extended by Bloch[119] and Redfield[120]. In the liquid state N.M.R. experiment this treatment is very useful, since the spin couplings within the molecule are stronger than the couplings to the lattice and molecules may be regarded as separate units.

We may define the density matrix operator as a statistical operator which relates the average behaviour of one molecule to the measured values of a property of an ensemble of systems. It contains the information necessary to describe an ensemble of identical systems and its time dependence.

The approximation is restricted in its application to liquids where the correlation time is very short and molecular collisions weak in the sense that they do not change the density matrices to a considerable extent.

In a system described by a wave function, ψ, at some instant of time, the expectation value of an operator $\hat{M}$, is given by

$$\langle M \rangle = \langle \psi^* | \hat{M} | \psi \rangle \quad \text{---------- 1}$$

(The expectation value of a function of variate is the mean value in repeated sampling). Now, if we expand ψ as a linear combination of time independent orthonormal functions ϕ_n, then

$$\psi = \sum_n C_n \phi_n \text{----------2}$$

The expectation value of M can be written as

$$\langle \hat{M} \rangle = \sum_{n,m} {}^*C_m C_n \langle m \mid \hat{M} \mid n \rangle \text{---------3}$$

If we consider wave function ψ' different from ψ, $\langle M' \rangle$ will be different from $\langle \hat{M} \rangle$ because of different coefficients but the matrix elements will be the same. Conversely, the expectation value of an operator N is calculated with the same ${}^*C_m C_n$ but different matrix elements.

The coefficients ${}^*C_m C_n$ can conveniently be written in a matrix form, defining an operator P as

$${}^*C_m C_n = \langle n \mid \hat{P} \mid m \rangle \text{----------4}$$

It is possible now to write equation 3 in the form

$$\langle \hat{M} \rangle = \sum_{m,n} \langle n \mid \hat{P} \mid m \rangle \langle m \mid \hat{M} \mid n \rangle \text{---------5}$$

The system under consideration is a superposition of different systems described by wave functions. The average value of the operator $\hat{M}$ is obtained by finding the average value of the operator calculated for each individual system.

If we use a bar to denote an ensemble average, equation 5 can be written as

$$\overline{\langle M \rangle} = \sum_{m,n} \overline{\langle n \mid \hat{\rho} \mid m \rangle} \langle m \mid \hat{M} \mid n \rangle \text{ ---------6}$$

If we define

$$\overline{\langle n \mid \hat{\rho} \mid m \rangle} = \langle n \mid \hat{\rho} \mid m \rangle \text{ ----------7}$$

where $\hat{\rho}$ is the density matrix operator, which is the average of average value of the operator $\hat{P}$, we have then

$$\begin{aligned} \overline{\langle M \rangle} &= \sum_{m,n} \langle n \mid \hat{\rho} \mid m \rangle \langle m \mid \hat{M} \mid n \rangle \\ &= \text{Tr } \hat{\rho}\hat{M} \\ &= \text{Tr} \left[\hat{M}\hat{\rho} \right] \text{ ----------8} \end{aligned}$$

(Tr, denotes the trace, the sum of the diagonal elements of the matrix $\left[\hat{M}\hat{\rho}\right]$). This means that the average of average value of the operator M acting on the system is equal to the trace of the matrix product $\left[\hat{M}\hat{\rho}\right]$. In their use, we shall omit the bar indicating an ensemble average, keeping in mind that the density matrix is an average of average values.

Section VI.5.2 The Time Dependence of the Density Matrix

So far we have neglected the time dependent properties of the density matrix. In a liquid due to random molecular motion, modulating nuclear interactions, the states of nuclei become time dependent. An equation is now found to

describe the time dependence of the density matrix when the system is acted upon by a time dependent perturbation.

Introducing time dependence in equation 2 we can write

$$\psi(t) = \sum_n C_n(t) \quad \Phi_n \qquad \text{----------9}$$

where Φ_n are the time independent eigenfunctions of the system and $C_n(t)$ are the complex time dependent constants. Substituting into Schrodinger's time dependent equation

$$\left(-\frac{\hbar}{i}\frac{\partial \psi}{\partial t} = \hat{\mathcal{H}}\psi\right)$$

we obtain

$$-\frac{\hbar}{i}\sum_n \frac{\partial c_n}{\partial t}\Phi_n = \hat{\mathcal{H}}\sum_n c_n \Phi_n \qquad \text{----------10}$$

multiplying by Φ_m^* and integrating, and using the fact that

$$\int \Phi_m^* \Phi_n \, dt = \delta_{mn}$$

where δ mn is the Kronecker delta function which is equal to one when m = n and zero when $m \neq n$. The result can be written as

$$-\frac{\hbar}{i}\frac{\partial c_m}{\partial t} = \sum_n c_n \langle m | \hat{\mathcal{H}} | n \rangle \qquad \text{----------11}$$

We have defined already that

$$\langle m | \hat{\rho} | n \rangle = c_m^* \, c_n$$

on differentiation

$$\frac{\partial}{\partial t}\langle m|\hat{\rho}|n\rangle = c_n \frac{\partial c_m^*}{\partial t} + \frac{\partial c_n^*}{\partial t} c_m \quad \text{--------12}$$

substituting equation 11 into 12

$$\frac{\partial}{\partial t}\langle m|\hat{\rho}|n\rangle = \frac{i}{\hbar}\sum_n \left[c_m c_n \langle n|\hat{\mathcal{H}}|m\rangle - \langle m|\hat{\mathcal{H}}|n\rangle c_n c_m \right] \text{-------13}$$

and defining $\hbar\hat{\mathcal{H}}$ as the spin Hamiltonian it can be written that

$$\frac{\partial\hat{\rho}}{\partial t} = i\left\{\hat{\rho}, \hat{\mathcal{H}}\right\} = -i\left\{\hat{\mathcal{H}}, \hat{\rho}\right\} \quad \text{----------14}$$

where $\{\hat{\mathcal{H}}, \hat{\rho}\}$ is the commutator of two operators. The equation expresses the time dependence of the density matrix and can be solved if the Hamiltonian is independent of time. By using the exponential operators one can obtain the formal solution to the equation of motion.

$$\hat{\rho}(t) = e^{(-i\hat{\mathcal{H}}t)}\, \rho(o)\, \exp(i\hat{\mathcal{H}}t) \quad \text{----------15}$$

In an N.M.R. experiment, the Hamiltonian consists of two parts, the time independent $\hat{\mathcal{H}}_o$, which represents the interaction of nuclei with the static magnetic field, and the $\hat{\mathcal{H}}_1(t)$ represents the time dependent part which can be split into two parts, one describes the interaction of nuclei with the rotating magnetic field, the second part expresses the interaction among nuclei and

with the surroundings, which becomes time dependent due to molecular motion.

If we define a quantity $\hat{\rho}^*$ by the equation 16

$$\hat{\rho}^*(t) = \exp(-i\hat{\mathcal{H}}_0 t)\ \hat{\rho}(t)\ e^{i\mathcal{H}_0 t} \quad \text{----------16}$$

and rewriting the Hamiltonian in equation 14 we have

$$\frac{\partial \hat{\rho}}{\partial t} = -i\left\{\hat{\mathcal{H}}_0 + \hat{\mathcal{H}}_1(t), \rho\right\} \quad \text{----------17}$$

where

$$\hat{\mathcal{H}}_1(t) = e^{-i\hat{\mathcal{H}}_0 t}\ \hat{\mathcal{H}}_1^*(t)\ e^{i\hat{\mathcal{H}}_0 t} \quad \text{----------18}$$

This representation of the operators $\hat{\rho}^*(t)$ and $\hat{\mathcal{H}}(t)$ is known as the interaction representation. Substituting the equation 16 into the left-side of equation 17 gives us the time differential equation obeyed by $\hat{\rho}$

Removing the commutator of $\hat{\rho}$ with $\hat{\mathcal{H}}_0$ from both sides and multiplying the left hand side by $e^{i\mathcal{H}_0 t}$ and R.H.S. by $e^{-i\hat{\mathcal{H}}_0 t}$ we get

$$\frac{\partial \hat{\rho}^*}{\partial t} = -i\left\{\hat{\mathcal{H}}_1^*(t), \hat{\rho}\right\} \quad \text{----------19}$$

integrating it by successive approximation up to the second order, then taking the time derivative

$$\frac{d\rho^*}{dt} = -i\left[\hat{\mathcal{H}}_1^*(t), \hat{\rho}_{(0)}^*\right] - \int_0^t dt\left[\hat{\mathcal{H}}_1^*(t), \hat{\rho}_{(0)}^*\right] \quad \text{----------20}$$

This is the master equation for the time dependence of the density matrix which is equivalent to ordinary second order time dependent perturbation theory.

The average ensemble behaviour of spins can be described by an average density operator, assuming that the Hamiltonian describing the spin lattice interactions is random and its average value is zero, i.e. $\overline{\hat{\mathcal{H}}_1(t)} = 0$. , and neglecting any correlation between $\hat{\mathcal{H}}_1(t)$ and $\hat{\rho}^*$.

Extending the upper limit of the integral to $+\infty$, the equation of motion for the average density matrix becomes

$$\frac{d\hat{\rho}^*}{dt} = -\int_0^{\infty} \left[\hat{\mathcal{H}}_1(t), \left[\hat{\mathcal{H}}_1(t-\tau), \hat{\rho}^*(t)\right]\right] d\tau \qquad \text{----------21}$$

Section VI. .3 The Operator Form of the Master Equation

The randomly variable Hamiltonian $\hbar\hat{\mathcal{H}}_1(t)$ which contains the spin variables and the lattice functions can be written as

$$\hat{\mathcal{H}}_1(t) = \sum_q F^{(q)}(t)\, A^{(q)} \qquad \text{----------22}$$

where $F^{(q)}(t)$ are time dependent randomly variable functions of position and $A^{(q)}$ are the spin operators acting on the system. The product $F^{(q)}(t)\, A^{(q)}$ is hermitian because the operator $\mathcal{H}_1(t)$ is hermitian, an assumption is made that $F^{(-q)} = (F^{(q)})^*$ and $A^{(-q)} = (A^{(q)})^{\neq}$ where asterisk and $\neq$ signifies the complex conjugate and hermitian conjugate respectively.

The Hamiltonian form of $\hat{\mathcal{H}}^{*}(t)$ is given by

$$\hat{\mathcal{H}}_1^{*}(t) = e^{-i\hat{\mathcal{H}}_o t}\ \hat{\mathcal{H}}_1^{*}\ e^{i\hat{\mathcal{H}}_o t}$$

$$= F^{(q)}\ A^{(q)}\ e^{i\omega^{(q)} t} \qquad \text{----------23}$$

with $\omega^{(q)} = \omega^{(-q)}$

Defining an autocorrelation function

$$g_{qq'} = \overline{F^{(q)}(t)\ F^{(q')}(t-\tau)} \qquad \text{----------24}$$

By substituting 22 and 23 into 21 we obtain the master equation in the operator form

$$\frac{d\rho^{*}}{dt} = -\frac{1}{2}\sum_q \left[A^{(-q)}, \left[A^{(q)}, \rho(t)\right]\right] \int_0^{\infty} g_q(\tau)\, e^{-i\omega^{(q)} t}\, d\tau$$

$$= -\frac{1}{2}\sum_q J_q(\omega)^{(q)} \left[A^{(-q)}, \left[A^{(q)}, \rho(t)\right]\right] \qquad \text{----------25}$$

where $J_q(\omega)^{(q)}$ are the spectral densities obtained by the Fourier transformation of the autocorrelation function of $F^{(q)}$.

Section VI 5.4 Macroscopic Differential Equations.

According to the properties of the density matrix, as defined earlier, the average value of an operator acting on a macroscopic system is given by

$$q(t) = \langle \hat{M} \rangle = Tr \left\{\hat{M}\hat{\rho}\right\}$$

or

$$q^{*}(t) = \langle \hat{M}^{*} \rangle = Tr \left\{\hat{M}\hat{\rho}^{*}\right\}$$

The equation of motion of the average density Matrix 21 is multiplied on both sides by M and we get an equation of motion for $\langle \hat{M}^{*} \rangle$ as

$$\frac{dq^*}{dt} = -(b^* - b_o^*) \qquad \text{----------26}$$

where $b^* = \langle B^* \rangle = \text{Trace} \{\hat{B}^* \rho\}$

$b_o = \text{Tr} \{B \rho_o\}$

and $B = \int_o^\infty \frac{}{[\mathcal{H}_1(t-\tau), [\mathcal{H}_1(t), M]] d\tau}$

expanding $\hat{\mathcal{H}}_1(t)$ as in 23 and following it up to 25 it is possible to write

$$B = \tfrac{1}{2} \sum_q J_q(\omega)^q [A^{(q)}, [A^{(-q)}, M]] \qquad \text{------27}$$

In the case of extreme narrowing the equation is simplified as

$$B_{\substack{\text{extreme} \\ \text{narrowing}}} = \tfrac{1}{2} \sum_q J_q(o) [A^{(q)}, M] \qquad \text{-------28}$$

Defining the Bloch's longitudinal relaxation time equation 26 can be written as

$$\frac{d\langle I_z \rangle}{dt} = \frac{(\langle I_z \rangle - I_o)}{T_1}$$

and replacing operator $\hat{M}$ by an operator $\hat{I}_z$ in the equation 28, the expression can be written as

$$\frac{1}{T_1} = \tfrac{1}{2} \sum_q J^{(q)}(\omega)^{(q)} [A^{(q)}, [A^{(-q)}, I_z]] \qquad \text{----------29}$$

T_2, is also obtained from 29 by replacing $\hat{I}_z$ by $\hat{I}_x$.

CHAPTER VII

MECHANISMS OF RELAXATION IN LIQUIDS

In general, any mechanism capable of producing fluctuating magnetic fields is a possible mechanism for relaxation. Nuclear magnetic relaxation may be characterised by a time constant T, which is related to the microdynamic behaviour of molecules in liquids described by a time dependent function f (t). It is possible to write

$$\frac{1}{T_1} = E^2 f(t)$$

where E, is the energy of the particular interaction. The possible mechanisms for the relaxation are discussed in the following sections.

The time dependent function f (t) is a complex function of intra and intermolecular rotational and translational motions. In the general case, molecular reorientations are anisotopic and the form of f (t) depends on the reorientational model used to describe the molecular motion (e.g. Rotational Diffusion, Inertial Rotation, conditional rotational diffusion and conditional inertial rotation).

In the simplest case that of isotropic motion f (t) represents the correlation time τ_c defined as the "average" time between molecular collisions for a molecule in some state of motion.

Due to random motion of molecules in a liquid sample, there exists a spectrum of molecular motional frequencies. The components of this spectrum vary from zero to 10^{12} Hz. The intensity of these components as a function of frequency is referred to as the spectral density $J(\omega)$. It is the fluctuating magnetic

fields associated with these motional frequencies that provide the mechanisms for nuclear spin relaxation. For spin lattice relaxation the components at the Larmor frequency ω_o and $2\omega_o$ are effective since for a spin lattice relaxation mechanism there must be an interchange of energy between the spin system and the lattice.

Section VII.1. Dipole Dipole Relaxation

Consider two spin ½ nuclei I and S at a distance r apart, in the same molecule and subjected to a static magnetic field. The nucleus I is not only experiencing the applied field but also a small local field due to the dipole of nucleus S. The magnitude of this local field depends on the magnetic moment of nucleus S, r, and the angle θ, which is the angle between the applied field and vector joining I and S. As the molecule moves about, θ becomes a time dependent function and gives rise to a fluctuating magnetic field which provides a mechanism for nuclear spin relaxation.

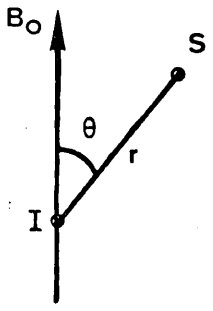

The quantitative derivation usually is based on some form of time dependent perturbation theory. The most usual methods of approach are those of the semi-classical density operator technique[116,122] and the linear response theory of Kubo

and Tomita.[113] In their classic paper on nuclear magnetic relaxation B.P.P.[111] used ordinary time dependent perturbation theory.

The energy of interaction between two spins I and S can be written in the form of the Hamiltonian

$$\hat{\mathcal{H}}_{DD} = \gamma_I \gamma_S \hbar^2 \left[\frac{\hat{\underline{I}}_I \hat{\underline{I}}_S}{r^3} - \frac{3(\hat{\underline{I}}_I \cdot \underline{r})(\hat{\underline{I}}_S \cdot \underline{r})}{r^5} \right]$$

It is convenient to split $\hat{\mathcal{H}}_{DD}$ into its various parts. This is done be expressing the above equation in spherical coordinates and rewriting the operators $\hat{I}_x, \hat{I}_y$ and $\hat{I}_z$ in terms of raising and lowering operators

$$\hat{\mathcal{H}}_{DD} = \frac{\gamma_I \gamma_S \hbar^2}{r^3} \left[A + B + C + D + E + F \right]$$

where

$$A = (1 - 3\cos^2\theta)\, \hat{I}_z \hat{S}_z$$

$$B = \frac{1}{4}(1 - 3\cos^2\theta) \left[\hat{I}^+ \hat{S}^- - \hat{I}^- \hat{S}^+ \right]$$

$$C = \frac{3}{2} \sin\theta \cos\theta\, e^{-i\phi} \left[\hat{I}_z \hat{I}^+ + \hat{I}^+ \hat{S}_z \right]$$

$$D = \frac{3}{2} \sin\theta \cos\theta\, e^{+i\phi} \left[\hat{I}_z \hat{S}^- + \hat{I}^- \hat{S}_z \right]$$

$$E = -\frac{3}{4} \sin^2\theta\, e^{-2i\phi}\, \hat{I}^+ \hat{S}^+$$

$$F = -\frac{3}{4} \sin^2\theta\, e^{+2i\phi}\, \hat{I}^- \hat{S}^-$$

where θ , ϕ and r are the usual spherical coordinates in which B_o is along the positive z direction.

The time dependent Hamiltonian may be written:-

$$\hbar \hat{\mathcal{H}}_{DD} = \sum_q A^{(q)} F^{(q)}_{(t)}$$

where $F^{(q)}_{(t)}$ are randomly variable the function of position (r, θ and ϕ), and $A^{(q)}$ terms are spin operators acting on spin variables given by

$$F^{(1)} = \frac{\text{Sin}\,\theta \quad \text{Cos}\,\theta \quad e^{-i\phi}}{r^3}$$

$$F^{(2)} = \frac{\text{Sin}^2\,\theta \quad e^{-2\,i\phi}}{r^3}$$

$$F^{(0)} = \frac{1 - 3\,\text{Cos}^2\theta}{r^3}$$

and

$$A^0 = a \left[-\frac{2}{3} \hat{I}_z \hat{S}_z + \frac{1}{6} (\hat{I}_+ \hat{S}_- + \hat{I}_- \hat{S}_+) \right]$$

$$A^{(1)} = a \left[\hat{I}_z \hat{S}_+ + \hat{I}_+ \hat{S}_z \right]$$

$$A^{(2)} = \tfrac{1}{2}\, a\, \hat{I}_+ \hat{S}_+$$

where $a = -\frac{3}{2}\ \gamma_I\ \gamma_S\ \hbar$

Relaxation times are related to the average behaviour of an ensemble of nuclei and we are interested in the average persistence in time of any given arrangement of nuclear moments relative to each other. The correlation functions give us this information. In general it is assumed that the motion of molecules in fluids is statistically stationary. This means that the value of a particular correlation function depends only on the difference between time t and $(t + \tau)$ and not on the absolute value of t. The correlation function can be written as (see section V.2.1).

$$G(\tau) = F_q(t)\ F^*(t+\tau)$$

$$G(\tau) = F^{(q)}_{(t)}\ F^{*(q)}_{(t)}\ \exp(-\tau/\tau_c)$$

The Fourier Transform gives the spectral density function

$$J(\omega) = \int_{-\infty}^{+\infty} G(\omega)\ \exp(-i\omega\tau)\, d\tau$$

We are particularly interested in the average way in which nuclei move about, the correlation functions $G_o(\tau)$, $G_1(\tau)$ and $G_2(\tau)$ give this information, can be written as

$$G_q(\tau) = G_q(o)\ \exp(-\tau/\tau_c)$$

where

$$G(o)_{(q)} = \overline{F^{q}{}_{(t)}{}^2} = \overline{F^2(q)}$$

$$= \int_o^{2\pi} \int_o^{2\pi} F_q^2\ \sin\theta\ d\theta\ d\phi$$

straightforward integration gives

$$\left.\begin{aligned} G_o(o) &= \frac{12}{15}\ r^{-6} \\ G_1(o) &= \frac{2}{15}\ r^{-6} \\ G_2(o) &= \frac{8}{15}\ r^{-6} \end{aligned}\right\} \qquad \text{----------2}$$

as described previously we can determine the motional frequencies and their intensities present in the correlation function. That is

$$J_q(\omega) = \int_{-\infty}^{+\infty} G_q(\tau)\ \exp(i\omega\tau)\, d\tau$$

$$= \int_{-\infty}^{+\infty} G_q(o)\ \exp(-\tau/\tau_c)\ \exp(i\omega\tau)\, d\tau \quad \text{----3}$$

By substituting equation (2) into equation (3) and integrating

$$J_o(\omega) = \left(\frac{24}{15r^6}\right)\left(\frac{\tau_c}{1+\omega^2\tau_c^2}\right)$$

$$J_1(\omega) = \left(\frac{4}{15r^6}\right)\left(\frac{\tau_c}{1+\omega^2\tau^2}\right)$$

$$J_2(\omega) = \left(\frac{16}{15r^6}\right)\left(\frac{\tau_c}{1+\omega^2\tau_c^2}\right)$$

The spin lattice relaxation time T_1^I is calculated by writing equation (26) as

$$\frac{d\langle I_z\rangle}{dt} = -(b_z^I - b_o^I)$$

and we know that

$$b_z^I = \langle {}^*B_z^I \rangle = Tr\{B_z \rho^*\}$$

According to equation (27), B_z^I can be written for two unlike spins I and S as

$$B_z^I = \frac{a^2}{72} J^{(o)}(\omega_I - \omega_S)\left[\hat{I}_-\hat{S}_+, \left[\hat{I}+\hat{S}_-, \hat{I}_z\right]\right] + h.c.$$

$$+ a^2 J^{(1)}(\omega)_I \left[I_-S_z, \left[\hat{I}_+\hat{S}_z, \hat{I}_z\right]\right] + h.c. +$$

$$+\frac{a^2}{4} J^{(2)}(\omega_I + \omega_S)\left[\hat{I}_-\hat{S}_-, \left[\hat{I}_+\hat{S}_+, \hat{I}_z\right]\right] + h.c.$$

If we consider the case of two like spins it becomes easier to derive the equation of motion for the quantities $\langle I\rangle$ and $\langle S\rangle$ together; we can write

$$\frac{d}{dt}\langle I_z + S_z\rangle = -(b_z - b_o)$$

where $b_z = Tr\{B_z \rho^*\}$

writing $S_z = I_z'$ for like spins

$$B_z = \tfrac{1}{2} J^{(1)}(\omega_I)\left[A^{(-1)}, \left[A^{(1)}, I_z + I_z'\right]\right] + h.c. +$$

$$+ \tfrac{1}{2} J^{(2)}(2\omega_I)\left\{\left[A^{(2)}, \left[A^{(2)}, I_z + I_z'\right]\right] + h.c.\right.$$

where h.c. = hermitian conjugate

With the help of standard commutation relations, we get

$$\left[A^{(-1)}, \left[A^{(1)}, I_z + I'_z \right] \right]$$

$$= 2a^2 I_z I'^2_z + 2a^2 I'_z I^2_z - a^2 (I_+ I'_- + I_- I'_+)(I_z + I_z),$$

$$\left[A^{(-2)} \left[A^{(2)}, I_z + I'_z \right] \right]$$

$$= a^2 I_z (I'^2_x + I'^2_y + I'^2_z) + a^2 I'_z (I^2_x + I^2_y + I^2_z)$$

$$B_z \approx \frac{2a^2}{3} I(I+1) \langle I_z + I'_z \rangle \left\{ J^{(1)}_{(\omega_I)} + J^{(2)}_{(2\omega_I)} \right\}$$

The macroscopic equation for T_1 has the form

$$\frac{d}{dt} \langle I_z + I'_z \rangle = -\frac{1}{T_1} \left\{ \langle I_z + I'_z \rangle - \langle I_z + I'_z \rangle_o \right\}$$

where $$\frac{1}{T_1} = \frac{3a^2}{2} I(I+1) \left\{ J^{(1)}_{(\omega_I)} + J^{(2)}_{(2\omega_I)} \right\}$$

$$= \frac{3}{2} \gamma^4 \hbar^2 I(I+1) \left\{ J^{(1)}_{(\omega_I)} + J^{(2)}_{(2\omega_I)} \right\}$$

For intermolecular motion the values of $J_q(\omega)$ are given by equation

are valid, we can write

$$\frac{1}{T_1} = \frac{3\gamma^4 \hbar^2 I(I+1)}{10 r^6} \left[\frac{\tau_c}{1 + \omega_o^2 \tau_c^2} + \frac{4\tau_c}{1 + 4\omega_o^2 \tau_c^2} \right]$$

In the case of extreme narrowing when $T_1^{-1} = T_2^{-1}$ and the frequency term in the denominator can be neglected

$$\therefore \quad \frac{1}{T_1} = \frac{1}{T_2} = \frac{3}{2} \frac{\gamma^4 h^2}{r^6} \tau_c$$

Following the same procedure for two unlike spins I and S we arrive at

a similar equation for the spin lattice relaxation

time of spin I, we get

$$\frac{1}{T_1}I = \gamma_I^2 \gamma_S^2 \hbar^2 S(S+1)\left\{ \tfrac{1}{2} J_o(\omega_I - \omega_S) + \frac{3}{2} J_1(\omega_I) + 3/4\, J_2(\omega_I + \omega_S) \right\}$$

evaluating the spectral densities and applying the condition of extreme narrowing we can write

$$\frac{1}{T_1}I = \frac{1}{T_2}I = \frac{\gamma_I^2 \gamma_S^2 h^2}{r^6} \tau_c$$

comparing the T_1 values in case of like and unlike spins it is found that

$$\left(\frac{1}{T_1}\right)_{like} \Big/ \left(\frac{1}{T_1}\right)_{unlike} = \frac{3}{2}$$

This is known as the 3/2 effect.

Both translational and rotational motions contribute to the spin lattice relaxation, the former being mainly responsible for the interactions between spins in different molecules, the latter for the interactions between spins in the same molecule. The term rotation corresponds to intramolecular mechanism and the translation corresponds to an intermolecular mechanism.

Section VII 2.1 Scalar Relaxation

In the case of spin-spin coupling of two nuclei I and S (where $I = \frac{1}{2}$ and $S > \frac{1}{2}$) inside a molecule, the interaction is described as

$$\hat{\mathcal{H}}_{S.C.} = \hbar \hat{\underline{I}} \cdot \mathcal{A} \cdot \hat{\underline{S}}.$$

where $\mathcal{A}$ is a spin coupling interaction tensor. In liquids due to isotropic motion, the components of the tensor are averaged out and

we can write that

$$A = \frac{1}{3} \text{ Tr } [\mathcal{A}]$$

Now, the Hamiltonian can be represented as

$$\mathcal{H}_{S.C.} = \hbar \text{ I.A.S}$$

where A is the coupling constant in rad S^{-1}. Suppose that the magnitude of coupling $\hbar$ A is such that $| \gamma_I - \gamma_S | \text{ Bo} \gg A$.

In a static magnetic field Bo both spins are quantized, ignoring all other interactions, the total Hamiltonian for these two spins is given by

$$\mathcal{H} = -\hbar \gamma_I . \text{Bo} . \hat{\underline{I}} - \hbar \gamma_S . \text{Bo} . \hat{\underline{S}} - \hbar A . \hat{\underline{I}} . \hat{\underline{S}} \qquad (1)$$

$$= -\hbar \gamma_I \text{ Bo } \hat{I}_z - \hbar \gamma_S \hat{S} . \text{Bo} - \hbar A [\hat{I}_x \hat{S}_x + \hat{I}_y \hat{S}_y + \hat{I}_z \hat{S}_z]$$

changing $I_z = \pm 1$, the Hamiltonian becomes

$$= -\gamma_I \hbar (\hat{I}_z - 1) \text{ Bo} - \gamma_S \hbar \hat{S}_z \text{Bo} - \hbar A [\hat{I}_x \hat{S}_x + \hat{I}_y \hat{S}_y + (\hat{I}_z - 1)\hat{S}_z] \qquad (2)$$

the energy change ΔE of the spin I, is given by

$$\Delta E = \hbar \gamma_I \text{ Bo } + h \text{ A } \hat{S}_z$$

Since S_z is quantized as well there are (2S + 1) energy levels separated by $\hbar$ A.

The Scalar coupling becomes a mechanism of spin relaxation when it is modulated at a rate greater than A. This occurs, when the relaxation time of S is short compared with the 1/A then the local fluctuating field at the nucleus I by nucleus S has a correlation time equal to T_1^S. In this event only the average value of the spin coupling interaction

is "seen" by nucleus I and its spectrum is averaged to one broad line instead of expected mutiple structure.

The modulation of scalar coupling can occur by either of the following two ways Fig (a) and (b).

1. Spin S is time dependent due to chemical exchange (scalar relaxation of the first kind) see fig. a.
2. A is time dependent, due to fast relaxing coupled nucleus/nuclei, (scalar relaxation of the second kind) see fig. b.

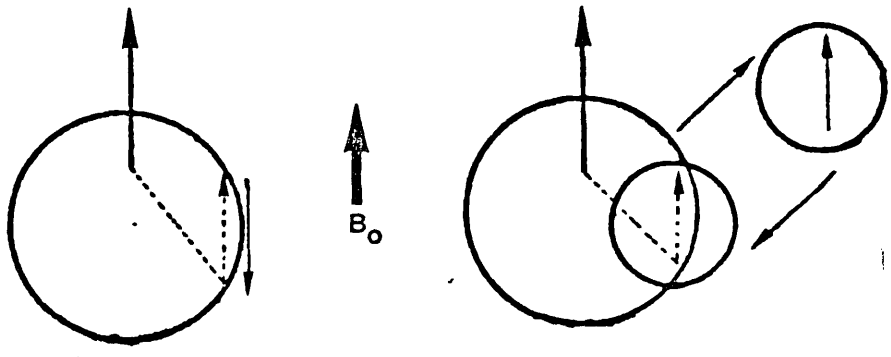

(b) One nucleus relaxing very rapidly.

(a) Relaxation due to chemical exchange.

In this work only the relaxation of the second kind will be dealt with which is described briefly here.

Section VI.2.2 Scalar Relaxation of the Second Kind.

Writing the perturbing Hamiltonian as

$$\mathcal{H}_1 = \hbar \hat{\underline{I}}.A.\hat{\underline{S}}.$$

$$= \hbar \sum_q F^{(q)} A^{(q)}$$

in this case the spin operators are as follows

$$A^{(o)} = \hat{I}_z$$

$$A^{(1)} = \hat{I}+$$

$$A^{(-1)} = \hat{I}-$$

and the randomly variable functions ("lattice operators") are

$$F^{(o)} = AS_z$$

$$F^{(1)} = \tfrac{1}{2} AS-$$

$$F^{(-1)} = \tfrac{1}{2} AS+$$

The macroscopic equation for longitudinal relaxation time is given by

$$\frac{d\langle \hat{I}_z \rangle}{dt} = \frac{\{\langle \hat{I}_z \rangle - \hat{I}_o\}}{T_1}$$

and for transverse relaxation time

$$\frac{d\langle \hat{I}_x \rangle}{dt} = \frac{1}{T_2} \langle \hat{I}_x \rangle$$

According to equation (29) of Section VI.3. T_1 can be given as

$$\frac{1}{T_1} = \sum_q J^q (\omega_I)^{(q)} \left\{ A^q, \sqsubset A^{(-q)}, I_z \sqsupset \right\}$$

or $$\frac{1}{T_2} = 2\, J^{(1)} (\omega_I)$$

and similarly replacing I_z by I_x we get

$$\frac{1}{T_2} = J^{(1)} (\omega_I) + \tfrac{1}{2} J^{(o)}_{(o)}$$

where $$J^{(1)}_{(\omega)} = \int_{-\infty}^{+\infty} G^{(1)}(\tau)\, e^{-i\omega\tau}\, d\tau$$

$$G^{(1)}(\tau) = \frac{1}{4}\overline{A^2 S_+(o).\ S_-(\tau)}$$

and

$$J^{o}(\omega) = \int_{-\infty}^{+\infty} G^{(o)}_{(\tau)}\, e^{-i\omega\tau}\, d\tau ,$$

$$G^{(o)}(\tau) = A^2 S_z(o)\ S_z(\tau)$$

If we denote τ_S, as the relaxation time of nucleus S, we may write

$$G^{(1)}(\tau), = \frac{1}{4} A^2 S_+(o) S_-(o)\, e^{i\omega_S\tau}\, e^{-\tau/\tau_s}$$

$$\simeq \frac{A^2 S(S+1)}{6}\, e^{i\omega_s\tau}\, e^{-i\omega_s\tau/\tau_s}$$

and in the same way

$$G^{(o)}(\tau) = \frac{A^2 S(S+1)}{3}\, e^{i\omega_s\tau - \tau/\tau_s}$$

Relaxation times are given as

$$\frac{1}{T_1}I = \frac{2A^2}{3} S(S+1) \frac{\tau_s}{1+(\omega_I - \omega_S)^2\tau_S^2}$$

$$\frac{1}{T_2}I = \frac{A^2}{3} S(S+1) \left\{ \frac{\tau_s}{1+(\omega_I - \omega_S)^2 \tau_S^2} + \tau_S \right\}$$

Scalar relaxation contributes to T_1 when the coupling constant is large, and correlation time very short or the coupled nuclei have very close resonance frequencies.

Section VII.3 Relaxation via Chemical Shift Anisotropy

A nucleus does not experience exactly the same applied magnetic field, because it is shielded by electrons. The magnitude of this shielding depends on the orientation of the molecule in the static magnetic field. In liquids due to rapid motion of molecules these nuclei experience an averaged shielding. If the chemical shielding is not isotropic it means that the nucleus is subjected to a magnetic field which is modulated by the molecular motion. This provides a mechanism for relaxation.

Unlike other mechanisms the value of the secondary magnetic field depends on B_o. Consequently the relaxation rate is proportional to B_o^2.

In the case of extreme narrowing the following expressions are found for axially symmetric situations

$$1/T_1 = \frac{2}{15} \gamma^2 B_o^2 \quad (\sigma_{\parallel} - \sigma_{\perp}) \tau_c$$

$$1/T_2 = \frac{7}{45} \gamma^2 B_o^2 \quad (\sigma_{\parallel} - \sigma_{\perp}) \tau_c$$

Where $\sigma_{\parallel}$ and $\sigma_{\perp}$ are the shieldings parallel and perpendicular to the symmetry axis. In the absence of axial symmetry the calculations become complicated. It is noteworthy that even in the case of extreme narrowing

$$T_1 \neq T_2 \quad \text{in fact } T_1/T_2 = 6/7$$

Section VII. 4 Spin Rotation Relaxation

The interaction between a spin I and the rotation of the molecule containing the spin is a source for relaxation because currents arising from the rotation of charges produce a magnetic field at a point fixed inside the molecule i.e. at a nucleus. Molecules possess energy associated with their rotational motion. In the gaseous state this rotational energy is quantized. If we denote the rotational quantum number J and moment of inertia of the molecule by I, the rotational frequency ω is given by

$$\omega = \frac{h\mathbf{J}}{2\pi \mathbf{I}}$$

If rotation is free, $\mathbf{J}$ is clearly an angular momentum operator. However, in the case of a liquid $\mathbf{J}$ is not a good quantum number. It is unlikely that a molecule in a liquid makes at least one revolution without interruption and so the free molecule rotational levels are blurred out by life time broadening. Since this effect is proportional to the moment of inertia of the molecule, we may say in general that the smaller the molecule the more important will be spin rotation.

Hubbard[65] has derived the following formula for the relaxation by spin rotation of a nuclear spin in a molecule .

$$\frac{1}{T_1} = \frac{2}{3} k T h^{-2} \mathbf{I} (2 C_{\perp}^2 + C_{//}^2) \tau_{s.r.}$$

where k is the Boltzmann's constant, T is an absolute temperature,

$C_{\perp}$ and $C_{//}$ are the components of the spin rotation interaction tensor (perpendicular and parallel to symmetry axis respectively).

For a spherical molecule undergoing small step diffusional motion the angular momentum correlation time $\tau_{s.r.}$ is related [65, 66] to the molecular reorientation time τ_c as

$$\tau_{s.r.} \quad \tau_c = \frac{I}{6 k T}$$

This equation, often called Hubbard's relation, only holds at temperatures well below the boiling point of a liquid. The opposite temperature behaviour of $\tau_{s.r.}$ compared to τ_c, helps to separate the spin rotation contribution from other mechanisms as $\tau_{s.r.}$ becomes longer with increasing temperature whereas τ_c becomes shorter.

CHAPTER VIII

GENERAL THEORY FOR THE MEASUREMENT OF SPIN LATTICE RELAXATION TIME.

There are several methods, in principle, by which one can measure the spin lattice relaxation time. In this work the inversion recovery method has been used, which is described briefly here.

Section VII.1 Use of Rotating Coordinates

Many N.M.R. experiments are conveniently described in terms of a system of rotating coordinates. In Figure a nuclear spins are shown by arrows precessing about the z axis at the Larmor frequency. Suppose the observer now imagines himself to be in a system of coordinates x', y' and z', z' along z and B_o, but rotating in the same sense and at the same frequency as the nuclei, all the nuclei will now appear to be stationary as in Figure b.

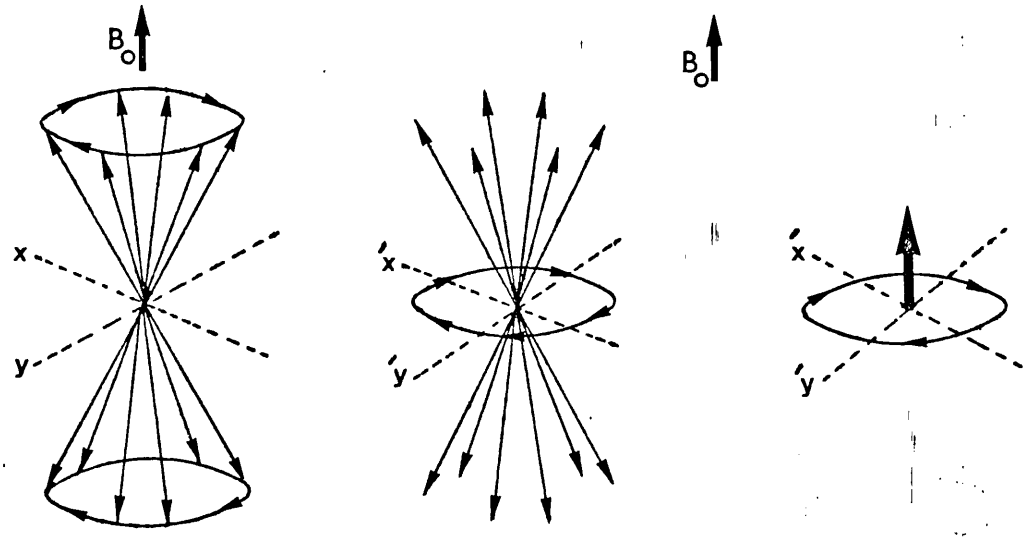

(a) (b)

The nuclei will appear to be in zero field to the rotating observer. We shall make use of this helpful concept in the discussion which follows.

Section VII. 2 Magnetization in the Rotating frame

Classically the motion of magnetic moment M can be described by the equation

$$\frac{dM}{dt} = \gamma \underline{M} \times \underline{B} \quad (\underline{M} = \gamma h \underline{I}) \qquad \ldots\ldots 1$$

In a frame of reference rotating with respect to the laboratory frame with an angular velocity ω . According to the general law of relative motion a relation between the time derivative $\frac{dM}{dt}$ of this time dependent vector M(t), and its partial time derivative $\frac{\partial M}{\partial t}$ in the moving frame, is given by an equation

$$\left(\frac{dM}{dt}\right)_{\text{fixed}} = \left(\frac{\partial M}{\partial t}\right)_{\text{rot}} + \underline{\omega} \times \underline{M}$$

$$\left(\frac{\partial M}{\partial t}\right)_{\text{rot}} = \gamma \underline{M} \times \underline{B} + \underline{\omega} \times \underline{M} = \gamma \underline{M} \times (\underline{B} + \frac{\omega}{\gamma}) \qquad \ldots\ldots 2$$

where the total derivative represents the overall motion of M in the fixed frame and the partial derivative represents the explicit dependence of M on time in the rotating frame. The term ω/γ is called the "fictitious field" and has the dimensions of magnetic field. Alternatively, the equation can be written in terms of "effective" field, where $B_{eff} = B + \omega/\gamma$ and in a rotating frame magnetization precesses about B_{eff}. When the frame rotates at an angular

frequency $\omega_L = -\gamma B_o$, the Larmor frequency, B_{eff} is zero and the magnetic moment is a fixed vector.

Now in addition to the applied field B_o an r.f. field B_1 rotating at Larmor frequency ω_L rad s^{-1} is applied perpendicular to it. At resonance, the fictitious field cancels B_o and B_1 is left in the x' axis

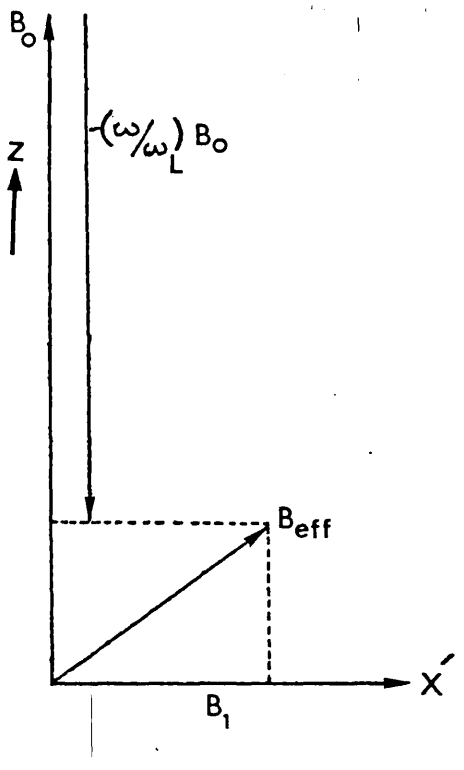

Fig.VIII . Magnetic fields in a rotating frame. The direction of B_{eff} depends on the ratio of ω/ω_L of the applied and Larmor angular frequencies.

Precession of M about x' is at the Larmor frequency γB_1.
In pulse experiments, where the r.f. field B_1 is applied for a short time t_a, the angle a, through which M precesses is known as the flip angle and is given by

$$a = \gamma B_1 t_a \qquad \text{rad sec}^{-1}$$

Section VII.3 Free Induction Decay

If we apply a 90^o pulse along the x' axis in the rotating frame, the nuclear magnetization will turn through an angle of 90^o and be directed along y'. When the pulse is turned off, the magnetization will be left to rotate in the xy plane. This magnetization induces a signal (free induction signal) in the detector coil, placed along the y' axis. The magnetization in the x'y' plane is due to the nuclei which are no longer precessing about B_o with random phase, but they have been drawn together to precess about B_o in a bunch.

As the transverse relaxation occurs, the signal decays to zero, since at thermal equilibrium in a static field there is no net transverse magnetisation. In a perfectly homogeneous field, the rate constant for this decay is $1/T_2$ where T_2 is the spin-spin relaxation time which involves the exchange of energy among the spins themselves.

In actual practice the transverse magnetization decays with a time constant T_2^* that includes the effects of field inhomogeneity.

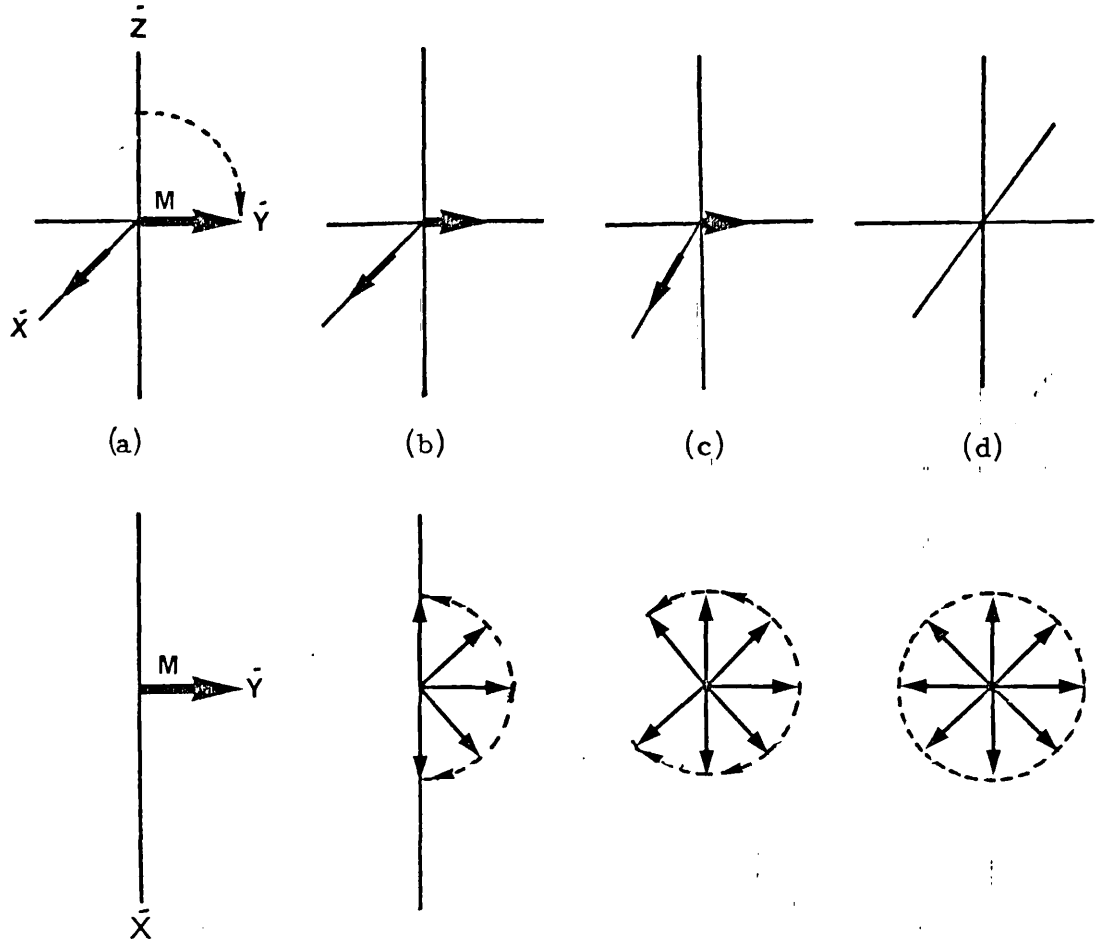

Fig. VIII.1. (a) A 90° pulse is applied along the $\acute{x}$ axis to rotate M along the y' axis

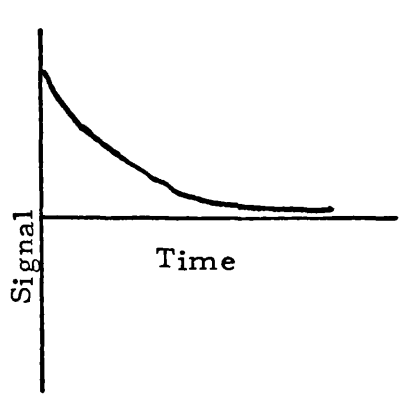

(e) F. I. D at ω_o

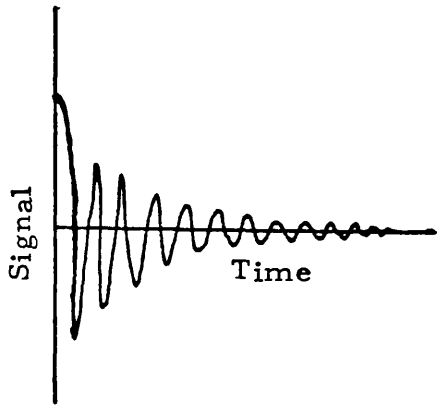

(f) F. I. D for slightly different ω_o

In an inhomogeneous magnetic field there is a range of precession 174
frequencies distributed on either side of the mean frequency ω_o. Hence, this produces an additional means by which nuclei will lose phase in the x y plane. Figure VIII.1 a, b, c and d and Figure VIII.1.e, shows the exponential decay of this magnetization when the r.f. pulse is precisely at the resonance frequency of a single type of nucleus.

When an r.f. pulse is applied slightly off resonance, the detector displays not only the exponentially decaying value of M_{xy} but also interference effects as M_{xy} and the reference frequency alternatively comes in and out of phase with each other. A typical pattern of such an F.I.D. is shown in Figure VIII.1.f. In the case of several magnetically non equivalent nuclei of the same species, that have different Larmor frequencies, the F.I.D. will be a complex signal.

Section VII.3 Measurement of T_1

The spin lattice relaxation time characterizes the decay of nuclear magnetization along the z axis. There are different methods but a convenient technique involves the sequence of two pulses, summarized as

$$(P.D. - P_1 - t - P_2 - AT)_n$$

where

PD = A pulse delay before the r.f. pulse and after the acquisition time

P_1 = first r.f. pulse (180° pulse)

t = delay time between pulses

P_2 = second or observing pulse

A.T = acquisition time, the time that the free induction decay is observed, and

n = the number of times this sequence is repeated

This inversion recovery pulse sequence is described in Figure VIII.II.

At thermal equilibrium the sample has a net macroscopic magnetization in the z direction, which can be represented by a vector arrow whose length indicates the amount of this magnetization. By applying a suitable amount of radiofrequency power at an appropriate frequency, in the form of a pulse, the original magnetization vector is tipped through 180°. After the application of a 180° pulse the spin system finds itself no longer in thermal equilibrium with its environment (lattice), and it will start to relax back to the equilibrium value. A 90° pulse is now applied which tips the residual magnetization into the x y plane where it induces a signal into the spectrometer receiver. The F.I.D. signal so obtained is stored, following digitization. The system is then given a time roughly equal to 5 T_1 to establish equilibrium and the sequence is repeated with a slightly different t.

The F.I.D's consist of a series of overlapping sine-waves and contain all the information concerning the N.M.R.

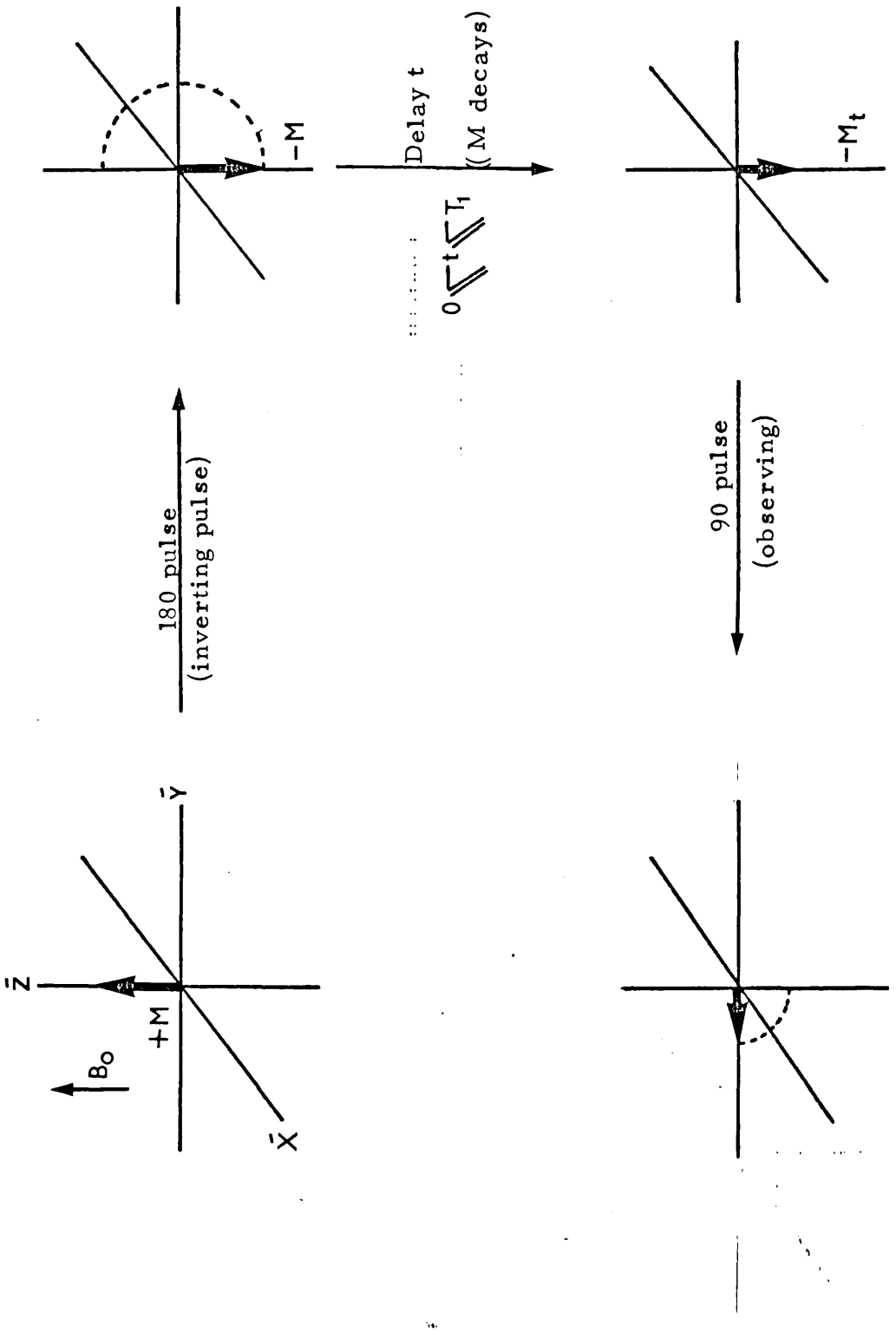

Fig.VIII.11. The rotating reference frame model for the measurement of spin lattice relaxation time

spectrum. This is then converted into the frequency domain by the mathematical manipulation known as Fourier Transformation. Quantitatively, the decay of M_z is given by the Bloch equation

$$\frac{dM_z(t)}{dt} = - \frac{(M_z(t) - M_o)}{T_1}$$

Integration with $M_z(t) = - M_o$ at $t = 0$

$$M_z(t) = M_o (1 - 2 \exp (-t/T_1)$$

or $$\ln (M_o - M_z(t)) = - \ln 2 M_o + \frac{t}{T_1}$$

From this equation one can determine the value of T_1 by plotting $- \ln (M_o - M_z(t)$ versus t. The resultant straight line plot will have a slope of $1/T_1$ and interpret $-\ln (2 M_o)$.

The time t, where the magnetization vector becomes zero is equal to $T_1 \ln 2$.

CHAPTER IX

RESULTS AND DISCUSSION

For a given molecule in the liquid phase, measurements of nuclear relaxation times may be exploited as an important tool for the study of microdynamic behaviour of liquids.[46, 48, 50] Although the precise details of the microdynamic behaviour of the liquid are not available from the relaxation data, the results do allow semi-quantitative evaluation of the molecular motion. A model for the nuclear motion is required. The most evident manifestationson the macroscopic level of the microscopic movement of the molecules of a liquid are the viscosity and Brownian movement. Early workers assumed isotropic rotational diffusion,≠ based on a model when a macroscopic particle was rotating in a continuous medium, and the problem therefore is to find expressions for angular displacements as a function of time. Using the Stoke-Einstein hydrodynamic model it has been shown[46] that when a molecule changes its orientation by $\Delta\Theta$ (Θ being an angle between a chosen axis on the molecule and a fixed axis) during a time t, the following relationship is valid

$$(\Delta\Theta)^2 = 2Dt$$

where D is the rotational diffusion constant and describes the molecular motion of the molecule by random instantaneous jumps. If the jumps are too large the model is not a good approximation. In the present model the molecule rotates like a macroscopic sphere immersed in a

---

≠ Diffusion: This term denotes the process by which molecules or other particles intermingle as a result of their random thermal motion. The diffusion constant is the measure of the rate of diffusion. The diffusivity has the dimensions of length times a velocity.

viscous liquid. For non-spherical molecules a different shape factor must be introduced. In any system which obeys the rotational diffusional model, the rotational diffusion constant an be evaluated from the experimentally determined correlation times. It has been shown[41, 42] that this assumption leads to calculated relaxation times that are usually much shorter than the observed values - even for roughly spherical molecules.

In more recent work[42-44] molecular motion was described in terms of microviscosity with a friction constant as a parameter. The model is applied most readily to the cases where only intramolecular interactions are important and the molecule is undergoing isotropic rotational diffusion, where the motion can be described by a single diffusion constant.[47, 49] The great disadvantage of this approach is that it is extremely difficult to calculate or to measure the frictional constant. In all the models the correlation time is related to the viscosity and temperature. However, the various models predict different proportionality constants between the correlation time and $\eta/_T$. If the molecule reorients by a rotational-diffusion mechanism and the shape of the molecule remains constant the correlation time would be directly proportional to viscosity regardless of the actual shape of the molecule. This should occur because the rotational diffusion coefficients of the Stokes-Einstein hydrodynamic model for reorientation about the various molecular axes at a given temperature are directly proportional to the viscosity and a function of molecular

symmetry.[45] The correlation time for a spherical molecule immersed in a continuous viscous fluid is calculated from the following expression:

$$\tau_c = \frac{V\eta}{k\,T}$$

(V is the molecular volume).

An isotropic movement (the simplest case) can be represented by a correlation time τ_c, a dynamic parameter which describes the total reorientation of the molecule. However, in general the molecular motions are anisotropic in non-symmetric molecules. In explaining the results obtained here a crude assumption of isotropic reorientation has been made.

In this work proton spin-lattice relaxation times have been measured for the hydride features in various organo tin hydrides and the correlation times appropriate to the tin-hydrogen vector were calculated from the satellite spectra as explained in the foregoing statement.

It has been shown[67,68] previously that ^{13}C satellites in proton spectra have shorter relaxation times than the central feature corresponding to non-magnetic carbon ^{12}C. This was explained in terms of the extra contribution from the intramolecular dipole-dipole interaction for the satellites. This prompted the present investigation of the analogous features in the spectra of tin hydrides. Experiments reported here confirm the expectation that the ^{119}Sn and ^{117}Sn satellites of hydride protons do have shorter relaxation times than the central feature corresponding to the non-magnetic tin nuclei. The results of measurements of proton

spin-lattice relaxation times for the main resonance and satellites are summarized in table X.1.

As the difference in relaxation rates between the central features and satellites is due to the additional contribution from ^{119}Sn-H dipole dipole coupling in the latter it is possible to write that

$$\left(\frac{1}{T_1}\right)_{\text{dipole dipole}} = \left(\frac{1}{T_1}\right)_{\text{satellite}} - \left(\frac{1}{T_1}\right)_{\text{central band}}$$

where $\left(\frac{1}{T_1}\right)_{\text{dipole dipole}}$ is given by

$$\left(\frac{1}{T_1}\right)_{\text{dipole dipole}} = \left(\frac{\gamma_{1H}\ \gamma_{119_{Sn}}\ \hbar}{r^3_{Sn\text{-}H}}\right)^2 \tau_c$$

and r_{Sn-H} is the internuclear distance. Taking[71] a value of 1.70 Å the correlation times, τ_c, for the rotational motion of these molecules were calculated using the above equation and are listed in Table X.1.

Several points arise from the T_1 data and the calculated correlation times reported in Table X.1. One general point needs to be made is about the trends observed in the dipolar relaxation times. These values are consistent with the structural features. From the geometry of the phenyl stannanes. the molecular motion is expected to be anisotropic. The effect of increased moment of inertia in going from di- to tri-substituted stannanes or in passing from methyl to butyl stannanes is also reflected in the dipolar rates as these

TABLE X.1

Experimental proton spin-lattice relaxation times and correlation times in some organo-tin hydrides

Molecule	Central feature T_1 sec	$(1/T_1)$sec^{-1}	Satellite T_1 sec	$(1/T_1$ sec$^{-1})$	#Dipole dipole contribution T_1 sec	$(1/T_1$ sec$^{-1})$	τ_c x10^{-12} sec	Conditions/ footnote
$(C_6H_5)_3SnH$	11.3± 0.5	0.0885	7.6± 0.4	0.1315	23.11± 0.64	0.04327	13.20	27°C †
$(C_6H_5)_2SnH_2$	13.4±0.4	0.0746	9.5± 0.6	0.1052	32.6 ± 0.7	0.0306	9.37	25°C ≠
$(CH_3)_3SnH$	30.6±1.2	0.0326	24.3±1.0	0.0412	117.34±1.56	0.00852	2.60	27°C †
$(CH_3)_2SnH_2$	33.2±1.0	0.0301	26.3±0.8	0.0380	126.58±1.2	0.00789	2.40	26°C ≠
CH_3SnH_3	43.7± 1.0	0.0228	38.2±0.8	0.0261	303.95±1.28	0.00329	1.00	-10°C ≠
$(C_6H_{11})_2SnH_2$	18.8± 0.7	0.0532	-	-	-	-	-	30°C †
$(C_3H_7)_3SnH$	19.1± 0.4	0.0523	16.5±0.7	0.0606	121.21±0.80	0.00820	2.50	29°C †
$(C_2H_5)_3SnH$	32.5±0.4	0.0307	26.5±1.0	0.0377	142.13±1.07	0.00703	2.14	29°C †
$(n\text{-}C_4H_9)_3SnH$	15.3±0.3	0.0653	13.4±0.4	0.0746	107.21±0.5	0.00932	2.84	28°C †

† values were obtained on a Brucker WH-90 spectrometer

≠ Varian CFT-20 spectrometer

$\left(\frac{1}{T_1}\right)_{dd} = \left(\frac{1}{T_1}\right)_{satellite} - \left(\frac{1}{T_1}\right)_{central}$

changes should result in longer correlation times and more efficient dipolar rates. The large difference in dipolar rates for tri- and di-substituted stannanes is greater than expected from the increase in overall correlation time due to increased molecular size in tri-substituted stannanes. This can be attributed to the preferred rotation of tri-substituted stannanes about the C_3 axis which is less effective in averaging out the dipole-dipole contribution than motion about the C_2 axes of di-stannanes. In all the alkyl tri-substituted stannanes listed in Table X.1, the calculated correlation times lie between 2.14 to 2.84×10^{-12} sec, and a higher value of 13.2×10^{-12} for tri-phenyl stannane also tends to suggest an anisotropic tumbling of the molecules resulting in non-systematic variation of relaxation time.

Contributions other than the intramolecular Sn-H dipole dipole mechanism obviously are responsible for relaxation of the central hydride feature. Possible mechanisms are the spin rotation interaction, scalar coupling, anisotropy of the chemical shift and internuclear dipole dipole interaction. Scalar coupling can be ignored as there is no rapid exchange going on in the molecule; chemical shift anistropy may be insignificant for protons. As the measurements were made in 10% solution in benzene-d_6 the internuclear dipole dipole contribution is not expected to be important and since the molecules are small a significant spin rotation contribution might be expected.

Carbon-13 NOE and T_1 data for $(^{13}CH_3)_2SnH_2$:

Table X.2 summarizes the $^{13}C-\{^1H\}$ NOE and the ^{13}C spin-lattice relaxation times under decoupled conditions for the methyl carbons of dimethyl tin dihydride at 25°C and -40°C. A 10 mm OD. N.M.R. tube containing 90% hydride in C_6D_6 was used. The experiments were run on a Varian CFT-20 spectrometer described elsewhere (see page 37). The enhancement factor was determined from the ratio of the integrated ^{13}C decoupled peak to that of the coupled spectrum. The dipolar relaxation times were calculated from the experimental quantity η , the enhancement factor and T_1 by using the relation:

$$(T_1)_{DD} = \gamma_{1_H} T_1 / 2\gamma_{^{13}C}\, \eta^{^{13}C\text{-}H}$$

If the dipolar mechanism is the sole contributor to T_1, the maximum value of the $^{13}C-\{^1H\}$ NOE becomes $1+\eta = 2.988$ ($\eta = 1.988$). While the NOE does not distinguish between inter and intramolecular effects, however, intermolecular dipolar relaxation is relatively unimportant for ^{13}C nuclei owing to the r_{CH}^{-6} distance dependence of the dipolar coupling[69, 70].

The less than maximum Overhauser enhancement indicates that other relaxation mechanisms are effectively competing with the dipolar mechanism. CSA can be ignored especially for methyl carbons. The reduced non-dipolar contribution at the lower

TABLE X.2

^{13}C spin-lattice relaxation times (T_1) and nuclear Overhauser enhancement (η) for the methyl carbons of $(^{13}CH_3)_2 SnH_2$

Temperature (°C)	η ≠	T_1 sec (total)	T_1 sec (dipole dipole)	T_1 sec (other mechanisms)
25	0.35	17.35± 0.54 sec (0.0576)* sec^{-1}	98.55 sec (0.0101) sec^{-1}	21.07 sec (0.0475) sec^{-1}
-40	1.56	10.78± 0.47 sec (0.0927) sec^{-1}	13.74 sec (0.0727) sec^{-1}	50.20 sec (0.0199) sec^{-1}

≠ The estimated accuracy of η (the intensity ratio - 1) is ± 8%

* figures in parenthesis show the corresponding relaxation rate.

temperature suggests the presence of spin rotation interaction as might be expected for small molecules. There is no other major interaction present in the system, any small contribution from chemical shift anisotropy (if there is any) can safely be ignored in the presence of two dominant relaxation mechanisms like dipole-dipole and spin rotation interaction. $(1/T_1)_{DD} = 0.0101\ sec^{-1}$ out of the total relaxation rate of $0.0576\ sec^{-1}$ at 25°C, shows that the dipolar contribution is small and the relaxation at this temperature is evidentally dominated by spin rotation.

At a lower temperature, the longer correlation times (slow molecular motion) for the dipole-dipole mechanism increase the efficiency of the process. From $\eta = 1.56$ and the total relaxation rate $(\frac{1}{T_1}) = 0.0927\ sec^{-1}$ at -40°C one finds the proton dipolar contribution $(\frac{1}{T_1})_{DD} = 0.0727\ sec^{-1}$ while $(\frac{1}{T_1})_{\text{other mech.}} = 0.0199\ sec^{-1}$, indicates that the relaxation is dominated by the dipolar contribution.

CHAPTER X

BAND SHAPE ANALYSIS

Section X.1 Quadrupole Effects. Interaction of Electrons with the Nucleus.

Classically, the energy of interaction of an electronic cloud and the electrostatic potential of the nucleus of finite dimensions is given by

$$W = \iint \frac{\rho_e(r_e)\ \rho_n(r_n)}{|r_e - r_n|}\ d\tau_e\ d\tau_n \qquad (1)$$

where ρ_n, $d\tau_n$, and $\rho_e d\tau_e$ are the nuclear and electric charge densities, $\bar{r}_n$ and $\bar{r}_e$ are shown in Fig. X.I.

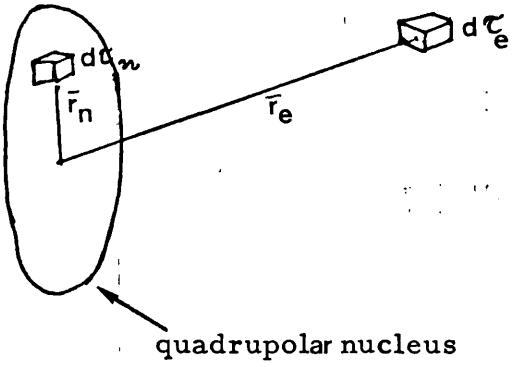

Fig. X.I.

A nucleus with a spin $I \geqslant 1$ possesses an electric quadrupole moment which corresponds classically to a non-spherical charge distribution. If a quadrupolar nucleus is situated in an inhomogenous electric field, it possesses a potential energy that depends upon the orientation of the quadrupole moment with respect to the electric field. The term $\frac{1}{|r_e - r_n|}$ in equation 1 can be written in spherical harmonics

$$\frac{1}{r_e - r_n} = 4\pi \sum_{l=o}^{\infty} \sum_{m=-1}^{m=1} \frac{1}{2l+1} \frac{r_<^l}{r_>^{(l+1)}} Y_l^{+m}(\theta_e, \phi_e)\ Y^{-m}(\theta_n\ \phi_n) \qquad (2)$$

where $Y_e^m(\theta, \phi)$ are the spherical harmonics of the electric and

nuclear coordinates and $r_<$, $r_>$ signify the smaller and larger of the two radius vectors respectively, r_e or r_n and the larger of the two is denominator.

Neglecting the weak perturbation arising from the electron penetration of the nucleus, because only s electrons penetrate, they do not contribute to the quadrupole effects since the charge distribution is spherically symmetric. By factorization of the interaction energy w, we can separate electric and nuclear variables as

$$W = \sum_{l} \sum_{m} N_l^m \cdot E_l^m \qquad (3)$$

$$\text{where } N_l^m = \left[\frac{4\pi}{2l+1}\right]^{\frac{1}{2}} \int \rho_n(r_n)\, r_n^l\, Y_l^m(\theta_n, \phi_n)\, d\tau_n \qquad (4)$$

$$\text{and } E_l^{(-m)} = \left[\frac{4\pi}{2l-1}\right]^{\frac{1}{2}} \int \rho_e(r_e) r_e^{(-l+1)}\, Y_l^{-m}(\theta_e, \phi_e)\, d\tau_e \qquad (5)$$

Replacing the charges by the average value (expectation value) of operators of charge density at the point r_n, transforming the function W, N and E into operators, where the integrals are replaced by sums on all the charges, we get

$$\mathcal{N}_l^m = \left[\frac{4\pi}{2l+1}\right]^{\frac{1}{2}} \sum_j e_j R_j^l Y_l^m(\Theta_j, \Phi_j) \qquad (6)$$

and

$$\mathcal{E}_l^{-m} = \left[\frac{4\pi}{2l+1}\right] \sum_k r_k^{-(l+1)} Y_l^{(-m)}(\theta_k, \phi_k) \qquad (7)$$

where R, Θ, Φ , and r, θ, ϕ are the spherical coordinates of nucleons and electrons.

The Hamiltonian of the quadrupole interaction can be written as

$$W_Q = \sum_{l} \sum_{m} \mathcal{N}_{l}^{(m)} \mathcal{E}_{l}^{-m}$$

These operators are tensors of the order l and the expectation value of the operator $\mathcal{N}_{l}^{m}$ is called the nuclear multipole moment of order l and has m components where $m = 2l + 1$. The multiple moments are only observed if $l \leqslant 2I$. If we consider spin $I = 1$ then $l = 0, 2$ and there will be five components of this moment.

Applying the Wigner Eckart theorem to equation 6 of spherical harmonics of order two, the components of quadrupole moment become

$$\left.\begin{aligned} Q^{o} &= \tfrac{1}{2} \frac{e\,Q}{I\,(2I-1)} \left[3\,\hat{I}_z^2 - \hat{I}^2 \right] \\ Q^{\pm 1} &= \frac{\sqrt{6}}{4} \frac{e\,Q}{(2I-1)} \left[\hat{I}_z \hat{I}_{\pm} + \hat{I}_{\pm} \hat{I}_z \right] \\ Q^{\pm 2} &= \frac{\sqrt{6}}{4} \frac{e\,Q}{I(2I-1)} \hat{I}_{\pm}^2 \end{aligned}\right\} \quad 9$$

Expressing in the same way the electronic tensor components are

$$\left.\begin{aligned} E_o &= \frac{e}{2} q_{zz} \\ E^{\pm 1} &= \pm \frac{e}{\sqrt{6}} (q_{xz} - q_{yz}) \\ E^{\pm 2} &= \frac{-e}{\sqrt{6}} (q_{xx} - q_{yy} - 2iq_{xy}) \end{aligned}\right\} \quad 10$$

If we denote V as the electrostatic potential at the nucleus which is in fact the electric field gradient, denoted by

q, at the nucleus produced by electrons. This gradient is a tensor quantity and the coordinate axes are selected such that its off diagonal elements are zero, i.e. can be diagonalized, the tensor components about x, y and z axes can be written as

$$q_{zz} = \frac{\partial^2 V}{\partial z^2}, \quad q_{yy} = \frac{\partial^2 V}{\partial^2 y} \quad \text{and} \quad q_{xx} = \frac{\partial^2 V}{\partial^2 x}$$

The sum of the components is zero (Laplace's equation), so that only two parameters are required to specify the field gradient tensor. By convention these two quantities are q_{zz} and the asymmetry parameter η which can be defined as

$$\eta = \frac{q_{xx} - q_{yy}}{q_{zz}} \quad \text{where} \quad 0 \leqslant \eta \leqslant 1$$

When $q_{xx} = q_{yy} = q_{zz}$, the field gradient is spherically symmetrical and there is no electrical quadrupole interaction. In the case of cylinderical symmetry $q_{zz} > q_{xx} = q_{yy}$, i.e. the maximum component of field gradient lies along the z axis.

Before the electric field gradient can be interpreted in terms of molecular electronic structure, it is necessary to know the orientation of the field gradient in the principal axis system in the molecular framework. This requires further three values α, β and γ representing Eulerian angles between the two axis systems. In the system of principal axis the electronic tensor components will be

$$\left.\begin{aligned} F^{0} &= \tfrac{1}{2}\, e\, q \\ F^{\pm 1} &= 0 \\ F^{\pm 2} &= 2\frac{1}{\sqrt{6}}\, \eta\, e\, q \end{aligned}\right\} \qquad 11$$

Now, the general form of the Hamiltonian of quadrupole interaction can be written as

$$h\hat{\mathcal{H}}_Q = \frac{e^2 q Q}{4 I (2I - 1)} \left[3 \hat{I}_z^2 - I (I + 1) + \tfrac{1}{2} \eta \left(\hat{I}_+^2 + \hat{I}_-^2 \right) \right] \qquad 12$$

The quantity $e^2 q Q/h$ is known as the quadrupole coupling constant has the units of length^2 ($Q \times 10^{-28}$ m^2), and is measured by spectroscopic methods described briefly here.

Section X. 1.1 N.Q.R.[103,104]

In an axially symmetric field ($\eta = 0$), the energy of interaction arising from[a] quadrupole moment in a field q is given by an equation of type

$$\Delta E = h \nu = \frac{e q Q \left[3 m_I^2 - I (I + 1) \right]}{4 I (2 I - 1)}$$

where m is the magnetic quantum number which can take (2I + 1) values. Transitions are induced by an electromagnetic field of frequency ν. Pure N.Q.R. measures the quadrupole resonance frequency in solids where the electric field required to remove m_I degeneracy is provided by the electrons in the molecule.

Section X. 1.2 Microwave Spectrum [105]

In gases where molecules rotate freely, the nuclear spin couples with the angular momentum of the molecule and the quadrupole coupling energy can be obtained from the fine structure of the spectrum.

(133–135)

X. 1.3 Liquid Crystal Method

The N.M.R. spectra of partially oriented molecules can contain valuable information about the molecular structure, anisotropies of the chemical shift and the spin-spin coupling tensors. "Liquid crystals" are used for such studies. In the case of quadrupolar nuclei such as deuterium a value for the quadrupole coupling constant may also be obtained.

The spectrum of a deuteron in a C-D bond is a doublet, the splitting (Δ) of which is

$$\Delta = \frac{3}{2} q \left| S_{C-D} \right|$$

where S_{C-D} is the degree of reorientation of the axis passing through C and D. This degree of orientation say S_{ij} along the axis joining the two nuclei i and j is given by

$$D_{ij} = - \frac{h \gamma_i \gamma_j}{4\pi^2 r_{ij}^3} S_{ij}$$

where D_{ij} is the direct coupling between the two nuclei at a distance r apart.

If S is determined from the proton spectrum of the molecule, q can be determined from the spacing of the D.M.R. spectrum in the nematic phase. The precesions of the measurement of the quadrupole coupling constant is limited by the accuracy to which interproton distances are known.

Section X. 1 .4 Mössbaur Spectroscopy[106]

Mössbaur resonance measures the resonant absorption of nuclear γ rays in crystals. Gamma rays are emitted or resonantly absorbed via transitions between a nuclear excited state and the ground state. Even in the case of the most favourable Mössbaur isotopes (^{57}Fe, ^{121}Sb) nuclear quadrupole coupling constants, local magnetic fields, etc., cannot be measured precisely as with N.Q.R. and N.M.R.

Section X.2 Nuclear Electric Quadrupole Relaxation

The relaxation occurs due to the modulation of the interaction between the nuclear quadrupole moment and the electric field gradient at the nucleus by molecular motion. Quadrupolar relaxation depends only on intramolecular motion, since internuclear contribution to local electric field gradients are weak. If a nucleus of spin $I = \frac{1}{2}$ is coupled to a quadrupolar nucleus, the electric quadrupole mechanism operates only on the high spin nucleus but affects the multiplet structure of the spin $\frac{1}{2}$ nucleus as well, depending on the quadrupolar relaxation time of higher spin nucleus. Quadrupolar relaxation mechanisms for quadrupolar nuclei are dominant since quadrupolar interaction is much stronger than the dipolar interaction.

Following the treatment of Abragam,[116] the Hamiltonian for the quadrupolar interaction can be written in terms of spin operators $A^{(m)}$ and lattice functions $F^{(m)}$ as

$$\hbar \hat{\mathcal{H}}_Q = \sum_{m=-2}^{m=+2} F^{(m)}(\Omega) A^{(m)}(I)$$

197

where Ω stands for the Eulerian angles α, β, γ and describe the orientation of the molecule with respect to the laboratory frame. According to the relation 9 of section X.1 we can write that

$$A^{o} = \left[\left(\frac{1}{2I(2I-1)} \right) \left(3\hat{I}_z^2 - I(I+1) \right) \right]$$

$$A^{\pm 1} = \left[\frac{\sqrt{6}}{4} \right] \left[\left(\frac{1}{2I(2I-1)} \right) \left(\hat{I}_z \hat{I}_{\pm} + \hat{I}_{\pm} \hat{I}_z \right) \right]$$

$$A^{\pm 2} = \left[\frac{\sqrt{6}}{4} \right] \left[\left(\frac{1}{2I(2I-1)} \right) \left(\hat{I}_{\pm}^2 \right) \right]$$

and the $F^{(m)}$ functions are given by

$$F^{o} = eq \frac{eQ}{4I(2I-1)}$$

$$F^{\pm 1} = 0$$

$$F^{\pm 2} = \frac{\eta eq}{\sqrt{6}} \frac{eQ}{4I(2I-1)}$$

The relaxation time can be calculated by writing the equation 27 in the form

$$B = \frac{1}{2} \sum_{m} J(m\omega) \left[A^{(m)}, \left(A^{(m)}, \hat{I}_z \right) \right] \quad \text{---------- 30}$$

By introducing the reduced spectral densities $\tilde{J}(m\omega)$ which is the Fourier Transform of the reduced correlation function we can write

$$B = \frac{1}{2} \sum_{m} \overline{\left| F^{m}(\Omega) \right|^2} \tilde{J}(m\omega) \left[A^{-m}, \left[A^{(m)}, \hat{I}_z \right] \right]$$

Making the assumption that the correlation function is of the same form for all $F^{(m)}$ i.e. an exponential function with characteristic τ_Q.

The reduced correlation function is given by

$$\tilde{G}(\tau) = \frac{\overline{F^{(m)}_{(t)} \; F^{(m)*}(t+\tau)}}{\left| F^{(m)}_{(t)} \right|^2} = e^{-\tau/\tau_\Omega}$$

The spectral density is then

$$\tilde{J}(\omega) = \frac{2\,\tau_\Omega}{1 + \omega_o^2\,\tau_\Omega^2}$$

The functions $F^{(m)}_{(\Omega)}$ have been described so far in a reference frame of molecule which is linearly related to the functions in the laboratory frame $F^{(m')}_{(0)}$ through

$$F^{(m)}_{(\Omega)} = \sum_{m'} a_{mm'}(\Omega)\; F^{(m')}$$

The coefficient $a_{mm'}$ is random due to molecular motion in a liquid

$$\overline{a_{mm'}(\Omega)\, a^*_{mm''}(\Omega)} = \frac{1}{2\,1+1}\,\delta\, m'm'' = \frac{\delta\, m'\, m''}{5}$$

because $1 = 2$

The spectral density in the laboratory frame is then $\frac{J(m\omega o)}{5}$

The equation 30 can be written as

$$B = \frac{1}{10}\left\{ \sum_{m'} \left| F^{(m')} \right|^2 \right\} \times \sum_{m} \tilde{J}_i(m\,\omega_o)\, [A^{(-m)}, [A^{(m)}, \hat{I}_z]]$$

where $F^{(m')}$ are the lattice functions in the molecular frame and can be written

$$\sum_{m} \left| F^{m'} \right|^2 = \frac{1}{4}\,(e^2\, q\, Q)^2\,(1 + \eta^2/3)$$

The commutator $[A^{(-m)}, [A^{(m)}, I_z]]$ is solved by using commutation relations and is evaluated by using expression of $A^{(m)}$ on page 197

$$[A, B] = [-B, A]$$

$$[A, B + C] = [A, B]$$

$$[A, BC] = [A, B]\, C + B\, [A, C]$$

$$[A, [B, C]] + [B, [C, A]] + [C, [A, B]] = 0$$

we obtain

$$[A^{o}, [A^{o}, I_z]] = 0$$

$$[A^{(-1)}, [A^{(1)}, I_z]] = \frac{3}{2} [16 \hat{I}_z^3 - \hat{I}_z [8 I (I + 1) - 2]]$$

$$[A^{(-2)}, [A^{(2)}, I_z]] = \frac{3}{2} [-16 \hat{I}_z^3 [16 I (I + 1) - 8]]$$

we can write

$$B = \frac{3}{16\ 0} \left[\frac{e^2 q Q}{I (2 I - 1)}\right]^2 \left[(1 + \frac{\eta^2}{3}) (\tilde{J} (\omega) (16 I_z^3 - I_z [8I(I+1)-2]\right]$$

$$+ [\tilde{J} (2 \omega) (- 16 I_z^3 + \hat{I}_z^3 + \hat{I}_z [16 I (I +1+ -8]]$$

In a general way the term I_z^3 is not eliminated but if we consider a particular case when $I = 1$, $I_z^3 = 1$ then we have

$$\frac{1}{T_1} = \frac{3}{8\ 0} (1 + \frac{\eta^2}{3}) (e^2 q Q)^2 (\tilde{J} (\omega) + 4 \tilde{J} (2 \omega)$$

Applying the extreme narrowing conditions $\tilde{J} (\omega) = 2 \tau_Q$, we obtain a general formula which is valid whatever the spin is

$$\frac{1}{T_1} = \frac{3}{4\ 0} \frac{2 I + 3}{I^2 (2I - 1)} (1 + \frac{\eta^2}{3}) (eq^2 Q)^2 \tau_Q$$

Similarly T_2 is obtained by replacing I_z by I_x in the commutation relations and the application of extreme narrowing condition gives

$$T_2 = T_1 .$$

Section X.3 Band shape analysis

X.3.1 Introduction

In nuclear magnetic resonance experiments one observes transitions between nuclear Zeeman levels of nuclei. In general, the intensity of the absorption line depends on the difference of populations in the upper and lower states. This spectral information in N.M.R. is recorded by a plot of signal intensity versus frequency. In many applications of high resolution N.M.R. spectroscopy, the shapes of the lines are of secondary importance. But studying the breadth and shape of these lines, interactions responsible for relaxation and life times of the energy states can be studied.

In actual practice, we always have an ensemble of nuclei present in a sample, nuclei being small dipoles change each others magnetic environments, which result in perturbing their energy states and also show hyperfine structure interaction. As the line is obtained from the precession of magnetic moments, non-magnetic interactions present in the system cannot affect it directly. The magnetic interactions which have been described in Chapter VII are however, affected by non-magnetic interactions. The motion of molecules in a liquid is an example of such non-magnetic factors which control the line shape by the phenomenon of narrowing.

Consider an N.M.R. spectrum of a single "isolated" nucleus which will be a single sharp line at the Larmor frequency.

It has no width at all because energy levels are exactly defined, but this is never the case, in actual practice they have some width due to an uncertainty in the energies of these states. This uncertainty can be estimated according to Heisenberg's uncertainty principle.

Interactions with the neighbour spin (dipole-dipole) also broaden the lines. If we resolve the precessing nuclear moment into its components, one along the direction of the applied field and the other rotating at the right angles to it. This transverse component can induce transitions in the neighbouring nucleus.

This spin exchange or flip flop does not change the overall energy but shortens the life time of the states and energy levels are not sharply defined and should be properly represented as Fig.X.II.

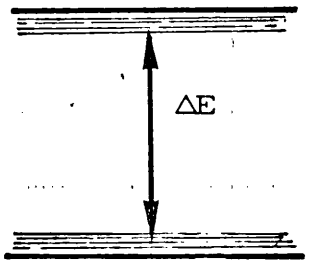

Fig. X.II.

Inhomogeneity of the applied magnetic field also broadens the N.M.R. spectrum lines. In an inhomogeneous magnetic field, the nuclei in different parts of a sample experience different intensities of the field, therefore, there will be a spread of Larmor frequencies over a small region of frequencies and the

overall signal will be a collection of signals from the same kind of ensemble of nuclei.

The line shape of a multiplet proton resonance changes greatly as the rate of relaxation of a nuclear spin to which the proton is coupled changes. If the proton is coupled to nuclei with quadrupole moments, the effects of quadrupolar relaxation are also observed in the proton spectra. The origin of these effects is discussed in detail in the following section.

X.3.2 The effect of quadrupole relaxation on the proton line shapes

Consider two spins I and S where S is a quadrupolar nucleus, coupled together by a scalar interaction of type $h\,\underline{I}.J.\underline{S}$. In a magnetic field both spins are quantized and the proton spectrum consists of a multiplet of lines corresponding to the (2S + 1) states of the quadrupolar spin. The frequency of the components being

$$\omega_{I\,m_s} = \omega_o + \omega' m_s \quad (m_s = -I \ldots I)$$

where ω_o = unperturbed angular resonance frequency of the proton

ω_{m_s} = shift arising from perturbation

Due to relaxation, the spin S can jump from a state $|m\rangle$ to a state $|m'\rangle$ causing random jumps of an effective field $JS_z = J_{m_s}$ acting on the proton. The frequency of these jumps depends on the life time of the spin states. When the relaxation time is long, the proton signal splits up into a multiplet, as the relaxation time decreases, the life time of the spin states decreases and the lines of the multiplet

broaden. As the relaxation time continues to decrease, the proton spectrum coalesces into a single broad line centred on the Larmor frequency. Finally, when the relaxation time is very short so that it becomes comparable with the Larmor frequency of the proton, the quadrupolar relaxation of spin S acts as a relaxation mechanism of the proton(s) via scalar coupling and the proton line will sharpen and effectively a decoupled signal is obtained.

To study the changes of the structure of a multiplet as a function of transition frequency Γ, let us first consider the case when $\Gamma \ll J$, i.e. long relaxation time.

The transition between two spin states of a proton are

$$|a\rangle = |+, m'_s\rangle \quad \text{to} \quad |b\rangle = |-, m'_s\rangle$$

corresponding to a frequency $\omega_{ab} = \omega_o + J m_s$

and the line width at half height is given by

$$\frac{1}{T_2} = \frac{1}{T_2^*} + \tfrac{1}{2}\left[\frac{1}{t_a} + \frac{1}{t_b}\right] \quad \text{-----1}$$

where $\frac{1}{T_2^*}$ is the broadening due to the magnetic field inhomogeneity (in fact, it is the broadening due to any mechanism other than the relaxation of spin S), t_a, t_b denote the life times of spin states a and b respectively, which is equal to the life time of the spin state m_s and we can write that $t_a = t_b = \tau_{m'_s}$

This "life time" broadening is the natural line width and according to the Heisenberg uncertainty principle, ω_{ab}, the width of the transition is given by $\omega_{ab} = \frac{1}{\tau_{m'_s}}$

The inverse life of a state m'_2 due to relaxation, denoting $P_{m'm''}$ as the transition probability between these two states we can write

$$\frac{1}{\tau_{m'_s}} = \sum_{m''} P_{m'm''} \quad ---2$$

If $\mathcal{H}_1$ is the Hamilitonian responsible for the transition between state $|m'_s\rangle$ and $|m''_s\rangle$, the probability of the transition can be written as

$$P_{m'm''} = |\langle m'_s | \mathcal{H}_1 | m''_s \rangle|^2 \quad ---3$$

but since we are considering here the perturbation Hamiltonian of the type

$$\mathcal{H}_1 = \sum_q F^{(q)} A^{(q)}$$

where $F^{(q)}$ and $A^{(q)}$ have their usual meanings, we can write that

$$P_{m\,m''} = \left|\left\langle m'_s \left| \sum_q F^{(q)} A^{(m'_s - m'_s)} m'' \right\rangle\right|^2 \quad ---4$$

as we are dealing here with the quadrupolar relaxation mechanism, the allowed transitions will be where $\Delta m = \pm 1, \pm 2$. For simplicity, without harming the generality of the treatment we apply the conditions of extreme narrowing, we have

$$P_{m'_s,\, m'_s \pm 2} = \frac{3}{80}\left[\frac{e^2 q Q}{S(2S-1)}\right]^2 (1 \pm \frac{\eta^2}{3}) |\langle m'_s | S_\pm | m' \pm 2 \rangle|^2 \tau_c \quad ---5$$

and

$$P_{m'_s,\, m' \pm 1} = \frac{3}{80}\left[\frac{e^2 q Q}{S(2S-1)}\right]^2 (1 + \frac{\eta^2}{3}) |\langle m'_s | S_\pm S_z + S_z S_\pm | m' \pm 1 \rangle|^2 \tau_c$$

calculating the integrals according to the properties of angular moments and introducing the quadrupole relaxation time Tq, the probabilities are given by

$$P_{m,\ m \pm 1} = \tfrac{1}{2} \frac{(2m \pm 1)^2 (S \pm m + 1)(S \mp m)}{(2S - 1)(2S + 3)} \quad \frac{1}{T_q} \quad \text{---- 7}$$

$$P_{m,\ m \pm 2} = \tfrac{1}{2} \frac{(S \mp m)(S \mp m - 1)(S \pm m + 1)(S \pm m + 2)}{(2S - 1)(2S + 3)} \quad \frac{1}{T_q} \quad \text{---- 8}$$

According to equations 1 and 2 we can calculate the line widths of the multiplet components as

$$\frac{1}{T_2} = \frac{1}{T_2^*} + \sum_{m''} P_{m'm''} \qquad 9$$

When T_q is longer as compared to T_2^*, we can ignore T_2^*, we can write that the respective width of the multiplet components is proportional to $\sum_{m''} P_{m'm''}$, we have

$$\frac{1}{\tau}_{m'_s} = \frac{1}{T_q} \frac{1}{2(4S(S+1)-3)} \left[\left\{ (2m+1)^2 (S+m+1)(S-m)(2m-1)^2 (S-m+1)(S+m) \right\} + \left\{ (S-m)(S-m-1)(S-m+1)(S+m+2)(S+m)(S+m-1)(S-m+1)(S-m+2) \right\} \right] \qquad 10$$

when $S = 1$ we get

$$\frac{1}{\tau_{m_1}} = \frac{1}{\tau_{m_{-1}}} = \frac{3}{5} \frac{1}{T_q} \quad \text{---- 11}$$

and

$$\frac{1}{\tau_o} = \frac{2}{5} \frac{1}{T_q} \quad \text{---- 12}$$

The spectrum of the proton coupled to the spin S is a triplet with the central line width $\frac{2}{5}$ ($\frac{1}{T_q}$) and the side lines $\frac{3}{5}$ ($\frac{1}{T_q}$), i.e. these widths are in the ratio of 3:2:3.

Several authors have developed expressions for the total band shape of a spin $\frac{1}{2}$ nucleus coupled to a quadrupolar nucleus.

The theory underlying the shape of the absorption band was developed by Pople[76] following the treatment of exchange processes described by Sack[80]. The Pople expression is given by

$$I(x) = \frac{45 + \eta^2 (5x^2 + 1)}{225 x^2 + \eta^2 (34 x^4 - 2 x^2 + 4) + \eta^4 (x^6 - 2 x^4 + x^2)}$$

where the intensity of absorption of the spin $\frac{1}{2}$ spectrum I(x) is given as a function of dimensionless parameters

$$x = {}^{\Delta\nu}/_{J}$$

$$\eta = 10 \pi T_1 J$$

where $\Delta\nu$ is the distance from the centre of the band, T_1 is the quadrupolar relaxation time and J is the coupling constant between the spin $\frac{1}{2}$ and the quadrupolar nucleus.

These authors did not take into account the natural line width of the proton signal in the absence of quadrupolar relaxation. This term must be included for an accurate line shape analysis. The theory was later modified to include the natural line width $(\pi T_2)^{-1}$ by Kintzinger et al[81] who obtained quadrupolar relaxation times of deuterium and nitrogen by fitting the experimental data to computer calculated band shapes.[82-85] Recently Pyper[86,87] has shown using a more rigorous approach based on Redfield's[88] relaxation theory that for a spin system consisting of first order groups of magnetically equivalent spin $\frac{1}{2}$ nucleuscoupled to one another and to a single quadrupolar nucleus, the spectrum of the spin $\frac{1}{2}$ nuclei consists of overlapping bands centred at the normal first order positions and

with normal intensities. The origins of the individual bands in the multiplet are to be taken at the frequencies of the multiplet components calculated in the absence of splitting from the quadrupolar nucleus. The line shape function is given by

$$L(\nu) = \sum_{E} \left(\prod_{i \neq q} g_{iE} \right) \sum_{c.p.t.} \langle \psi_i | M_x | \psi_j \rangle \, P(\nu, E)$$

where g_{iE} is the degeneracy of the composite particle state of the i th magnetically equivalent group in the wave functions ψ_i and ψ_j $P(\nu, E)$ is just a Pople type function centred at E which is the transition frequency from $|\psi_j\rangle \longrightarrow |\psi_j\rangle$ in the absence of splitting from the quadrupolar nucleus. The summation over all the composite particle transitions (c.p.t.) of $\langle \psi_i | \hat{M}_x | \psi_j \rangle$ is a constant for all E. The equation shows that the line shape is composed of contributions from a number of particles of total spin I_q, corresponding to all the possible total spins of the q th group executing stationary random Markovian jumps ≠ between three sites of different precessional frequencies. In qualitative terms this behaviour can best be understood by considering a $^3A^2X$ system (e.g. the HD sub spin system for the non magnetic tin species is $(C_6H_5)_2SnHD$). The six eigenstates of the spin system and the corresponding three transitions are shown in Fig. X.III. The relaxation of the A spin causes the X spin to jump between sites of different resonance frequency corresponding to different spin states of A. As the rate of

---

≠ Markov Process: A stochastic process (randomly variable) such that the conditional probability distribution for the state at any future instant, given the present state is unaffected by any additional knowledge of the past history system.

Fig. X. III. Energy levels of a spin $\frac{1}{2}$ nucleus coupled to a spin I = 1 nucleus by scalar interaction

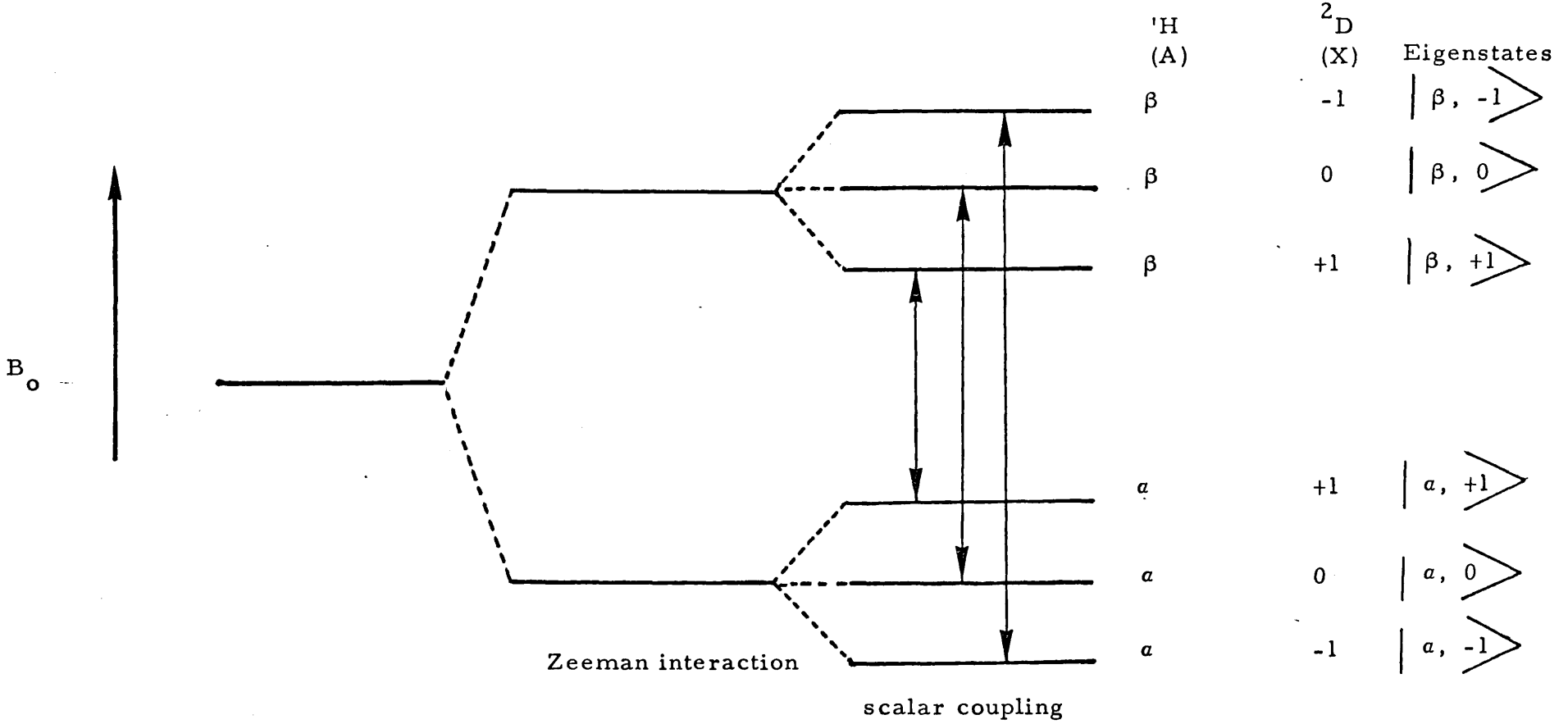

The energies of these three transitions (of X spectrum) are as

$$|\alpha, 1\rangle \longrightarrow |\beta, 1 \quad = \nu X + J_{AX}$$
$$|\alpha, 0\rangle \longrightarrow |\beta, 0 \quad = \nu X$$
$$|\alpha, -1\rangle \longrightarrow |\beta, -1 \quad = \nu X - J_{AX}$$

relaxation of A increases, the X transitions broaden and then collapse into one transition centred at ν_x, which is then further narrowed for more rapid relaxation of A.

Section X.4 Curve fitting program.

The curve fitting of the experimental band shape was done with a computer program QUADRUCALC. This program was written by N.C.Pyper[86], of the University of East Anglia, to iteratively fit band shapes of first order NMR spectra of spin-$\frac{1}{2}$ nuclei for systems containing a quadrupolar nucleus. The maximum number of spin-$\frac{1}{2}$ nuclei is seven. The program accepts as input (on punched cards) the experimental band shape (including baseline information) an estimated value for the coupling constant to the quadrupolar nucleus and a trial relaxation time. A least squares fit of

$$L(\nu) = \sum_{E} \left(\prod_{i \neq q} g_{i E} \right) \sum_{c.p.t.} \langle \psi_i | M_x | \psi_j \rangle P(\nu, E)$$

is performed by the computer. In order to obtain a "smooth" baseline an arbitrary reference point is taken on the left hand side and all the intensities of experimental curve are measured from it. This program deals only with the intensity differences. The data was processed on a CDC 6600 computer via a 200 user terminal. The data is read in as below.

NN Name — NN is the number of spin $\frac{1}{2}$ nuclei and name of the file.

NWANT — number of nuclei being observed.

IRT — the trial longitudinal relaxation time T_1 of the quadrupolar nucleus, is variable.

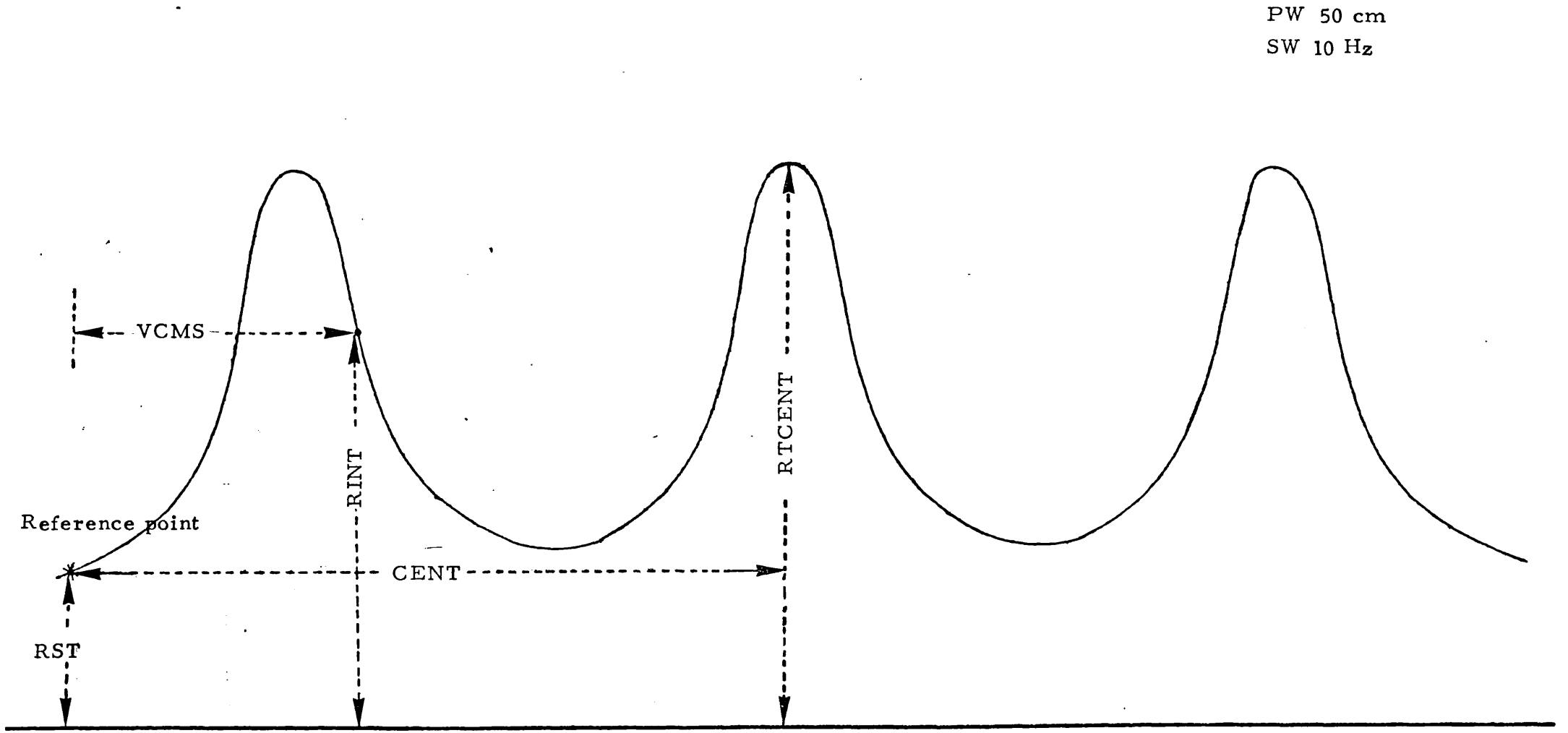

Fig. X.IV. Calibration of the experimental curve.

NITIT is the number of iterations required

CQ is the coupling constant (J_{HD})

RMFI the line width at half height of a standard line to which no quadrupolar nucleus is attached.

EPR the percentage correction

CORIT is the fraction of correction

(Both EPR and CORIT have standard values 0.05 and 0.08 respectively)

RT is the initial value of quadrupolar relaxation time

CENT an arbitrary origin, is taken on the extreme left of the chart and the distance of the centre of the multiplet from that arbitrary origin

RTCENT is the height of the central feature of the multiplet from the origin of the paper

VST the horizontal distance of any point on the experimental multiplet from the arbitrary point on the left hand

RST is the height of the reference point from the left hand origin of the paper

SW and PW are the sweep width and paper widths respectively

VCMS distance of points in cm from the origin (98 numbers taken in this case)

RINT is the height of a point on the curve from the same origin as RTCENT

Fig.X.IV. shows the calibration of the experimental curve according to the above program.

The program prints relaxation times, scaling factor and their calculated corrections. At the last iteration, the root mean square errors are printed with the final values of quadrupolar relaxation time and scaling factor.

Errors. The computer program calculates the orthogonalized root-mean-square errors on parameter two (relaxation time of quadrupolar nucleus). These errors actually indicate the degree to which the observed line shape can be fitted to a theoretical model, so they do not reflect the true error where less than 0.1 per cent. Another source of error is the variation of iterated parameters from one spectrum to another and uncertainty as to the correct value for the magnetic field inhomogeneity. The magnetic field inhomogeneity was measured in every case from the line width of undeuterated species to minimise the above mentioned error.

Section X .5 Results and discussion

The deuterium nucleus in deuterated di-phenyl tin hydride $\square$ $(C_6H_5)_2SnHD$ $\square$ can relax by quadrupolar and dipole-dipole mechanisms (The spectrum of this compound has been described in Chapter III). Its relaxation time being

$$\left(\frac{1}{T_1}\right)_{\text{total}} = \frac{1}{T_q} + \frac{1}{T_{H\text{-}D\ (\text{dipole-dipole})}}$$

The quadrupole relaxation is by far the dominant relaxation mechanism of a quadrupole nucleus and much more effective than the dipolar relaxation of H-D. In addition quadrupole relaxation depends only on intramolecular motion. Intermolecular contributions to the local electric field gradients are very weak, therefore no separation is necessary. We will consider that the relaxation of deuterium is due to a purely quadrupole mechanism.

A value of 0.488 sec for the quadrupole relaxation time was obtained by band shape analysis at room temperature of the proton resonance. To check the above value, further measurements on the half widths of lines of the triplet were evaluated. Taking into account the "natural" line width in the absence of quadrupolar relaxation, the "pure" quadrupole broadening $\Delta \nu_q$ can be obtained for the central and 3/2 $\Delta \nu_q$ for the outer peaks. The broadening $\Delta \nu_q$ is given by [76]

$$\Delta \nu_q = \frac{1}{\pi \tau_o}$$

where τ_o, is the life time of the non magnetic spin state (m = o) of deuterium. The inverse life time (probability of transition per

unit time) is given by

$$1/\tau_o = \frac{6}{40} \left(\frac{e^2 q Q}{\hbar} \right)^2 \tau_c$$

The quadrupole relaxation time T_q can be written as

$$\frac{1}{T_q} = p_{o,1} \pm 2 p_{-1,1} = \frac{3}{8} \left(\frac{e^2 q Q}{\hbar} \right)^2 \tau_c \quad \ldots(A)$$

(where p_{ij} is the transition probability between the two states)

Therefore

$$\frac{1}{T_q} = \frac{3}{8} \times \frac{40}{6} \times \frac{1}{\tau_o}$$

$$= \frac{5}{2} \pi \Delta \nu_q$$

similarly for the outer peaks the expression can be written as

$$\frac{1}{T_q} = \frac{5}{3} \pi \Delta \nu_q$$

Comparison of T_q values gave the following results

$(C_6H_5)_2SnHD$

Line shape analysis	Line width measurements
0.488 sec	0.454 sec (central peak)
	≠ 0.477 sec (outer peaks)

≠ calculated from the average width.

The agreement between these T_q values is fairly good. It is interesting to compare the results obtained here for T_q with similar molecules. A suitable example[94] is that of $(C_6H_5)_2CD_2$ where the deuterium quadrupole relaxation time has been measured as 0.19 sec by the direct method. The difference of these relaxation times may be explained in terms of a lower quadrupole coupling constant for Sn-D in $(C_6H_5)_2SnHD$

as compared to C-D in $(C_6H_5)_2CD_2$ (the reported values for the quadrupole coupling constant C-D are between 170 and 350 kHz depending on the compounds).

Similar measurements on the line shape of deuterated dimethyl tin hydride yielded the following T_q values

2.21 sec (central peak)

2.38 sec (outer peaks)

The exact value of the Sn-D quadrupole coupling constant is not known. Since both proton and deuteron relaxation in diphenyl tin dihydride and deuterated diphenyl tin hydride arise from intramolecular interaction (for ^1H relaxation time, see Chapter IX), a calculated value of τ_c, from the intramolecular dipole-dipole relaxation time can be used to estimate the quadrupole coupling constant from the expression (A), by substituting a value of T_q. Previous [89-91] such attempts to determine the quadrupole coupling constant gave poor results because of difficulty in separating various intramolecular contributions. Molecules in the liquid state tumble anisotropically. The dependence of the deuterium relaxation time on this anisotropic motion is the same as that of proton. The angular dependence of Sn-H dipole-dipole relaxation is exactly the same as that of Sn-D quadrupole relaxation. Taking 9.37×10^{-12} sec as a correlation time (Table X.1) and $T_q = 0.488$ sec and substituting these values in equation (A), a value of $(e^2q\,Q/\hbar)$ was found to be 121.5 kHz. This value can be compared with that of mono-phenyl

silane-d_3 (91 $\pm$ 2 kHz) calculated from the proton deuterium magnetic resonance studies in liquid crystal solutions by Fung et al.[93] Since the quadrupole coupling constant does not change much if the bond connecting deuterium is of similar nature in different compounds. Taking a value of 121 kHz and $T_q = 2.12$ sec for deuterated dimethyl tin hydride one obtains

$$\tau_c = 2.18 \times 10^{-12} \text{ sec}$$

The correlation time derived here is somewhat lower than the value of 2.40×10^{-12} sec (Table X.1) calculated from the measurement of proton intramolecular dipole-dipole relaxation time of di-methyl tin hydride. However, one is tempted to suggest that the value of the quadrupole coupling constant for the systems studied here is close to the real value of the Sn-D quadrupole coupling constants in these compounds.

A suggestion for further work in this area would be variable temperature studies to observe the effect on the line shape and measure quadrupole relaxation times, from which correlation times for molecular motion can be calculated. The temperature dependence of T_q leads to the calculation of activation parameters for molecular reorientation.

REFERENCES

REFERENCES

1. H. C. Clark, J. T. Kwon, L. W. Reeves and E. J. Wells, Can. J. Chem., 41, 3005 (1963)
2. Jeanine Dufermont et J. C. Maire, J. Organometal. Chem., 7, 415, (1967).
3. P. E. Potter, L. Pratt, and G. Wilkinson, J. Chem. Soc., 524,(1964)
4. N. Flitcroft and H. D. Kaesz, J. Amer. Chem. Soc., 85, 1377, (1963).
5. Eberhard Amberger, Heinz P. Fritz, Cornelius G. Kreiter und Maria-Regina Kula, Chem. Ber., 96, 3270, (1963).
6. M. T. Ryan and W. L. Lehn, J. Organometal. Chem., 4, 455, (1965).
7. C. Schumann and H. Dreeskamp, J. Magn. Resonance, 3, 204, (1970).
8. J. C. Maire and J. Dufermont, J. Organometal. Chem., 10, 369, (1967).
9. M. L. Maddox, N. Flitcroft and H. D. Kaesz, J. Organometal. Chem.,
10. H. J. Bernstein, and N. J. Sheppard, J. Chem. Phys., 37, 3012 (1962)
11. J. D. Kennedy, and W. McFarlane, Revs. Si, Ge, Sn and Pb, 1. (3), 235, (1974).
12. D. G. Gillies, R. Walder and M. A. Ward, unpublished results
13. Y. Kanazarva, J. D. Baldeschwieler and N. C. Craig, J. Mol. Spec., 16, 325, (1965).
14. G. Fraenkel, Y. Asahi, H. Batiz-Hernandez and R. A. Bernheim, J. Chem. Phys., 44, 4647 (1966).
15. D. G. Gillies and I. D. Cresshull, unpublished results.
16. C. S. Peters, R. Codrington, H. C. Walsh and P. D. Ellis, J. Magn. Resonance, 11, 431, (1973).

17. J.J.Burke and P.C.Lauterber, J.Amer.Chem.Soc., 83, 325,(1961)

18. B.K.Hunter and W.Reeves, Can.J.Chem., 46, 1399, (1968).

19. D.L.Alleston, A.G.Davies, M.Hancock and R.F.M.White, J.Chem.Soc., 5469 (1963).

20. W.J.Considine, G.A.Baum and R.C.Jones, J.Organometal. Chem., 3, 308, (1965)

21. Alw yn G.Davies, P.G.Harrison, J.D.Kennedy, T.N.Mitchell, R.J.Puddephatt and W.McFarlane, J.Chem.Soc.(C), 1136, (1969).

22. P.G.Harrison, S.E.Ulrich and J.J.Zuckerman, J.Amer.Chem. Soc., 93:21, 5398 (1971).

23. P.J.Banney, D.C.McWilliam and Peter R.Wells, J.Magn. Resonance, 2, 235, (1970).

24. E.V.Van der Berghe and G.P. Van der Kelen, J.Organometal. Chem., 26, 207, (1971).

25. G.M.Ford, L.G.Robinson and G.B.Savitsky, J.Magn.Resonance, 4, 109, (1970).

26. N.F.Ramsey, Phys.Rev., 87, 1075, (1952).

27. H.Baitz-Hernandez and R.A.Bernheim, Prog.N.M.R.Spectroscopy, 3, 63, (1967).

28. R.A.Bernheim and H.B.Hernandez, J.Chem.Phys., 45, 6, 2261, (1966)

29. A.Saika and H.Narumi, Can.J.Phys., 42, 1481, (1964).

30. R.G.Gillespie and J.W.Quail, J.Chem.Phys., 39, 2555, (1963).

31. R.K.Harris, J.Mol.Spectry., 10, 309, (1963).

32. R.A.Bernheim and H.Baitz-Hernandez, J.Chem.Phys., 40, 3446, (1964).

33. A. Tupciauskas, N. M. Sergeyev and Yu. A. Ustynk, Mol. Phys., 21, 1, 179 (1971)

34. W. McFarlane, J. Magn. Resonance, 10, 9, 98 (1973)

35. A. A. Borisenko, N. M. Sergeyev and Yu. A. Ustynk, Mol. Phys., 22, 715, 1971

36. C. N. Banwell, J. N. Murrell and M. A. Turpin, Chem. Comm. 1466, (1968).

37. G. Fraenkel and W. Burlant, J. Chem. Phys., 42, 3724, (1965).

38. Pfisterrer and H. Dreeskamp, Ber, Bungsenges, Phys. Chem. 73, 654, (1969).

39. M. Murray, J. Magn. Resonance, 9, 326, (1973).

40. N. M. Sergeyev and V. N. Solkan, J. Chem. Soc. Comm., 17, 1975.

41. W. B. Moniz, W. A. Steele and J. A. Dixon, J. Chem. Phys., 38, 2418, (1963).

42. D. E. Woessner, J. Chem. Phys., 37, 647, (1962).

43. H. Shimizu, J. Chem. Phys., 37, 765, (1962).

44. W. A. Steele, J. Chem. Phys., 38, 2404, (1963).

45. F. Perrin, J. Phys. Radium, 5, 497, (1934).

46. P. Debye "Polar Molecules", Dover publications, Inc., New York, (1954).

47. A. Gierner and K. Wirtz, Z. Naturforsch, 8a, 532, (1953).

48. W. J. Taylor, D. D. Wagman, M. G. Williams, K. S. Pitzer and F. D. Rossini, J. Res. Nat. Bur. Stand. 37, 95, (1946).

49. N. F. Hill, Proc. Phys. Soc. London, 67B, 149, (1954).

50. N. Bloembergen, E. M. Purcell and R. V. Pound, Phys. Rev., 73, 679, (1948).

51. Hindermann, D.K., and Cornwell, C.D., J. Chem. Phys., 48, 2017, (1968).

52. Litchman, W.M., Alei A. and Florin A.E., J. Chem. Phys., 80, 1897 (1969).

53. H. S. Gutowsky, V. D. Mochel and B. G. Sommers, J. Chem. Phys., 36, 1153 (1962).

54. E. A. V. Ebsworth and J. J. Turner, J. Chem. Phys., 36, 2628 (1962).

55. P. Piehl and Th. Liepert, Helv. Chim. Acta, 47, 545, (1964).

56. H. Wantabe, T. Totani and M. Ohtsuru, Mol. Phys., 367 (1968)

57. G. Fraenkel and W. Burlant, J. Chem. Phys., 42, 3724, (1963).

58. H. Coli, V. Gold and J. Pearson, J. C. S. Chem. Comm., 408 (1973)

59. H. Schmidbaur and W. Siebert, Z. Naturforsch 20b, 596, (1965).

60. E. Dayan, G. Widenlocher and M. Chaigneau, Compt. Rend. 275, 2255 (1963).

61. George Van Dyke Tiers, J. Am. Chem. Soc., 79, 5585 (1957).

62. M. McFarlane, Ann. Rev. N. M. R. Spectroscopy, 1, 135, (1968).

63. A. Saika and C. P. Slichter, J. Chem. Phys., 22, 26 (1954).

64. H. J. Jakobsen and T. Bundgaard, J. Magn. Resonance ; 18 , 209, (1975).

65. P. S. Hubbard, Phys. Rev. 141, 1155 (1963).

66. R.E.D.McClung, J.Chem.Phys., 51, 3842 (1969).

67. A.Briguet, J.C.Duphan and J.Delman, Mol.Phys., 29, 3, 837 (1975).

68. Frank Heatley, J.Chem.Soc. Far.Trans.II., 70, 148, (1974).

69. J.J.Jones, D.M.Grant and K.F.Kuhlmann, J.Am.Chem.Soc., 91, 5013, (1962).

70. K.F.Kuhlmann, D.M.Grant and R.K.Harris, J.Chem.Phys., 52, 3439, (1970).

71. R.C.Poller, "The Chemistry of organo-tin compounds", Logos Press Ltd., London 1970.

72. J.N.Shoolery, Techn.Information Bull. Varian Associates, Palo Alto, Cali. No.3 (1959).

73. Ebsworth and Turner, J.Chem.Phys., 36, 2628, (1962).

74. Schneider and Buckingham, Discuss.Faraday Soc., 34, 154 (1962).

75. H.A.Bent, Chem.Rev., 60, 275, 1960 and Canad.J.Chem., 38, 1235 (1960).

76. J.A.Pople, Mol.Phys., 1, 168 (1958).

77. J.S.Waugh, "Molecular Relaxation Process" Academic Press, London (1966).

78. J.Bacon, R.J.Gillespie and J.W.Quail, Canad.J.Chem., 41, 3663, (1963).

79. M.Suzuki and R.Kubo, J.Mol.Phys., 7, 201, (1963).

80. R.A.Sack, Mol.Phys. 1, 163, (1958).

81. J.P.Kintzinger, J.M.Lehn and R.L.Williams, Mol.Phys., 17, 139 (1969).

82. Ch.Brevard, Doctorate d'Etat thesis, University of Strasbourg, (1971).

83. J.P.Kintzinger, Doctorate d'Etat thesis, University of Strasbourg, (1970).

84. Ch.Brevard, J.P.Kintzinger and J.M.Lehn, Tetrahedron., 28, 2429 (1972).

85. C.M.Sheppard, T.Schaefer, B.W.Goodwin and J.Traa, Canad. J.Chem., 49, 3158 (1971).

86. N.C.Pyper, M.Sc.thesis, University of East Anglia (1968).

87. N.C.Pyper, Mol.Phys., 19, 161 (1970)

88. A.G.Redfield, Adv.Magn.Resonance, 1, 1, (1965).

89. D.Woessner, J.Chem.Phys., 40, 2341, 1964

90. Bonera and A.Rigamonti, J.Amer.Chem.Soc., 42, 175,(1965).

91. M.Zeidler, Ber.Bunsenges Phy.Chem., 69, 659 (1965).

92. R.Figgins and M.Rhode, Mol.Phys., 17, 669 (1970)

93. B.M.Fung and I.Y.Wei, J.Amer.Chem.Soc., 92, 1497 (1970).

94. H.M.Mautsch, H.Saito, L.C.Leitch, I.C.P. Smith, J.Amer.Chem. Soc., 96:1,285 (1974).

95. W.P.Neumann and Niermann, Liebigs.Ann.Chem., 653, 164 (1962).

96. H.G.Kuivila, A.K.Sawyer and A.G.Armont, J.Org.Chem., 26, 1426, (1961).

97. G.W.Schaeffer and Sr.M.Emelius, J.Amer.Chem.Soc., 76, 1203, (1954).

98. C.R.Dillard, E.Holmes McNeill, D.E.Simmons and J.B. Yeldell, J.Amer.Chem.Soc., 80, 3607, (1958).

99. H.G.Kuivila and A.M.Bennual, J.Amer.Chem.Soc., 83, 1246, (1961).

100. H.J.Emeleus and S.F.A.Kettle, J.Chem.Soc., 2444 (1958).

101. A.E.Finholt, A.C.Bond, K.E.Wilzbach and H.I.Schlesinger, J.Amer.Chem.Soc., 69, 2692 (1947).

102. G.E.Coates, M.L.H.Green and K.Wade, "Organometallic Compounds" Vol.I, Methuen and Co.Ltd. London (1969).

103. E.A.C.Lucken, "Nuclear Quadrupole Coupling Constants" Academic Press, N.Y. (1969).

104. T.P.Das and E.L.Hahn, "Nuclear Quadrupole Resonance Spectroscopy", Academic Press, N.Y.(1955).

105. C.H.Townes and A.Z.Schawlow, "Microwave Spectroscopy", McGraw Hill, N.Y. (1955).

106. G.K.Wertheim "Mössbaur Effect, Principles and Applications", Academic Press, N.Y. (1960).

107. W.Low, "Paramagnetic Resonance in Solids" Academic Press, N.Y. (1960).

108. F.Bloch, W.W.Hansen and M.E.Packard, Phys.Rev., 69, 127, (1946).

109. E.M.Purcell, H.C.Torrey and R.V.Pound, Phys.Rev., 69, 37, (1946).

110. F.Bloch, Phys.Rev., 70, 460, (1946).

111. N. Bloembergen, E. M. Purcell and R. V. Pound, Phys. Rev., 73, 679 (1948).

112. P. W. Anderson, J. Phys. Soc. Japan, 9, 316, (1954).

113. R. Kubo and K. Tomita, J. Phys. Soc. Japan, 9, 888 (1954).

114. R. Kubo, J. Phys. Soc. Japan, 9, 935 (1954).

115. R. Kubo, Suppl. Nuovo Cimento, 6, 1064 (1957).

116. A. Abragam "The Principles of Nuclear Magnetism" Oxford University Press (1961).

117. F. Bloch and R. K. Wangsness, Phys. Rev., 89, 728 (1953).

118. F. Bloch, Phys. Rev., 102, 104, (1956).

119. F. Bloch, Phys. Rev., 105, 12o6, (1957).

120. A. G. Redfield, I. B. M. Res. Develop. 1, 19, (1957).

121. P. S. Hubbard, Rev. Mod. Phys., 33, 349, 1961.

122. C. P. Slichter, "Principles of Magnetic Resonance" Harper and Row, N. Y. (1963).

123. J. A. Pople, W. G. Schneider and H. J. Bernstein "High Resolution Nuclear Magnetic Resonance", McGraw Hill, N. Y. (1959).

124. P. L. Corio, Chem. Rev., 60, 363 (1960)

125. J. D. Roberts, "An Introduction to the analysis of Spin Spin splitting in High Resolution N. M. R. Spectra", W. A. Benjamin, N. Y. (1961).

126. Lamb, Phys. Rev., 60, 817 (1941).

127. E. Fermi, Z. Physik, 60, 320 (1930).

128. J. A. Pople and D. P. Santry, Mol. Phys. 8, 1, (1964).

129. Solomon, Phys. Rev., 99, 559 (1955).

130. K. F. Kuhlmann, D. M. Grant and R. K. Harris, J. Chem. Phys., 52, 3439, (1970).

131 P. S. Pregosin and E. W. Randall, "Determination of Organic Structure by Physical Methods" (F. C. Nachod and J. J. Zuckermann eds. Vol. 4.) Academic Press, N. Y. (1971).

132. R. Freeman, H. D. W. Hill and R. Kaptein, J. Magn. Res., 7, 327 (1972).

133 J. W. Emsley and J. C. Lindon, "N. M. R Spectroscopy Using Liquid crystal solvents", Pergamon Press (1975)

134 P. Diehl and C. Khetrapal, "N. M. R Basic Principles and Progress " Vol. I. Springer-Verlag.

135 R. Ader and A. Loewenstein, Mol. Phys. 30, 199, (1975).

136 M. E. Rose "Elementry Theory of Angular Momentum " John Wiley, (1955)